# Flapping wing actuation using resonant compliant mechanisms

## An insect-inspired design

# Flapping wing actuation using resonant compliant mechanisms

## An insect-inspired design

PROEFSCHRIFT

ter verkrijging van de graad van doctor
aan de Technische Universiteit Delft,
op gezag van de Rector Magnificus Prof. ir. K.C.A.M. Luyben,
voorzitter van het College voor Promoties,
in het openbaar te verdedigen op donderdag 21 oktober 2010 om 12.30 uur
door

Caspar Titus BOLSMAN

werktuigkundig ingenieur
geboren te Zaanstad

Dit proefschrift is goedgekeurd door de promotor:

Prof. dr. ir. A. van Keulen

Copromotor:

Dr. ir. J.F.L. Goosen

Samenstelling promotiecommissie:

| | |
|---|---|
| Rector Magnificus, | voorzitter |
| Prof. dr. ir. A. van Keulen, | Technische Universiteit Delft, promotor |
| Dr. ir. J.F.L. Goosen, | Technische Universiteit Delft, copromotor |
| Prof. dr. ir. drs. H. Bijl, | Technische Universiteit Delft |
| Prof. ir. R.H. Munnig Schmidt, | Technische Universiteit Delft |
| Prof. dr. ir. J.L. Herder, | Universiteit Twente |
| Prof. dr. ir. J.L. van Leeuwen, | Wageningen University |
| Dr. ir. D. Lentink, | Wageningen University |

DEVLAB DEVELOPMENT LABORATORIES     NWO Netherlands Organisation for Scientific Research     Agentschap NL Ministerie van Economische Zaken

Author email: casparbolsman@gmail.com

*For Marieke*

# Summary

**Flapping wing actuation using resonant compliant mechanisms**
**An insect-inspired design**

This thesis describes the analysis and design of the wing actuation mechanism for an insect inspired flapping-wing MAV Micro Air Vehicle. Insects are among nature's most nimble flyers and are an abundant source of inspiration for the development of flapping-wing MAVs. The human endeavor to design and realize flapping wing flight at insect scales has increased in recent years. The focus of this thesis is on the exploitation and application of resonant principles to achieve insect-like wing movement patterns. The insect thorax-wing system is in essence a tuned resonant system. Insects exploit resonance to reduce the energy required to realize the wing flapping motion and achieve large amplitude wing motion by resonant amplitude amplification. The application of resonant principles in a flapping-wing MAV is intended to achieve the same aspects. The insect wing movement can be divided into two parts; The first is the flapping motion and the second is the wing rotation or pitching motion. The research in this thesis is divided along these lines. The flapping-wing MAV body, which facilitates the flapping motion is designed separately but parallel to the wings, which facilitate the pitching motion.

In order to achieve resonance a significantly flexible structure has to be incorporated into the design of the flapping-wing MAV thorax. Various options are reviewed and an option based on the use of bending is chosen. The elastic structure used for the body of the flapping-wing MAV is a ring-type structure. Using the ring in this setting gives many options for both wing attachment and actuator placement. The ring is coupled to the wings by a compliant amplification mechanism which transforms and amplifies the ring deflection into the large wing root rotation required for the wing flapping motion. The development of the structures follows a two-step approach. The first step is the selection of four prototypes

used for determining the viability of the structures and proposed analysis methods, multi-body dynamics models and finite element models. The second set of structures is geared towards application level detailing and as such more emphasis is placed on reducing weight. After initial sizing, the structures are analyzed by finite elements (eigenvalue and transient analysis). Based on the analysis, the structures have been built, realized and tested. It appeared that the structures are capable of sustaining large amplitude flapping motion in a resonant manner.

The division of the design of the structure allows for independent analysis of the wings. In insects, the wing pitching motion, which is of paramount importance for efficient lift production, is predominantly passive in origin. An engineering equivalent requires the presence of a tunable elastic structure in the wing root to facilitate the passive wing pitching motion. A solution to this problem has been found by adding a simple elastic element in an existing, commonly used, wing design. The elastic element in the wing root is tuned by using a coupled quasi-steady aerodynamic and multi-body dynamics model. The reference used for the tuning is a simplified version of the wing kinematics portrayed by hawkmoths. The wings are realized and tested experimentally to see whether the wings reflect the performance found in the analysis.

The ring-shaped thorax structure is combined with the wings to test resonant performance of the assembled structure. A test setup is built to quantify lift production. Lift is tested by suspending the prototype on a flexible beam and measuring changes in deflection when the model is actuated. Significant lift is produced using the current prototype, in the order of the weight of the structure without the actuator. Kinematic patterns present during resonant actuation show correct timing of wing rotation.

The present developments have led to greater insight in the exploitation of resonance for driving wings in flapping-wing MAVs. Ring-type structures are a valid starting point and yield promising results. Further developments lie in the selection and tuning of actuators and the incorporation of control possibilities in the design.

*Caspar Bolsman*

# Contents

# Chapter 1

# Introduction

## 1.1 Motivation

The use of unmanned aerial reconnaissance drones has dramatically increased in recent years due to technology advancement in many fields: GPS systems, advancement in computational power, unsteady aerodynamics and battery technology, among others. Miniaturization in many fields, *e.g.*, electronics, sensors and actuators, has allowed smaller aerial platforms to become feasible. It is here that a great challenge and opportunity lie, namely indoor aerial reconnaissance. In fiction different cases exist in which these type of platforms are being used. One of the most notable example is Dan Brown's novel "Deception Point" [23] in which a weaponized insect-scale flapping wing platform is used for both surveillance and attack.

There exist many real life cases in which small aerial sensor platforms, capable of slow moving and hovering flight, would provide a huge benefit over terrestrial platforms or remote sensing capabilities. Imagine the following case from a search and rescue perspective. In the aftermath of an earthquake there will be many damaged buildings of which the structural integrity is questionable such that entry by rescue services will only be performed when it is certain that human lives are in danger inside. Now, imagine first entering the building with a small aerial platform capable of sensing life signs and maneuvering in the indoor environment. The information provided by such an aerial drone would be invaluable to the search and rescue workers to make a decision to enter the building and attempt to rescue the victims inside. This case stresses an immediate benefit of having such a platform. There are many other cases, in less life threatening circumstances, where an aerial sensor platform would provide useful information. Operating in clouds, the platforms can map concentrations of chemicals or temperature distribution including gradient information in indoor environments

which may prove to be invaluable information. The ability to perch would introduce methods of self distribution and thereby making distribution of small sensor nodes in a three-dimensional environment possible.

The possible uses for a hovering micro aerial vehicle are numerous, as can be seen from small selection of examples. Both the search and rescue and remote sensing/sensor cloud cases are highly inspirational and the field, although many large contributions have been made, is still in its infancy.

## 1.2   Micro Air Vehicles

The term Micro Air Vehicle (MAV) is a further development of the term Unmanned Aerial Vehicle (UAV) used for larger flying platforms, which are commonly deployed on the battlefield and are starting to trickle into every day surveillance such as traffic monitoring. The term micro is defined relative to normal aircraft and may be misleading when looking at technologies like MEMS. MAVs are at least an order smaller than UAVs, the United States Defense Advanced Research Projects Agency (DARPA) has defined the MAV as any flying vehicle which is limited to 150 mm or smaller in any linear dimension (wingspan, length).

Traditionally, UAVs are fixed-wing or rotary-wing aircraft. These wing configurations are used also at the MAV scale. Many projects exist that develop fixed-wing MAVs. Especially the battery and propulsion technology can be obtained with relative ease. The aerodynamics and corresponding wing structure of fixed-wing MAVs are being heavily researched. Large additions to this field have been made by research groups at universities around the world. Rotary-wing aircraft are also used often but mainly at larger scales, often based on radio-controlled helicopters and quad rotors. A notable exception is the Mesicopter project, see [90], which aimed at the development of centimeter-sized rotary-wing aircraft at Stanford University.

A small subset of the MAVs are the flapping wing flyers. Inspired by nature's flyers, these flyers try to benefit from the possibilities of flapping wing flight.

## 1.3   The Atalanta Project

The context for the developments within this thesis is the Atalanta project, which aims at the development of a flapping-wing MAV. The requirements set for the total project are that the flapping-wing MAV should eventually be able to:

- fly autonomously

- Hover and fly slowly

- Communicate with others and a base station

- Manage power storage

- Provide payload capacity

- Be adaptable for many situations

The Atalanta project includes development on different fields required for conforming to the requirements set in the list above. One major line in these developments is low power usage. At small scales management of power usage is very important, due to a generally limited ability to store energy onboard. The second, equally important, issue in this development is the aim for low mass. A reduction of the vehicle mass will make hovering flight less energetically demanding as well as provide more room for payload.

The intended dimension of the vehicle is 100 mm wingspan and maximum vehicle mass is set to 4 g. The work described in this thesis covers the development of the wing actuation mechanism for the Atalanta flapping-wing MAV. The targeted dimensions are feasible by making use of conventional technologies, such as: gears, links and electric motors, see, for example [59, 60, 74, 84]. These dimensions are also the starting point for other technologies, such as: linear actuators and compliant mechanisms, see, for example [29, 33, 34, 144], which are more relevant when moving to even smaller dimensions.

The focus is on the development of a structure which provides the ability to hover. More specifically, hovering flight should be the basic flying state. Hovering is the worst case scenario from an energy perspective, since no additional lift is created by induced flow by forward movement [40, 50]. In insects and hovering birds the ability exists to reconfigure the wing movement and wing stroke plane orientation to facilitate the change between hovering and forward flight. Although possible mechanically, this is not aimed for in the current project.

## 1.4   Inspiration from Nature

Flight in nature exists in many forms, from gliding squirrels to flying fish. However, powered flight is predominantly the realm of bats, insects and birds. The size range covered by flight in nature is huge from the smallest flying insect, 0.25 mm wingspan and 20–30 $\mu$g body mass for a small parasitic wasp, to the largest flying birds which sport wingspans up to 3.65 m (wandering albatross) and 21 kg body mass (Great Bustard). The range in which the humans have achieved powered flight is equally impressive, starting at aircraft like the Airbus A380 which has a 79.75 m wingspan and 560 $10^3$kg maximum take-off weight [2], ranging down to the smallest radio-controlled MAVs with 67.3 mm wingspan and 0.495 g vehicle mass [85].

Humans have historically always been interested in the flight capabilities of birds and insects, see, for example Lilienthal [83]. The development of flapping wing vehicles integrates human fascination for flight with ongoing miniaturization of technical designs. Understanding of the aerodynamics of insect flight has evolved over the years and the phrase 'The laws of aerodynamics prove that the
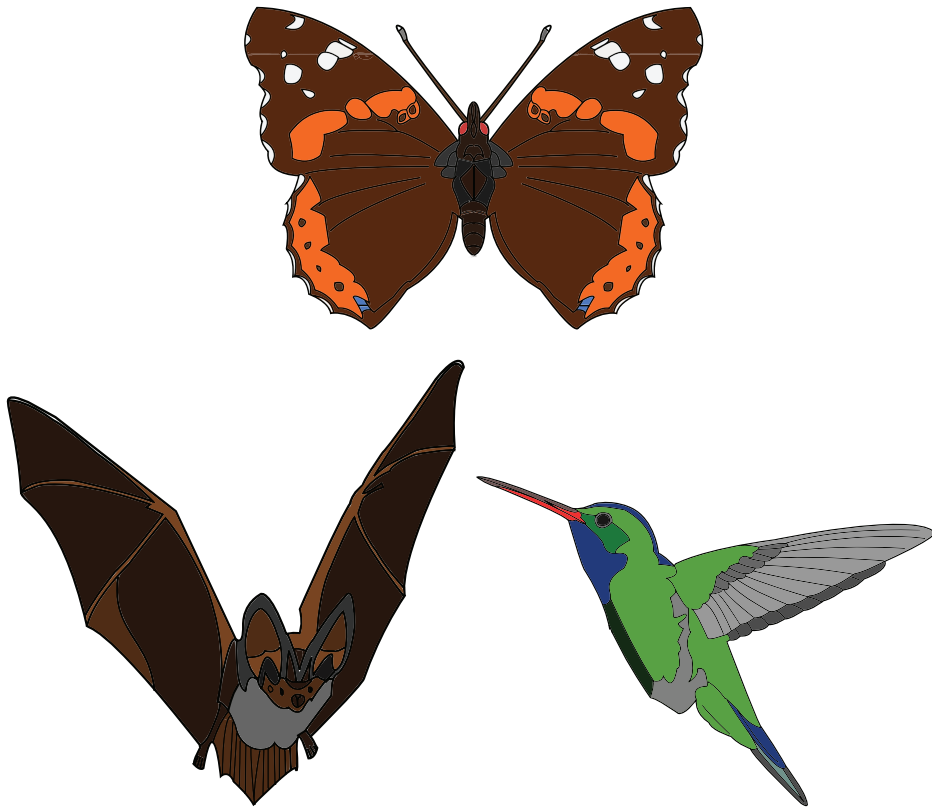
**Figure 1.1:** *Examples of powered flight in nature: The birds, mammals and insects.*

bumblebees are incapable of flight 'is of disputable origin as is proven by bumblebees everyday, from [88].

When looking at nature as an inspiration for the development of MAVs, and in general for bio-inspired design, one has to take care that direct copying of concepts found in nature will probably not lead to feasible designs, see Michelson and Naqvi [92]. The problem lies in finding the balance between the engineering implementation and the concepts extracted from nature.

## 1.5   Background

### 1.5.1   Why flapping flight?

The implementation of flapping flight at the smaller scales, and especially insect scales, is inherently more difficult than fixed-wing and rotary-wing implementations. Then, why is it so interesting to strive for insect sized flapping-wing MAVs?

This question can be answered from many perspectives. Firstly, the factor flying speed. Very small fixed-wing aircraft need high speeds to stay airborne, *i.e.*, the required induced flow over the wings needs to be high for sufficient lift production. These high speeds limit indoor usage due to short reaction times needed for the control. The second reason for flapping wing flight is the question of energy usage. The energy required for a hovering insect to stay aloft scales favorably with the dimensions and corresponding mass of the insect, see Ellington [49]. Therefore, when moving to smaller scales hovering, and slow moving flight becomes increasingly interesting. The ability to hover also exists in rotary-wing aircraft as well as some fixed-wing aircraft. This ability, or at least the ability of very slow flight, is of paramount importance for indoor applications.

More mechanically oriented issues result from the need for control. Rotary wing aircraft require additional rotors for control. Fixed-wing aircraft rely on control surfaces for control. Insects and birds combine control and propulsion in their flapping wing system. Other important factors include the reduced acoustic signature generated by flapping wing flight, as compared to helicopters. Very important is the engineering challenge that lies in the development of a flapping-wing MAV, and all the developments needed in supporting technologies to achieve the goal of lift-off.

## 1.5.2   Why insects?

The most obvious reason to look at insects is their ability to hover. Other animals such as birds and bats are also capable of true hovering flight. The most notable example of a true hovering bird is the Hummingbird. Hovering flight, as performed by hummingbirds and bats, is based on the same aerodynamic mechanisms that larger insects use to achieve hovering flight, see Muijres *et al.* [95] and Warrick *et al.* [131]. Scaling is important, the interesting size range for flapping-wing MAVs lies more towards that of insects than that of birds or bats. The developments in the context of this thesis are of such a scale that they are in the range of small birds and bats. However, in the long run, downsizing is more feasible when the principles by which developments are inspired are more suitable for smaller scales. Insects are therefore chosen of the prime sources of inspiration.

Mechanical in origin and no less important for the development of flapping-wing MAVs, is the system that drives the wings. In insects and birds muscles drive the wings. In insects the whole thorax structure functions as a spring and combined with the wings essentially forms a tuned mass-spring-damper system, see [62, 132]. This is possible due to certain elastic proteins in insects, which are absent in birds and bats, making resonance possible and efficient in insects.

The wings of insects are mechanically seen very interesting structures. Unlike the wings of birds, insect wings are predominantly passive structures. Bird wings can be actively deformed during flight because of muscles and joints present in the wing. These adaptations allow changing wingspan and wing shape during flight. The absence of active elements in the wing makes insects more suitable

for inspiration of flapping-wing MAV wings, due to lower complexity involved. Therefore focus will be on insect wings.

The insects are thoroughly studied by many sciences. Focus here is on the insect flight mechanism and the supporting structures. In nature the basic design for all flying insects is approximately the same. (With the note that two thorax designs exist, see Section 2.2.1.) These two thoraxes differ in the muscle wing coupling system, which can be either direct or indirect. These two thorax designs are the result of evolutionary differentiation and have led to various flight envelopes suitable for different needs, for example, long travel flight or aerial predation.

### 1.5.3  Approach

In the development of micro air vehicles two approaches are common. The first is the top–down approach in which an already flying platform is scaled down to reach smaller and smaller scales. The emphasis in this approach is on the ability to fly. The second approach, adhered to in this project, is the bottom–up approach in which a new concept is designed and developed as a basis for a flying platform. The obvious drawback of this last approach is the unavailability of a flying platform for the development of other disciplines in the Atalanta project such as control methods and sensors technology among others. It may lead, however, to novel applications due to legacy free designs.

## 1.6  Objective

Following the course set by the overall intentions of the Atalanta program and the motivation for the use of flapping wings presented in preceding sections, this section states the objective and scope of the research presented in this thesis.

### 1.6.1  Aim

The aim of this research is the development of a wing actuation mechanism for a flapping-wing MAV. This objective is motivated by the developments needed within the Atalanta project to obtain a flying structure. The wing actuation mechanism should preferably be based on principles extracted from research on insects. The development of the wings is an integral part of the wing actuation mechanism.

### 1.6.2  Scope

The scope of this work is the development of prototypes which show the feasibility of the chosen direction and allow the analysis of the design choices. It is not the

intention to have a fully controllable platform capable of sustained hovering flight and forward flight as is accomplished by, for example, the Delfly [31].

The second limitation is the use of a test bench setup. The prototype will not be able to achieve free flight. The prototype will therefore be fixed to the world by external means of stabilization. While this inherently limits the claims about performance to which can be measured in the test bench it also provides a controlled method for testing performance on specific issues of the design.

Furthermore, for the analysis of the performance of the prototype a set of wings is needed to test lift production. In order to provide an analysis of the flapping-wing MAV the wings are included as an integral part of the design and as such are treated in the development of the flapping mechanism.

## 1.7 Thesis structure and overview

This thesis is built up in four phases: The first phase consist of a review of insects and flapping-wing MAV research. The intention is to gain insight into the workings of hovering insects and a review of current flapping-wing MAV research. The corresponding chapters are Chapter 2 on insects and Chapter 3 on flapping-wing MAVs. The information gathered in these chapters is used to set up the second phase of this thesis: the framework for the analysis and development of the wing actuation mechanism. Conceptual ideas for the development of the wing actuation mechanism are presented in Chapter 4. The results of this chapter are the starting point of a bifurcation in the structure of this thesis. The body and the wings are reviewed and analyzed in two separate chapters, Chapter 5 which covers the wing actuation mechanism and Chapter 6 which covers the development of the wings. The third phase covers the integration of the wing and body as developed in the previous chapters, this is presented in Chapter 7 which also presents the test methods used to evaluate the prototypes. Finally, conclusions, recommendations and outlook are given in Chapter 8. The structure of the thesis is visualized in Figure 1.2.
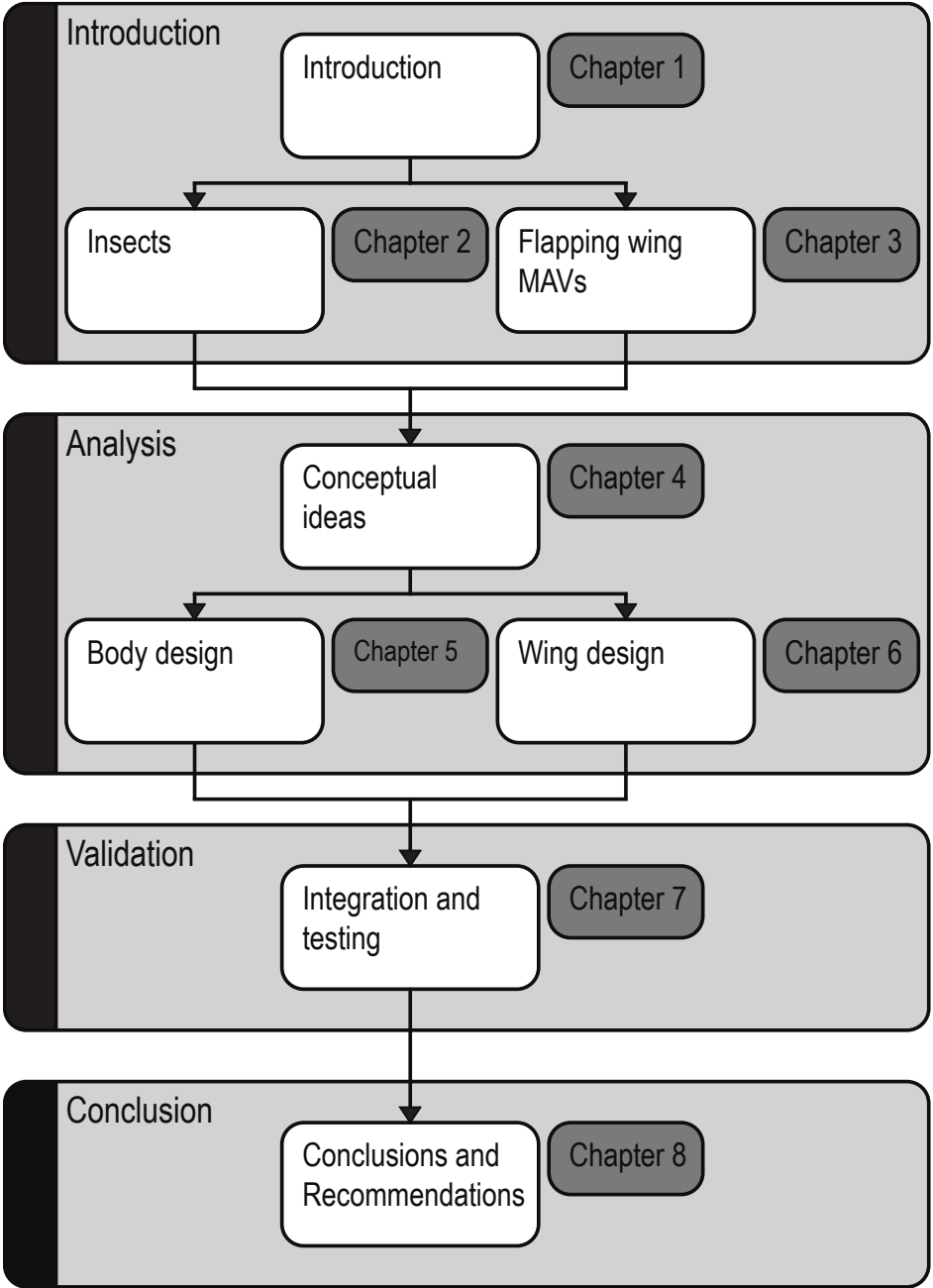
**Figure 1.2:** *Graphical overview of the structure of this thesis.*

# Chapter 2

# Insects

## 2.1 Introduction

As stated in the Chapter 1, flying insects provide the source of inspiration for the development of the flapping-wing MAV in this project. Insects in their many forms are among the most nimble flyers in nature. Their aerial performance will probably not be duplicated in the near future by manmade flying craft. For example the common fly, who is capable of landing upside down or successfully evading a fly swatter. Birds and other flyers in nature are less interesting as a source of inspiration. This aspect is size related. For larger MAVs or flapping-wing MAVs, *i.e.*, larger than 0.15 m wingspan, birds are a great source of inspiration. This can be explained by the higher flying speeds in birds which induces greater lift. For hovering capabilities, flapping wing setups are less suitable at larger scales due to wing root loading. The specific power required flight limits the maximum size at which an animal can sustain hovering flight, see Ellington [48].

When looking at insects as inspiration, it is necessary to place bounds around the area studied. Within the present setting, the mechanical development of the wing actuation mechanism, two aspects are of prime interest. First, the insect thorax, which constitutes the power source and wing driving mechanism. Second ,the wings which are an integral part of the flight mechanism in insects. In essence these structural elements form the chain which conveys the mechanical energy, which is generated in the muscles, via the thorax structures to the wings where eventually lift is produced. The mechanical aspects of insect flight studied in this chapter include the interfaces with bounding realms. Namely, physiology on the one side, in the form of muscles and nerve control and aerodynamics, in the form of fluid–structure interaction, on the other.

This chapter provides an overview of insect physiology, with a focus on the flying apparatus including the insect thorax structure, wing root, the wings and

**Figure 2.1:** *A typical flying insect (order* Diptera*), showing the high-level division of the anatomy into the head, thorax and abdomen. For the developments within this thesis focus is on the thorax as it contains the mechanical aspects of the insect flight apparatus.*

Head    Thorax    Abdomen
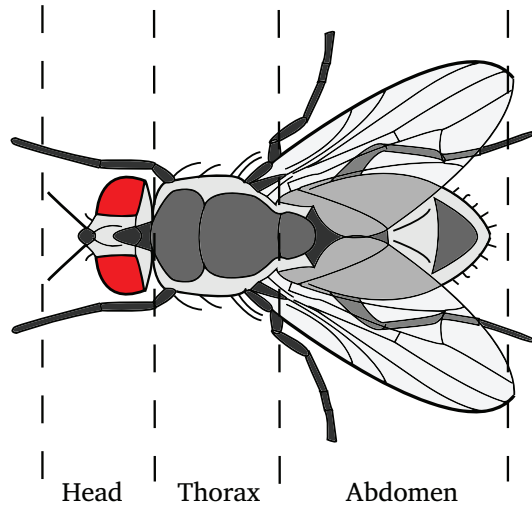
muscles. An analysis of insect wing kinematics follows to identify wing patterns suitable for flapping-wing MAV flight. The mechanical functioning of the thorax-wing system is analyzed in order to extract information on efficiency and resonant behavior. This will eventually provide information on how to extract valuable lessons from nature to develop the wing actuation mechanism for a flapping-wing MAV.

## 2.2   Insect anatomy

A short introduction is given here to the physiology of insects. The intention is to clarify the different parts of the insect that are important for flying. For more extensive views on insect physiology the reader is directed to one of the many textbooks on insect anatomy, see, for example Snodgrass [116], Chapman [26] or Blum [15]. The insect consists of three body parts: the head, thorax and abdomen, indicated in Figure 2.1. The head serves as carrier of the brain and sensors for perception of the larger neighborhood of the insect, for example, vision, olfactory and auditive information. Other sensors include tactile sensors and sensors in the form of hairs all over the body and the wings which are sensitive to air speed and direction for local air velocity information. The function of a gyroscope and feedback of wing movement is done by the halteres in *Dipterans*, see, for example Hengstenberg [66], which will be discussed in Section 2.5.1. The abdomen houses the reproductive organs, breathing apparatus and most of the digestive systems. The thorax is the structure of interest here. It houses the wing actuation mechanism including: drive muscles, control muscles and the wing-root joint which are the attachment points of the wings.

### 2.2.1  Insect thorax structure

The thorax drives the movement of the wings. The wing kinematics are at the basis of efficient lift production. The thorax couples the muscles to the wings in an elastic fashion. From an engineering viewpoint the wing-thorax structure is a compliant amplification mechanism. Two different thorax designs exist which differ in the way the wings are driven: namely, direct and indirect. In the directly driven case, the drive muscles are directly connected to the wing root. In the indirect case the drive muscles are connected to the thorax and the thorax deformation drives the wing via the wing root.

**Direct-drive mechanism**

The direct mechanism is for instance present in Mayflies (order *Ephemeroptera*) with reduced or absent rear wings and the dragonflies and damselflies (order *Odonata*) which are true four-winged insects. Because the muscles drive the wings directly, the left, right and possible fore and hind wings can have different flapping frequencies and amplitudes, allowing a very large range of force production and therefore large aerial agility. All species of *Odonata* are, not surprisingly, aerial predators. A schematic representation of the direct-drive mechanism is given in Figure 2.2. The direct-drive insects generally exhibit lower wing beat frequencies than those with an indirect-drive mechanism, see Brodsky [22].
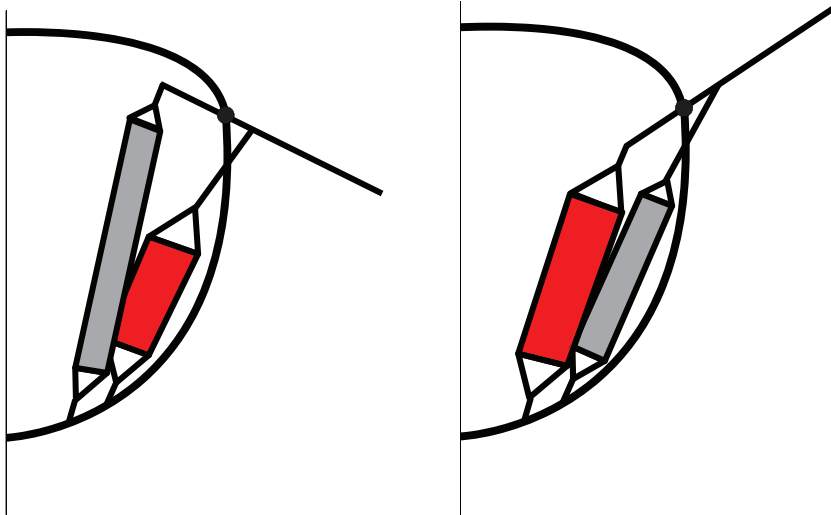


**Figure 2.2:** *Schematic representation of the direct-drive insect thorax. Wing down position shown on the left, wing up position shown on the right. One side of the thorax is shown, direct-drive insects are capable of driving each wing independent. Actuated muscles shown in red.*
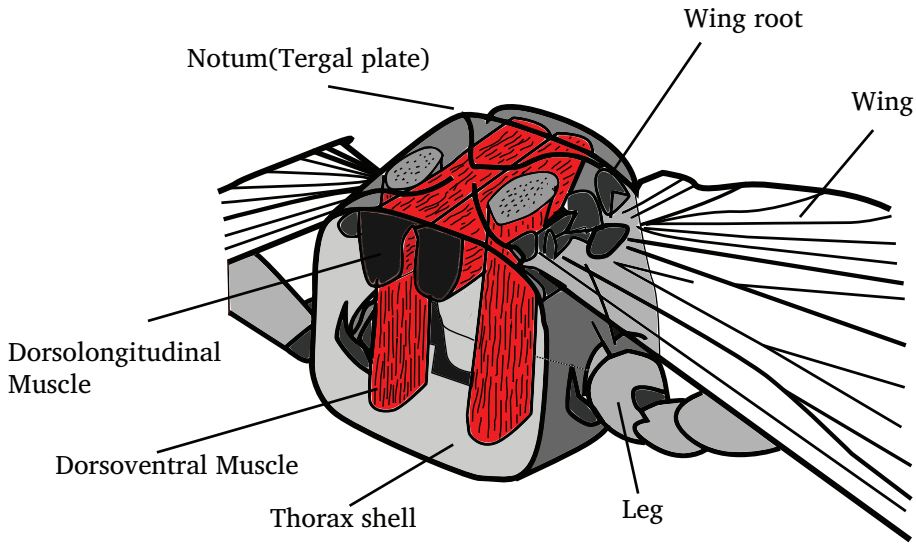
**Figure 2.3:** *The thorax of an insect of the order* Diptera *which has the indirect-drive mechanism. The two orthogonally placed main muscle groups can be clearly seen. Based on Snodgrass [116].*

The stroke amplitude is generally lower than direct-drive insects. Hovering capabilities are present in direct-drive insects. However, larger types cannot sustain hovering due to thermoregulation problems.

**Indirect-drive mechanism**

The indirect-drive mechanism is a defining feature of all members of the infraclass *Neoptera*. Notable members are the true flies (Order *Diptera*), butterflies (Order *Lepidoptera*), bees (Order *Hymenoptera*) and grasshoppers (Order *Orthoptera*). A typical indirect-drive thorax is shown in Figure 2.3 The deformation of the thorax is governed by the two muscle groups. A dorsal group deforms the thorax front to back mainly by bending the dorsal surface of the thorax which is known as the notum, causing a downward movement of the wing. A second group which is attached to the notum pulls the notum down when activated, as a result the wings move upward. The elastic properties of the thorax and muscles combined with the inertial properties of the wings and the thorax box form a tuned mass-spring-damper system. The two extreme positions of this movement can be seen in Figures 2.4 and 2.5. The indirect-drive insects generally exhibit higher wing-beat frequencies when compared to direct-drive frequencies [22]. A large stroke amplitude is usually present in the indirect-drive mechanisms, *e.g.* up to 125°for the Hawkmoth *Manduca Secta* [135]. Many species of insects ex-
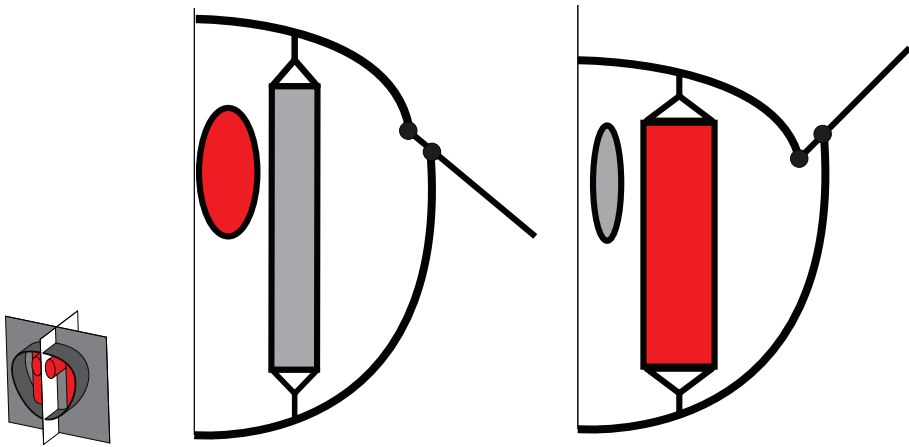
**Figure 2.4:** *Schematic representation of the indirect-drive insect thorax. Wing down position shown on the left, wing up position shown on the right. The orientation of the cut plane through the thorax is indicated by the gray plane on the lower left. Actuated muscles shown in red.*
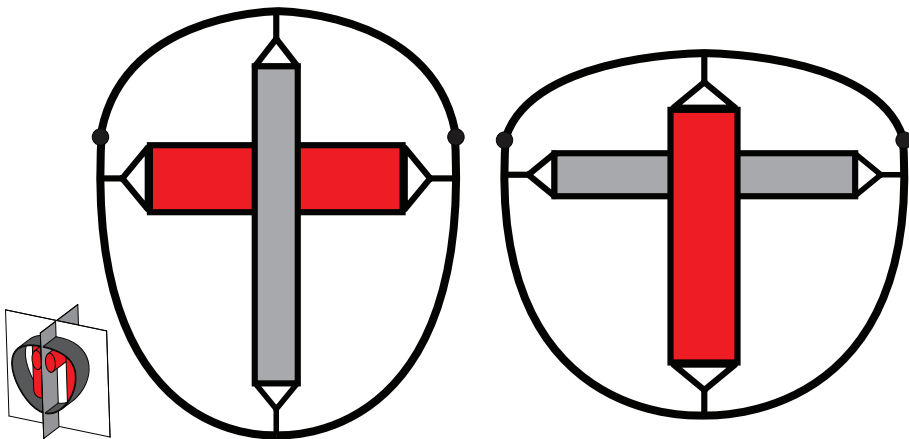


**Figure 2.5:** *Schematic representation of the indirect-drive insect thorax. The two extreme positions are shown. The orientation of the cut plane through the thorax is indicated by the gray plane on the lower left. Actuated muscles shown in red.*

ploiting the indirect-drive mechanism have the possibility to hover for extended periods of time.

The resonant properties which are described for the indirect-drive thorax are most interesting for application in flapping-wing MAVs. They may help to reduce the energy expenditure required for wing movement while also offering large stroke amplitudes through resonant stroke amplification. It is due to this reason that the present focus on the insects is shifted towards the indirect-drive insects.

### The wing root

The wing root, shown in Figure 2.3, is the structure that connects the thorax to the wings. The wing root is a multi-degree-of-freedom joint. The structure consists of a conglomerate of sclerites. These sclerites are connected by ligaments to each other and to the thorax. Control muscles are also attached to the wing root sclerites and by activation of these muscles the joint can be reconfigured on a wingbeat-to-wingbeat basis, see Dickinson and Tu [37]. This reconfiguration of the joint can influence parameters such as joint stiffness, transmission ratio and movement range for control purposes. These control methods do not drastically change the wing kinematics and control forces are mostly generated by influencing the finesses of aerodynamic flight force production. The control muscles are very small compared to the power muscles and therefore do not contribute significant power to the flight motion.

Since the insect wing-root-joint is very complex joints the innervation of the control muscles has been studied extensively, see, for example, Lehmann [80] and Balint and Dickinson [8]. Other studies have covered the wing root joint motions on structural level, see, for example, Miyake [94].

### Muscles

As mentioned in Section 2.2.1 insects which have an indirect-drive thorax, for example members of the orders *Diptera* and *Hymenoptera*, have a distinction between muscles for control and muscles for power generation. Besides obvious differences in size, there exists a more fundamental difference between the two muscle types: synchronous and asynchronous muscle. Both types are innervated by nerves but they differ in their response. Synchronous muscles contract when activated by the nerve, the amount of contraction is guided by the intensity of the signal. This is similar to mammalian muscle. Asynchronous muscles are activated and kept active by the nerve after which their contractions are guided by the strain levels present in, for example, the thorax structure, see Dickinson and Tu [37] and Josepson *et al.* [70]. This means that when the muscle is in use it contracts only when a certain strain level is reached. In an antagonistic setup this will result in a harmonic motion of the driven body part. The setup used in most indirect-drive insects is suitable to exploit the strain actuation in such a way that the two orthogonal muscle groups actuate each other in a cyclic fashion

due to elastic coupling between the muscle groups via the thorax structure, see Figures 2.3, 2.4 and 2.5.

The properties in the insect flight muscles which are of interest for flapping-wing MAV research are the power density, efficiency and strain. The power density is very interesting for comparison against possible actuator technologies which are candidate for the actuation of the flapping-wing MAV. The specific power output of insect muscles varies significantly. Typical numbers are 30–110 $W\,kg^{-1}$[39]. The efficiency of insect muscles is interesting in this setting of designing a flapping-wing MAV. Generally, insect muscles do not show high efficiency. However, excess heat cannot be seen as lost within insects because it adds to heating of the animal which is ectothermal. The analysis of strain in insect muscles showed that the main drive muscles show very small strain, in the order of 2–5% for asynchronous muscle types which is remarkable for muscle tissues. Insect muscle is extremely stiff relatively seen, so that small strains allow for storage of significant amounts of elastic energy, particularly if compared to the maximum kinetic energy of the moving thorax–wing system, see Ellington [47].

### 2.2.2 Wings

To indicate the intricate design of insect wings, an introduction to their anatomy is given here. The wings are, as seen from an engineering viewpoint, a structure which consists of load bearing members (longitudinal veins), crossbeams (cross-veins) and spanning between the veins and cross-veins is a sheet (membrane) as can be seen on a conceptual level in Figure 2.6. On a higher level, insect wings may be seen as flat plates, however, when zooming in the wings show a corrugated structure in chordwise direction, see Rees [107] and Wootton [142]. This corrugation greatly enhances bending stiffness of the wing. While the corrugation enhances the bending stiffness, the torsion stiffness may still be quite low, see Ennos [53], which is useful since passive wing torsion is an effective method to increase angle of attack. In this manner local angle of attack may be better suited to accommodate the increasing airspeed when moving towards the wing tip, similar to the twist present in the blade of a propeller.

Being passive structures, the wings are driven at the base where they connect to the thorax through the wing joint. The wing loading depends on their kinematics as well as their three-dimensional shape, see Daniel and Combes [30]. The deformation of the wing is the result of the inertia and aerodynamic loads. As mechanically and aerodynamically loaded structures, the wings form the coupling between the muscles, which generate mechanical energy, and the aerodynamics, in which energy is dissipated, see Wootton *et al.* [143]. The wings constitute the major part of the effective inertia of the moving thorax-wing system.

Elastic elements, in the form of the protein resilin, are present in many wings at key locations and are used to tailor the deformation patterns in loaded condition, see Haas *et al.* [63]. The deformable nature of insect wings is very intricate because they must conform to many different requirements, *e.g.*, stiffness require-
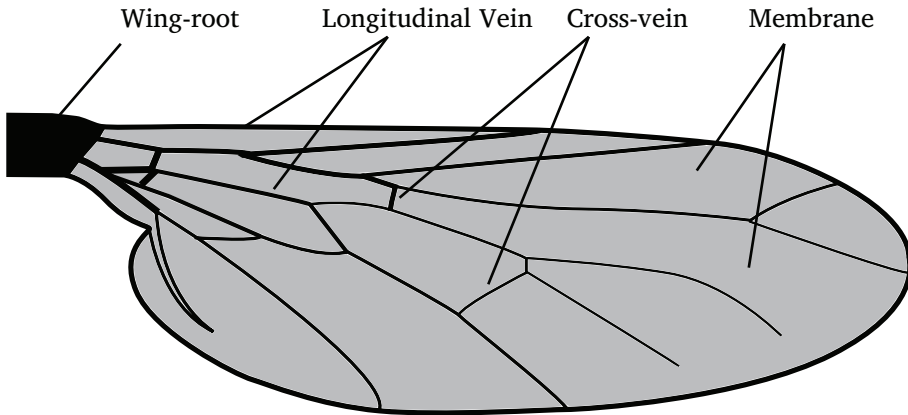
**Figure 2.6:** *Schematic view of an insect wing, Showing basic parts: Longitudinal veins, cross-veins and the membrane. The wing root is indicated and serves as the attachment point to the insect thorax. Based on work by Chapman [26].*

ments, deployability and visual signs for species recognition and genetic fitness for mate selection.

## 2.3   Resonance in insects

The resonant properties that indirect-drive insects exhibit help to reduce the inertial cost of wing movement. In the thorax-wing system the wings form the dominant part of the equivalent inertia. When an elastic element is introduced the muscle forces required to move the wing can, depending on the properties of the system, be reduced significantly. Smaller muscle forces imply smaller muscles and thus lower power usage. The insect thorax-wing system can then be seen as a tuned mass-spring-damper system. The mass is dominated by the inertia of the wings. The spring function is a combination of the elastic thorax shell, and the muscle properties, see Section 2.2.1. The aerodynamic loading on the wings can be seen as the damping force.

The resonant properties of the insect thorax have been subject of investigation for a long time. Greenewalt [62] stated, based on observations, that the wing-beat frequency does not change during varying flight conditions. To achieve resonance, an efficient spring has to be present. In insects the spring function is taken care of by the protein resilin, see Weis-Fogh [132], which shows very low hysteresis and can store energy efficiently. Weis-Fogh [133] showed that most insects have an elastic system to reduce energetic cost of wing movement. He also stated that, although specific proteins for elastic storage are available in birds, they are probably not used due to high damping specifically at flapping frequen-

cies. Dickinson and Lighton [36] show the energetic benefits of elastic storage and that above a certain value no further benefits are expected. This means that, depending on the ratio between inertial and aerodynamic loading on the wing an optimum value for the elastic storage may be found and that above a certain value improved elastic storage methods do not improve the efficiency of the system. Alexander [3] elaborated further on the topic of elastic storage and introduced coupling with muscle mechanics. When looking at flapping-wing MAVs an engineering equivalent has to be found for resilin to serve as the elastic unit when applying resonance in flapping-wing MAVs.

In order to exploit the resonant properties, the wing-beat frequency must be within certain bounds for optimum usage of resonant amplitude amplification. This frequency is determined by the inertia and stiffness properties of the thorax–wing system. The aerodynamic loading, which is dissipative, does not significantly influence the resonant frequency. The origin of this is the ratio between aerodynamic and inertia effects in the thorax-wing system, which can be up to 10, see, for example, Combes and Daniel [28] and Ennos [55]. Ellington [49] calculated the $Q$-factor, defined as the ratio between the total energy in the resonator and the energy dissipated per cycle, for various insects. The factor can in the order of 6.5, 10 and 19 for the fruit fly, hawk moth and bumblebee, respectively. Ellington remarked that these values are impressive for biological structures and that they indicate that the resonant response of these structures will, when driven outside the natural frequency, very rapidly fall effectively reducing the wing sweeping amplitude.

The presence of resonance in insects in the wing–thorax system has implications for the obtainable wing kinematics. The main flapping motion will be harmonic. Besides this, the aforementioned frequency band of the system is very small. Assuming that the steady-state motion of the insect corresponds to hovering or forward flight, the control moments needed for stability or direction control have to be the results from changes in kinematics by means of reconfiguring the wing root as described in Section 2.2.1. These changes will be restricted to variations of the harmonic motion. The description of kinematics of the insect will be presented in the following section.

## 2.4   Kinematics

Kinematics cannot be seen separate from the aerodynamics of the wing. The fluid–structure coupling between the wing and the air and the subtleties in insect wing aerodynamic load generation make insect flight possible. The approach followed here is that the analysis of the structure or insect is studied from a mechanical perspective. Therefore wing kinematics are treated before aerodynamics.

The insect wing movement can be split in two separate parts: a rigid body motion and an elastic deformation. The rigid body motion consists of three rotations facilitated by the wing-root joint. The elastic deformation consists mostly of

torsional deformation and bending, however the magnitude of the elastic deformation is small compared to the rigid body movement. In smaller insects elastic deformation is increasingly smaller due to increased relative stiffness by scaling effects. For small insects, this leads to the conclusion that the wing movement can be accurately described on a global level by only rigid body rotations. Therefore, the rigid body rotations will be described first and the bending and torsion in Section 2.4.2

### 2.4.1    Rigid body description

As mentioned in Section 2.4 the insect wing movement can be described by three angles. The main flapping or sweeping motion, which is the most characteristic
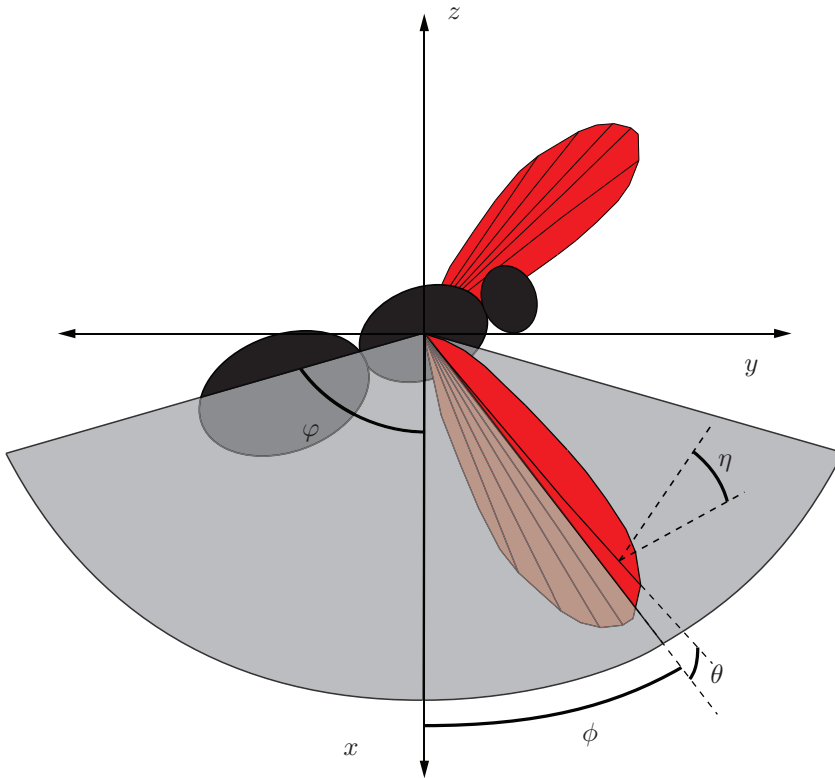
**Figure 2.7:** *The wing as a rigid body defined by three angles. The main sweeping angle is given by $\phi$, the wing pitching motion is described by $\eta$ and the out of plane motion is defined by angle $\theta$. The partial circle swept by the wing is bounded by the maximum sweeping angle of the wing, indicated by $\varphi$.*

motion of the wing, makes the wing trace a plane which is approximately horizontal for most hovering insects. The main flapping motion is the result of the resonant motion and as such is described by a harmonic motion.

The main flapping motion is indicated by $\phi$ in Figure 2.7. The stroke plane swept by this motion generally has a constant angle with the insect body, see Żbikowski [147]. The area swept by the wing is indicated by the circle segment in Figure 2.7 and is bounded by the maximum wing sweeping angle $\varphi$. The second motion, the wing rotation or wing pitching, is defined as the rotation of the wing about its radial axis. The pitching angle is defined in Figure 2.7 by the angle $\eta$. This motion, together with direction induced flow, defines the angle of attack of the wing. The wing pitching is generally a motion close a pure sinus. The frequency of the pitching motion is always the same as the main flapping motion. Generally, a phase shift exists between the two. A defining characteristic of the wing pitching motion is that the phase shift with respect to the sweeping motion is such that the same wing edge always remains the leading edge. The last motion is the out of plane motion or heaving motion which describes the deviations from the stroke plane, defined by the angle $\theta$ in Figure 2.7.

A typical wing stroke cycle can be roughly divided in four phases. The first are the up and downstroke. In these phases the wing moves with respect to the body with approximately constant wing rotation. The remaining two phases are the two stroke reversals, called supination after the downstroke and pronation after the upstroke. The wings rotate around an axis typically located 25–50% from the wings leading edge. These rotational phases typically last 10–20% of the total stroke cycle time, see Ellington [44].

Since it is difficult to visualize the wing motion in three dimensions, a two dimensional representation will be used here. This representation is constructed by using a two-dimensional projection of the movement of the wing chord located at the center of pressure of a typical insect wing, see Birch and Dickinson [14]. A typical symmetric movement of the chordwise slice of wing is shown in Figure 2.8, in which the phase delay between sweeping and pitching can be clearly seen. Note that no heaving motion is present. In most insects there is heaving, if heaving is present the wing tips describe a trajectory that is out of the main flapping plane and has the shape of a banana or figure eight, see Ellington [42] as is shown in Figures 2.9 and 2.10.

The description presented here is simplified. The purpose is to inform the reader of the general characteristics of insect-wing kinematics. This description is by no means exhaustive and covers only the flight mode of the wings. It is known that insect wings are folded when in the chrysalis stage and that most insects are able to fold their wing backwards and park them along their abdomen. These motions are not reviewed here and focus is on the sweeping, pitching and heaving motion. An extensive description of insect wing kinematics can be found in Dudley [39].

**Figure 2.8:** *Typical movement of a chordwise slice of insect-wing. Note the large amplitude of the wing pitching and absence of the feathering motion. The upstroke and downstroke are plotted vertically separated to avoid unclarity due to overlay. Upstroke indicated in blue, downstroke in red and leading edge by a circle.*
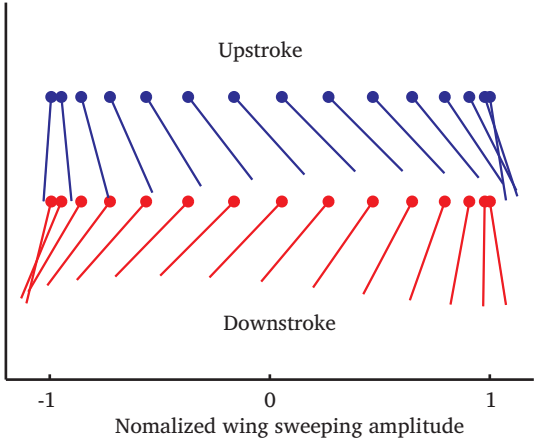


**Figure 2.9:** *Addition of a simple heaving motion which results in a banana-type motion of the leading edge, present in the Hawkmoths, for example. Upstroke indicated in blue, downstroke in red and leading edge by a circle.*
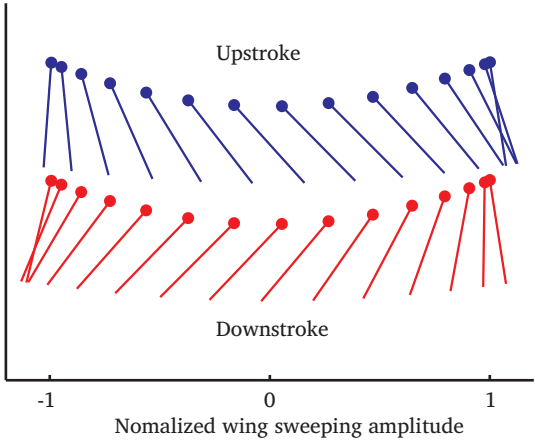


**Figure 2.10:** *Figure-of-eight wing tip motion present in some insects. Upstroke indicated in blue, downstroke in red and leading edge by a circle.*
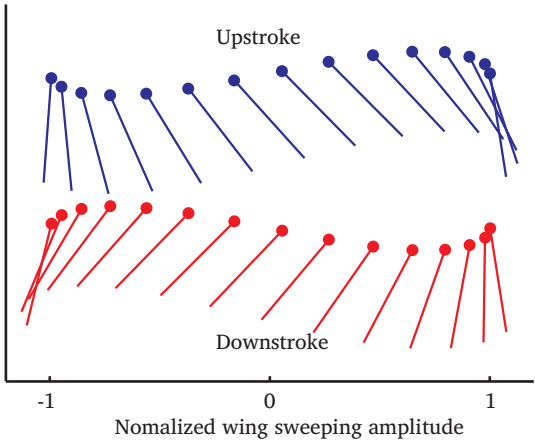
**Passive pitching**

As described, the origin of wing sweeping motion can be found in the resonant state of the thorax–wing system. The origin of wing pitching has been the subject of argument among biologists; is the pitching motion passive or active? Analysis of the insect thorax suggests that the control muscles are too small to generate the required power for wing pitching. However, pitching could be the result of a smart wing-root hinge configuration. The second option is passive pitching controlled by inertial and aerodynamic loads. Norberg [97] found that the mass distribution in Dragonfly wings generates a wing pitching moment during the acceleration phases of the wing sweeping motion. Ennos [52] found that the torsional compliance of the wing root joint is high. This low compliance combined with pitching moments generated by stroke reversal allows the wings to pitch passively, see Ennos [54, 55]. Bergou *et al.* [11] reviewed the energy balance of the wing motion and concluded that there is sufficient energy available for passive wing pitching indicating that control muscles do not need to do any work for wing pitching. The general consensus among biologists and engineers is that during steady-state flying or hovering wing pitching is passive. However, when the insect performs extreme maneuvers indications are that the reconfiguration of the wing joint is such that wing pitching is at least partially actively controlled.

## 2.4.2   Bending and torsion

The rigid body description as presented in the previous section provides an explanation of the major part of insect wing movement. Bending and torsion, however, do play a role in the insect wing kinematics. However, for the majority of applications within the current work the current rigid body description suffices. For both the aerodynamic description and kinematic description of the insect-wing.

In Section 2.2.2 a description of insect wing anatomy is given. The application of loads on the wings, both inertial an aerodynamic, results in wing deformation during the flapping motion. The shape of the wing can have significant influence on the production of aerodynamic loads as is shown by Daniel and Combes [30]. Combes and Daniel [28] show that bending is present in flapping insect-wings and mostly the result of inertial loading.

While bending is present in insect-wings, the aspect of torsion is more important. Torsion and more specifically the timing of torsion deformation during the wing stroke can directly influence the local wing pitching angle and, consequently, the local angle of attack. Ennos [53] discusses the magnitude of wing torsion and proposes structural explanations for the tailored torsional compliance in insect wings. Bergou *et al.* [11] show that the loading on Dragonfly wings during flapping is such that a torsional wave is introduced which induces increasing torsion from wing-base to wing-tip and thereby better adjust the local angle of attack. The angle of attack is more optimal due to increased structural velocities at the wing tip, as is the case in, for example, windmills for electricity production.

As mentioned earlier in this work, scaling effects effectively reduce the effects of bending and torsion when moving to smaller scales.

## 2.5   Aerodynamics

This section gives an introduction to the aerodynamics of flapping wing flight. Flapping flight by insects is characterized by unsteady incompressible flow at intermediate Reynolds ($Re$) numbers. The $Re$ number range within which flying insects have been studied is large. To quantify this: for large insects the $Re$ lies between 5000 and 10000. The smallest flying insects have $Re$ numbers which can go as low as 10, see Ellington [49]. At the small scales the viscous forces become more pronounced and as such extremely small insects appear to paddle more than fly. The range is large due to the large variance in the body mass of flying insects, which ranges from 20–30 $\mu$g to 2–3 g.

In order to generate enough lift for flapping-wing MAV flight a comprehensive understanding of aerodynamics concerning flapping flight is paramount. The production of lift and thrust follows from the complex interaction between the compliant wings, wing kinematics and the aerodynamics. This system is a complex example of fluid–structure interaction. There are serious challenges in unraveling the underlying principles of insect flight. Aerodynamic theory is well developed for larger scales and can be applied at insect scale with the incorporation of effects that are present at these smaller scales and, consequently, lower velocities. The flapping wing induces unsteady flow with a cyclic nature.

The production of lift and drag in insects is based on three mechanisms:

**The Leading Edge Vortex**  The Leading Edge Vortex (LEV) is the most important aerodynamic effect in insect flight, a typical LEV can be seen in Figure 2.11. Due to this LEV the flapping insect wing produces far more lift than can be explained using normal airfoil theory. Experiments, both numerical and experimental showed that when a wing moves through air, a large vortex starts at the leading edge of the wing and forms on top of the wing. The rotation in this vortex is very high. The associated high velocity creates a patch of low pressure on the wing surface facilitating lift production. This vortex grows in size during wing flap and after some chord lengths releases from the wing and removing the low pressure field and thus lift. Ellington *et al.* [51] showed that the leading edge vortex is stable in insect flight. This is due to span wise flow which takes energy out of the vortex, thus, controlling its growth and delaying stall. Usherwood and Ellington [124] showed that the LEV is a stable phenomenon for a large range of flying insects.

**Rotational circulation**  Dickinson *et al.* [35], found a force pattern that could not be explained even when the LEV was taken into account. They suggested that the rotation and especially the rotational speed of the wing contributed
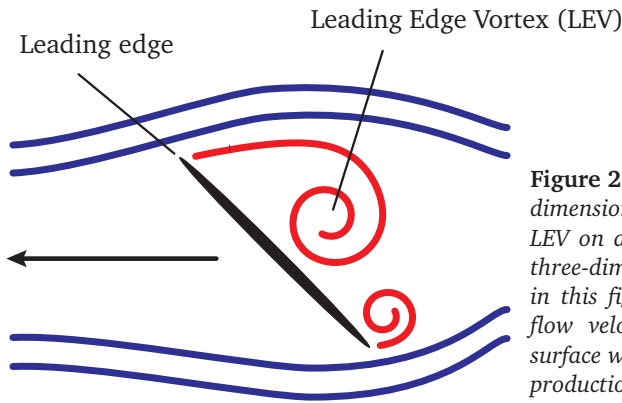
**Figure 2.11:** *Schematic two-dimensional representation of a LEV on a translating wing. Stabilizing three-dimensional effects cannot be seen in this figure. The LEV increases local flow velocities over the trailing wing surface which leads to an increase in lift production.*

to extra lift. Later experiments, experimental and numerical, see Fry *et al.* [58] and Ramamurti and Sandberg [105], showed that this rotational aerodynamics have significant influence on force production by flapping wings in insects. The rotational circulation effect is only present during phases where the rotational or pitching velocities are large, that is, during stroke reversal. Thus, by varying the wing rotation timing and rotation speed, causing advancements or delays in the wing kinematic pattern, the wing forces can be varied. The force will increase when the rotation is advanced and decreased when the rotation is delayed. It was shown that changes in rotation timing come with an increase in power usage, suggesting that these measures are only used for control purposes. This agrees with the observations made by Ramamurti and Sandberg [105].

**Wake capture** Wake capture is the effect where flapping wings interact with the vortex that was shed at the end of the previous stroke. This creates large load peaks at the beginning of the new stroke. This increase in lift is caused by the increase in fluid flow by the capture of the previous vortex, this was the explanation by Dickinson *et al.* [35]. The wake capture effect is most pronounced during stroke reversal and not during the period of relatively low pitching velocities during mid stroke. Another group suggested that the force peaks can be accounted for by the very high acceleration in this phase of the wing stroke, see Sun and Tang [120].

Two other effects are present in insects but are not directly responsible for lift production. The first is the effect known as added mass or virtual mass. The virtual mass can be seen as a region of influence where the air around the wing moves with the wing and thereby contributes to the effective inertia of the wing. The added mass can be of the same order of magnitude as the mass of the wing itself. These properties are very important when constructing quasi steady state models of the wing aerodynamics. Estimates for added mass can be found in Sane and Dickinson [109], Dudley [39] and Ellington [43].

Another effect present in insect flight is a very specialistic effect known as: clap and fling. This effect was first described by Weis-Fogh [134]. The effect consists of expanding the wing sweeping angle so far that the wings touch at the end of the upstroke above the body of the insect. When that downstroke starts the wings are rolled open in order to jump start the LEV. Since the formation of the LEV is independent of wing size, jump starting might be beneficial for very small insects which have a very small wing stroke in absolute sense. Questions still exist if this property has been properly interpreted. Sane [108] suggests that the wing touching is to maximize the wing sweeping stroke.

There exist great differences in the flight mechanisms of insects. For example, two or four wings, ability to hover, flight for predation or transportation. Recent investigations into the current state of understanding of insect flight have been presented by Sane [108] in 2003. Of prime interest for the understanding of insect flight is the modeling of the aerodynamics. The aerodynamic modeling of insects is supported by both experiments and simulations, which are both important to complete the understanding. In order to understand control strategies and maneuvers of insects, simple models may prove invaluable. Sane and Dickinson [109] cover a subject treated by many researchers, namely the existence and validation of a quasi-steady aerodynamic model for insect flight as proposed by Ellington in 1984 [42]. More work based on experimental studies on insects in both free and tethered flight has been performed by Usherwood and Ellington [124] on Hawkmoth wings. Later, Usherwood and Ellington [125] worked on a variety of wings actuated in a rotational fashion. Dragonfly flight has also been extensively studied, especially on the subjects of: power usage, wing kinematics and steady-state loads, see Wakeling and Ellington [128, 129, 130]. The current qualitative review of insect aerodynamics covers only a small subset of available research on insect aerodynamics. The mentioned subjects, experiments and simulation, are extensively covered for a large range of insects by both biologists and engineers alike. A very extensive overview of the field of insect aerodynamical modeling is not intended here and can be found in, for example, Ansari *et al.* [6].

### 2.5.1   Control

The subject of control in insects is very interesting. The aerodynamic features displayed by even the tiniest insect are remarkable. As demonstrated by the previous sections, the aerodynamics of insect flapping wings are far from trivial. Due to the unsteady effects in the aerodynamics even very small changes in wing kinematics may induce large changes in aerodynamic load production. In order to control the aerodynamics, insects make adjustments to the kinematics of the wings. In order to accomplish this, insects may control the power muscles, control muscles, wing root joint, wings, kinematics and aerodynamics. Four-winged insects introduce more challenges from a control standpoint due to wing-wing interaction. For two winged insects the possibilities for control are the increase in stroke amplitude, changes in stroke plane and changes in wing rotation timing.

Fry *et al.* [58] showed for the common fruit fly what is needed to make a 90° turn. It turned out that the control measures taken by the fly are very subtle changes in kinematics. Lehmann [80] provided an extensive overview on the control of flight forces in flying insects. Insects manipulate the LEV, rotational circulation and wake capture by very small perturbations in the wing kinematics. Since insects are very small, the scaling of inertia properties is in their favor with respect to making them agile.

## 2.6    Concluding remarks

The lessons which can be learned from insects can be used as a major source of inspiration for the development of effective flapping-wing MAVs designs. For this conclusion the source of inspiration is split into three subjects: the body or thorax of the flapping-wing MAV, the wing transmission system and the wings.

The thorax of the flapping-wing MAV can make use of the resonant principles which are present in insects. The goal is, as it is in insects, the reduction of energetic impact of wing movement. Besides this reduction, the resonant amplification of the wing sweeping motion can be used to obtain a large wing sweeping stroke. When this principle is used, care has to be taken that besides the obvious benefits, the same drawbacks are also introduced. The wing sweeping frequency becomes bounded by high sensitivity to changes in drive frequency. In order to realize this mechanical equivalent, an elastic element has to be used to store the kinetic energy. In insects a large part of the thorax structure participates in the resonant thorax–wing system. A mechanical equivalent should strive for the same, namely, a very high degree of integration.

The wings need to be driven by the thorax. In the insect thorax and, consequently, also a resonance based flapping-wing MAV thorax, the thorax deformation has to be transformed and amplified into a large sweeping motion at the wing base. In insects this property is integrated into the thorax-wing-root combination. The insect thorax and wing root together form a fully compliant system capable of generating complex kinematics. The compliant nature of this structure allows for low losses due to the absence of friction. While the most obvious motion in insect-wings is the sweeping motion, wing pitching also finds its origin in the wing-root. To accomplish the same features in a flapping-wing MAV thorax would be amendable but requires very high degree of integration. The challenges lie in the objective to integrate a compliant amplification mechanism with a passive wing pitching mechanism in an integrated fashion.

The wing is the place where the lift is produced. It will pose a significant challenge to design a mechanical equivalent of the insect wing. The subtleties in the tuned compliance, in both the wing-root and wing itself, of the insect wing are impressive. The lesson that should be learned from aerodynamics in flapping insects is that the wing pitching kinematics may be of passive origin, thereby reducing the need for a complex pitching mechanism. In the ideal case the correct

timing and amplitude of wing pitching will have to be obtained by a combination of a highly compliant wing root with a wing which is able to support a beneficial torsional wave to augment lift production. In this sense the system has to be designed in a highly integrated fashion, combining wing and wing root. The complex veined and corrugated structure of insect wings allow for a large degree of tuning of the compliance.

Lessons can be learned from why insects are such successful flyers. The engineer has to learn as much as possible from nature in order to make a successful attempt at producing a flapping-wing MAV. Direct copy of insect design is, however, not feasible due to the building blocks available to the engineer. Summarizing the above leads the engineer to be bio-inspired but not focused on biomimetic designs, as is also noted by Michelson and Naqvi [92].

# Chapter 3

# Flapping Wing MAVs

## 3.1 Introduction

The development of flapping-wing MAVs in general is based on either bird or insect flight. Several projects exist which are inspired by the aforementioned flight in nature. Historically, flapping-wing MAVs have been based on bird-like flight focusing on forward flight. Recently, interest has shifted towards miniaturization and thus, inspiration can then be found in small birds and insects. Especially hovering and slow moving flight is of interest for possible indoor usage of the flapping-wing MAV. Developments in actuator and battery technology have also widened the scope to smaller flapping-wing MAVs. Also recent advances in the understanding of aerodynamic principles of flapping wing flight have spurred renewed interest in flapping-wing MAVs.

In order to create an overview of the field of current projects and developments, an analysis of the currently running and past projects is given in this chapter. The intention of this overview is twofold, first to see what is being done in the field and, secondly, to extract ideas and good practice similar to the analysis of insects. The second part of this chapter is to set up a framework in which lessons and inspiration from insects and the various flapping-wing MAV projects are reviewed. The developments and lessons from this chapter and Chapter 2 will be used to design the actuation mechanism on a conceptual level in Chapter 4.

The review of the field is done in a structure similar to the analysis of the insect flight apparatus in Chapter 2. Thus, first an overview is given of the different projects, and how they achieve wing actuation. Subsequently, different aspects of the flapping-wing MAV implementations are reviewed, such as: actuation technology, wing technology, manufacturing techniques and control possibilities.

## 3.2   Projects

From a mechanical point of view, the wing actuation mechanism is the key component in the flapping-wing MAV. Consequently, there has been a large amount of research into the understanding and the functioning, on a biological level, and analysis and design on an engineering implementation level. Different levels can be identified at which research is aimed; for example, showcasing actuator technologies, exploring possibilities of wing kinematics and developing airframes amongst others. In this sense the projects described show a differentiation in their intentions and are treated here as such.

### 3.2.1   Overview of projects

In this section an overview is presented of projects performed around the world, in academia and private research groups, to develop a flapping-wing MAV. A selection has been made on the intention of the project. Either the development of a mechanism to drive wings in a kinematically correct manner or the intention to achieve lift-off. Projects are included that provide either a prototype of lesser or similar dimensions, as intended in this project, or an interesting mechanism.

### 3.2.2   The Lipca powered flapping-wing MAV

The developments within the Lipca powered flapping-wing MAV project [13] aim at two aspects. First, the application of smart actuator technology, see, for example Yoon *et al.* [146] and Lee *et al.* [79] and, second, the development of a wing actuation mechanism based on the new actuator technology. The actuator is a lightweight composite actuator based on a PZT piezoelectric ceramic as the active material, developed by the same group. This actuator, *i.e.* a designated lightweight piezo-composite curved actuator (LIPCA), uses lightweight materials



**Figure 3.1:** *Piezo powered (LIPCA actuator) flapping-wing MAV by Syaifuddin* et al. *[121]. Mechanical amplification by means of a four-bar linkage. Passive wing pitching by freely pitching augmented by rigid pitch limiters. Picture by Nguyen* et al. *[96]. Copyright: SAGE Publications, reprinted with permission.*
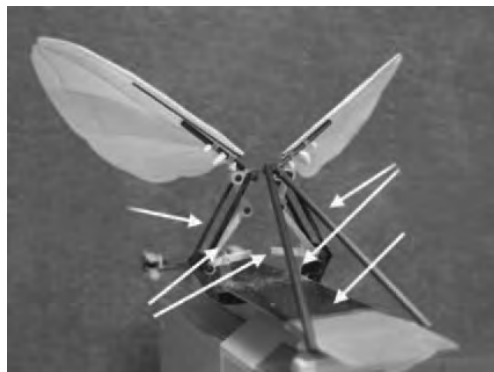
to make a bimorph setup to create large deflections needed for efficient usage in a flapping-wing MAV.

The second aspect is the development of a wing actuation mechanism for a forward flying MAV, see Syaifuddin *et al.* [121] and Nguyen *et al.* [96]. The mechanism is based on a four-bar linkage which is used to transform and amplify the linear deflection of the LIPCA actuator to drive the sweeping motion of the wing. The wing pitching degree-of-freedom uses mechanical limiters to limit the movement range, pitching moments are generated by inertial and aerodynamic loads during stroke reversal. The current setup exploits resonance to amplify motion. The LIPCA actuator doubles as the elastic storage element. The mechanism is shown in Figure 3.1.

### 3.2.3   The MFI project

The Berkeley Micromechanical Flying Insect (MFI) project, aims at the development of a 0.1 g, 25 mm wingspan flapping-wing MAV. The project started in 1998. In 2003 a lift force of 500 $\mu$N has been produced by a single wing on a test stand. Since 2003, work has been centered on reducing weight, increasing actuator power density, increasing air frame strength, and improving wing control of a real prototype, see Wood *et al.* [139, 140]. The MFI is shown in Figure 3.2.

The wing actuation mechanism is based on two parallel four-bar mechanisms. The two four-bar mechanisms are used to control wing base rotation and function as mechanical amplifiers for the small movement range exhibited by the piezo actuators used for actuation. Using the two compliant parallel mechanisms, the wing pitching can be controlled actively by the phase difference in rotation between the two. The piezo bimorph can also be integrated as part of the four bar mechanism, as is done in the realization of the prototype in Deng *et al.* [34]. The mechanisms exploits resonance by using the piezo actuators as the elastic storage element and to a lesser extent also the compliant links.



**Figure 3.2:** *The Berkeley MFI, a piezo actuator powered flapping-wing MAV. The MFI is based on two parallel four-bar mechanisms which provide the capability to actively control wing pitching movement. Image from [91]. Copyright: The Biomimetic Millisystems Lab, UC Berkeley, United States, reprinted with permission.*

**Figure 3.3:** *The Harvard fly [138], a piezo actuator powered flapping-wing MAV. The Harvard fly is based on a four-bar mechanism to transform and amplify the piezo actuator deflection into a large wing sweeping movement. Wing pitching is accomplished by passive means . This is currently the smallest flapping-wing MAV capable of achieving tethered lift-off. Note the dimensions with reference to the hand. Image by Wood from [138]. Copyright: IEEE Publications, reprinted with permission.*
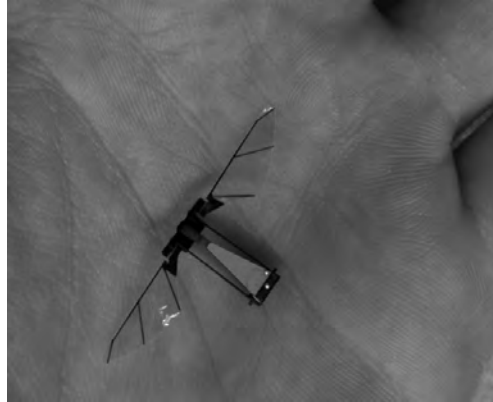


### 3.2.4   The Harvard fly

The Harvard fly [65] aims at the development of insect-scale flapping-wing MAVs. This project uses the manufacturing techniques and actuator technology as developed within the MFI project, see Section 3.2.3. The structure is based on a compliant mechanism which amplifies actuator movement and transforms it to the large rotations needed at the wing base. The structure is very small and light: 30 mm wing span and 60 $\mu g$.

The actuator is a PZT bimorph actuator with high specific energy density, see Wood *et al.* [141]. The mechanism is essentially a one degree-of-freedom system, based on a four-bar linkage. The wing pitching motion is passive in origin and provided by a wing pitching hinge with has tuned stiffness. The maximum pitching deflection is limited by end stops. The mechanism functions as a tuned resonator in order to minimize energy expenditure, see Wood [137]. The mechanism is capable of producing enough lift to propel itself upward along guide wires [138], it is the first linear actuator based mechanism capable of doing so. The realized structure is shown in Figure 3.3.

### 3.2.5   Clapping wing MAV of insect size

The clapping wing MAV project [73] aims at the development of a flapping-wing MAV based on a four-winged setup. The design uses an DC-motor which drives a reduction gearbox which in turn drives the wings which are placed in a cross-type setup, see Kawamura *et al.* [72]. The last step in the wing actuation is a linkage based four-bar mechanism. The wing setup is very similar to the precursors of the Delfly [32]. The prototype is capable of free flight using a tail with control surfaces. The wingspan of this prototype is 100 mmwith a corresponding mass of 2.3 g. The wings employ the clap and fling mechanism as described by Weis-Fogh [134] to jump start the leading edge vortex for efficient lift production. The prototype can be seen in Figure 3.4.
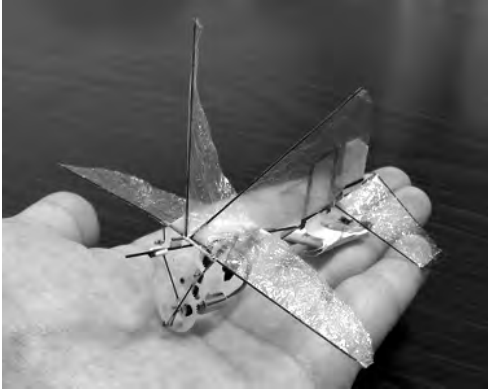
**Figure 3.4:** *Flapping wing prototype by Kawamura et al. [72] capable of controlled free flight. The wings are driven by a DC-motor via a gearbox and a four-bar linkage system. The four-winged prototype exploits the clap and fling mechanism described by Weis-Fogh [134]. Image by Kawamura et al. from [72]. Copyright: Springer Science and Business Media, reprinted with permission.*

### 3.2.6 Caltech Microbat

The Caltech microbat [74] is a MAV presented and developed before the year 2000 and refined since. The Microbat is a two-winged flapping-wing MAV. Its wing kinematics are more bird-like than insect-like and are aimed at forward flight. It has successfully flown. The wings are actuated by an DC-motor and a gear box driving a four-bar mechanism. In the current prototype there is no control over wing pitching and local angle of attack is due to wing membrane deformation. There are options for control over the wing bending pattern by the design of the wings which are based on titanium MEMS technology, see Pornsin-Sirirak *et al.* [104]. The Microbat is shown in Figure 3.5. Control is accomplished by means of a tail section with control surfaces. The mechanism does currently not offer possibilities for exploiting resonance.

### 3.2.7 Vanderbilt University

The Vanderbilt flapping-wing MAV is based on a resonating system excited by one or multiple piezo actuators, see Cox *et al.* [29]. The piezo actuators are coupled to the wings by means of a compliant four-bar or five-bar mechanism. There is control over the amplitude of the wing flap for both the left and right wing. This



**Figure 3.5:** *The Caltech Microbat [74], a flapping-wing MAV capable of free flight driven by a DC-motor. Image by M. T. Keennon from [74]. Copyright: M. T. Keennon, AeroVironment Inc, Monrovia, CA, United States, reprinted with permission.*

**Figure 3.6:** *The Vanderbilt flapping-wing MAV [29], resonance is exploited in such a way that the drive frequency can be used for control purposes. This is done by introducing a difference between the resonance frequency for the left and the right wing. Image by Cox* et al. *from [29]. Copyright: SAGE Publications, reprinted with permission.*
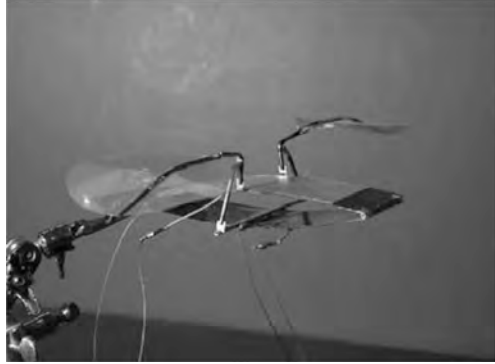
is accomplished by designing the structure such that the left and right wing have slightly different resonant frequencies, a change in drive frequency will therefore result in a different response amplitude for the left and right wing. A drawback will be the non-optimal amplification factor during symmetric flapping. Aerodynamically efficient wings are implemented and tuned to allow passive wing rotation. The prototype is depicted in Figure 3.6. There are no flying prototypes due to two reasons: The fact that the wing technology was suboptimal and the piezo actuator used was unable to convey sufficient energy into the structure for creating a large wing sweeping motion.

### 3.2.8   Georgia Tech Entomopter

The Entomopter project, see Michelson and Reece [93], is based on a chemical muscle which produces linear actuation strain. The mechanism between wing-base and actuator is not disclosed. The wing configuration is a four-winged setup. The wings are placed in two sets of rigid wings at the front and back of the flapping-wing MAV. The wings are actuated by a torsion mode induced in the body by the chemical muscle. Current prototypes of the chemical muscle are slow and heavy but future incarnations may exhibit large possibilities due to the inherent high energy density in chemical fuels.

### 3.2.9   Delfly Micro

The Delfly project [32] within the Delft University of Technology aims at the realization of free flying flapping-wing MAVs. The Delfly Micro is the result of two miniaturization steps of a single design. Two previous versions, namely the Delfly I and Delfly II [32], have successfully preformed controlled flight and inspired the creation of the Delfly Micro.

The Delfly Micro has 100 mm wingspan and 3 g vehicle mass. The Delfly Micro is currently the only flapping-wing MAV of this size and mass which has a
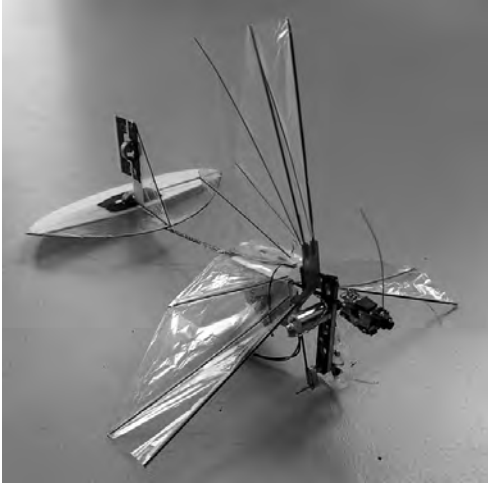
**Figure 3.7:** *The Delfly Micro [32]: a 100 mm wingspan four-winged flapping-wing MAV capable of controlled free flight. Notable is that it is capable to carry functional payload in the form of a camera. Photo courtesy of B. Remes. Copyright: Delfly.nl, reprinted with permission.*

video camera and is fully controllable by radio. The power is generated by a DC-motor while the control is accomplished via a tail section. Very small brushless motors are under development. The electric motor drives the four wings via a gear reduction and a linkage system. The system does not function as a resonator. The setup is capable to provide a clap and fling motion on one side of the stroke as described by Weis-Fogh [134] for very small insects. Wing pitching is obtained by tailored stiffness of spar reinforced membrane wings. The Delfly is depicted in Figure 3.7. The Delfly micro is like its predecessors capable of slow moving and near hovering flight.

### 3.2.10   FW-MAV

The flapping-wing MAV project in the group of Agrawal at Delaware University focuses on the creation of a flapping-wing MAV powered by an DC-motor [89]. The intention of the project is to develop a hovering flapping-wing MAV. The current project includes mechanisms for correct reproduction of insect wing kinematics in the form of precursors, see Banala and Agrawal [9] and parallel development in the form of more advanced mechanisms, see McIntosh *et al.* [87]. The center of the development is the flapping-wing MAV described in Khan and Agrawal [75, 76]. The mechanism is based on gears and links to accomplish the main wing sweeping motion. In order to exploit resonance, to reduce of the energetic cost of wing movement, springs are added to the mechanism. The springs are tuned to provide optimal reduction of energy usage of the mechanism while flapping at the intended frequency is performed. This addition of springs to a non-compliant linkage system to exploit resonance is a very interesting concept. Another very interesting property of the system is the incorporation of a tuned passive wing-pitching system.
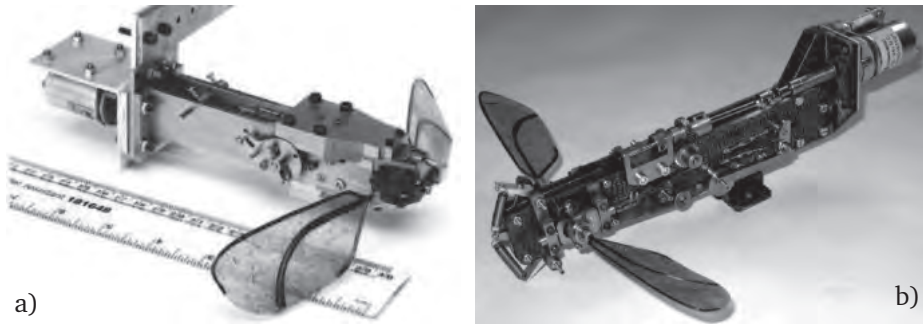
**Figure 3.8:** *The mechanisms proposed and realized by Galinski and Żbikowski in order to accurately reproduce insect wing kinematics: a) The Geneva wheel based mechanism. [60]. Image by Galinski and Żbikowski from [60]. Copyright: Elsevier Ltd., reprinted with permission. b) The mechanism based on a double spherical scotch yoke [59]. Note that these mechanisms are able to reproduce insect-wing kinematics although only a single actuator is used. Image by Galinski and Żbikowski from [59]. Copyright: The Royal Society publishing, reprinted with permission.*

### 3.2.11   Projects for reproducing kinematics

There exists a large interest in the development of flapping wing mechanisms to accurately reproduce insect-wing kinematics for testing purposes, both for biological sciences or as a test bed for flapping-wing MAV wing design. These projects are not intended to create lift-off immediately, but serve other purposes, such as: measurements of lift production, testing different wing designs, testing effects of kinematics on lift production and testing of various wing actuation mechanisms. Although not intended for lift production, these projects might function as inspiration for the design of prototypes that do produce lift. It is therefore that a short review of these projects is included.

**Cranfield University**

Galinski and Żbikowski [1] focus on the correct reproduction of insect wing kinematics. As described in Section 2.4, this movement consists of the wing sweeping motion, the wing pitching motion and a small out of plane motion or wing heaving. The latter introduces a banana or figure eight shape to the wing tip trajectory. Galinski and Żbikowski present two wing actuation mechanisms, which are not able or intended to fly. The first mechanism presented by Galinski and Żbikowski [59] is based on a double spherical scotch yoke, which provides the wing sweeping motion as well as the possibility for a banana or figure-of-eight type movement. A Geneva wheel provides the wing pitching.

The second is a mechanism which is based on the combination of a typical four-bar mechanism (Watt's linkage) and a Geneva wheel [60]. The Watt's linkage
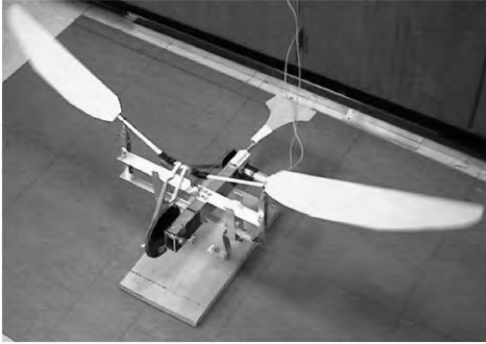
**Figure 3.9:** *The wing actuation mechanism developed by Banala and Agrawal [9]. The mechanism is based on a 5-bar linkage and offers the possibility to drive wing sweeping and pitching using a single actuator. Depending on configuration the trajectory of the wing tip can chosen to show figure-of-eight or banana type motion. Image by Banala and Agrawal from [9]. Copyright: ASME publications, reprinted with permission.*

provides the wing stroke and heaving motion. The Geneva wheel provides the wing pitching motion. The mechanism is shown in Figure 3.8a. Both mechanisms are mostly intended for study of forces on the wings and realization of insect wing kinematics. However, possibilities are proposed towards miniaturization and weight optimization of the mechanisms.

**Delaware University**

Banala and Agrawal [9] present a wing actuation mechanism which is able to produce wing sweeping and pitching kinematics. The mechanism is based on a compound configuration of a four-bar and a five-bar mechanism, see Figure 3.9. The four-bar mechanism is used to generate the wing sweeping motion, the coupled five-bar mechanism is used to introduce the wing pitching motion. The mechanism is driven via the four-bar mechanism using a single actuator.

By optimizing the two mechanisms the wing trajectory can be made to closely resemble a reference kinematics, for example, that of the Hawkmoth. By tuning the mechanism a figure-of-eight or banana type heaving motion can be obtained. The mechanism is intended for proof-of-concept purposes and currently no steps are suggested towards in-flight application.

**NASA Langley Research Center**

The test-setup presented by Raney and Slominski [106] is based on two electromechanical shakers which drive two hummingbird-inspired wings. By means of these two shakers the wings can be driven in a sinusoidal fashion. Phase difference in the driving signals can be used to introduce various wing tip kinematic patterns. Wing pitching is obtained by passive means. The interesting part of this setup is that it is essentially a compliant mechanism, driven by linear actuators. In this sense it is very similar to the insect thorax and bird wing actuation structure.

**The French aerospace laboratories (ONERA)**

Giraudo and Osmont [61] present a simple wing actuation test-bed inspired by the on the insect-thorax. The structure is an intermediate step towards the application of elastic storage in flapping-wing MAVs. The mechanism is based on an elastic shell-type structure similar in topology to the insect thorax. To facilitate resonance, elastic energy is stored in a U-type shell and upper shell which closes the structure. The top of the shell is prestressed by the sidewalls, this induced a curved shape. The dynamic behavior is analyzed and shows unstable behavior due to the prestressed top plate. The top plate has two stable positions. Passively pitching wings are proposed and analyzed independent of the structure. The realized test best shows large amplitude wing sweeping motion.

## 3.2.12   Comparison of actuation mechanisms

In this section a comparison is made between the different actuation mechanism concepts. Taken into account are the following aspects which serve as the explanation of the columns in Table 3.1. The columns of the Table provide information on the projects described in Sections 3.2.1–3.2.10

For some properties, assumptions have been made since data/papers did not provide enough clarity.

**Complexity** The complexity of the structure is indicated in this term. In most prototypes the complexity is inherent to the mechanism. However, in some cases the complexity of the actuator is dominant.

**Source of complexity** As mentioned this can be either the mechanism itself or the actuator technology.

**Number of joints** The number of joints present in the prototype. These can be compliant joints, hinges, bearings and other connections. The number of joints can be seen as an indicator of mechanism complexity.

**Actuator type** The type of actuator technology used.

**Flapping frequency** The flapping frequency of the wings when operated at the steady state motion, either hovering or forward flight. In this case <20 Hz means low frequency, >=20 Hz and <50 Hz is medium frequency and everything >=50 Hz is considered to be high flapping frequency. The flapping frequency is heavily size dependent.

**Flapping angle** The deflection angle of the wing sweeping motion.

**Control** The implementation of control, either by influencing the wing kinematics or by adding a tail with control surfaces.

**Table 3.1:** *Comparison of different flapping-wing MAV projects based on criteria defined in Section 3.2.12.*

| Project | LIPCA flapper | Berkeley MFI | Harvard fly | Clapping wing | Caltech Microbat | Vanderbilt University | Entomopter | Delfly Micro | FW-MAV |
|---|---|---|---|---|---|---|---|---|---|
| Complexity | Low | High | Low | Low | Low | Low | High | Low | Low |
| Src of Comp. | Mechanism | Mechanism | Mechanism | Mechanism | Mechanism | Mechanism | Actuator | Mechanism | Mechanism |
| ♯ joints | ~14 | ~22 | ~13 | ~9 | ~9 | ~8 | ~10 | ~9 | ~13 |
| Act. type | Piezo | Piezo | Piezo | Emotor | DC motor | Piezo | Chem | DC motor | DC motor |
| Freq | Med | High | High | Medium | Medium | High | Low | Medium | Medium |
| Flap. angle | Tail | Large | Large | Large | Large | Med | Small | Large | Large |
| Control | None | Wings | Wings | Tail | Tail | Wings | Other | Tail | Tail |
| Wing rot. | Passive | Active | Passive | Passive | Passive | Passive | Passive | Passive | Passive |
| Resonance | Yes | Yes | Yes | No | No | Yes | No | No | Yes |
| Scaling | + | + | + | - | 0 | + | - | - | - |
| Hovering | No | Yes | Yes | No | No | No | No | Yes | Yes |
| Flight | No | No | Yes | Yes | Yes | No | No | Yes | no |
| Wingspan | 150 mm | 25 mm | 30 mm | 100 mm | 100 mm | 150 mm | 200 mm | 100 mm | 150 mm |
| Section | 3.2.2 | 3.2.3 | 3.2.4 | 3.2.5 | 3.2.6 | 3.2.7 | 3.2.8 | 3.2.9 | 3.2.10 |
| Publication | [96] | [34] | [137] | [72] | [74] | [29] | [93] | [31] | [76] |
| Year | 2008 | 2006 | 2007 | 2008 | 2003 | 2002 | 1998 | 2009 | 2007 |

**Wing rotation** The character of the control over the wing pitching motion. This can be done actively by actuators or passively by a combination of inertial and aerodynamic loading.

**Resonance** Does the mechanism exploit resonance to reduce the cost of wing movement. This can only be accomplished by incorporating elastic elements into the design of the prototype.

**Scaling** Since miniaturization is a major factor in the design of flapping-wing MAVs this column indicates if the design used leaves room for scaling down the design. This can be hindered by: actuator technology or mechanism technology.

**Hovering** Is the prototype capable of producing wing kinematics that allow it to hover. Hovering flight is, when looking from an energy perspective, the most demanding task for a flapping-wing MAV.

**Flight** Has the prototype been used in real flight experiments. That is, does it generate enough lift to sustain its own mass.

**Wingspan** The wingspan gives an indication of the dimensions of the flapping-wing MAV for comparison purposes.

**Publication** The most relevant publication on the project covering the mechanics.

**Year** The year of this publication.

From this comparison, and the description of the mechanisms, it can be clearly seen that the different groups are following different paths. For example, the Harvard group has its focus on the attaining real flight and miniaturization. Other groups specialize in a certain type of actuator, for example, Georgia tech, which introduces other challenges.

Especially the complexity of some of these projects seems to be a major problem in producing enough lift for sustained flight, either forward or hovering. This can be seen when looking at the number of joints in the prototype and the flight success of the model. Other sources of complexity also introduce large problems, for example the chemical muscle in the Entomopter project. It should be noted that the complexity comparison is unfair when looking at the piezo driven prototypes, the control electronics are not included in this comparison but do add to the total complexity of the systems.

### 3.2.13   Wings

The wings are an integral and very important part of the flapping-wing MAV. Depending on usage, the loading conditions vary quite significantly. Intended

flapping frequencies influence loading conditions. The type of wing structure is dependent on the design. The size range is also quite large which introduces scaling issues.

Various methods exist to manufacture wings for flapping-wing MAVs. Perhaps the most common method of constructing wings for flapping-wing MAVs is the method of spanning a membrane by stiff rod type structures. The membrane is usually a biaxially stretched high strength Mylar film. The stiffening structures are usually unidirectional carbon rods of various cross sections. Wings constructed in this way are not only used for flapping-wing MAVs but also for non-flapping MAVs. Usually they have excellent strength-to-weight ratio, the projects which use these or related type of wings are discussed in Sections 3.2.1–3.2.10. Depending on the chosen method of realization, wings constructed this way can be very insect like.

Other methods for constructing wings usually rely on using a membrane and a stiffening structure which represents a vein like structure. For example, the wing presented by Pornsin-Sirirak *et al.* [102] in which a titanium skeleton is etched using MEMS techniques and combined with a parylene film. In this way it is possible to produce arched spars and more accurately control wing stiffness. A second method is the usage of electrospinning for depositing the membrane of flapping-wing MAV wings. The method is presented by Pawlowski *et al.* [99], using this method properties such as: thickness, local stiffness and surface tension can be controlled. Both these methods are very interesting when the design of the flapping-wing MAV includes accurate aerodynamic modeling for optimization of lift production and mass reduction. Lentink *et al.* [82] present a method for manufacturing corrugated wings for flapping-wing MAVs. These wings follow a design which is based on a real insect wing. The insect wing is scanned using a $\mu$CT scanner, the resulting data is converted into a FE model. The resulting FE model is then used to tailor the wing for a set of loading conditions present during hovering flight, both aerodynamic and inertial loads. The manufacturing technique allows for the addition of a corrugated structure to be able to carefully tune compliance, in accordance to real insects wings, see, for example Wootton *et al.* [143].

The currently available wing technologies are suitable for the current insect-sized flapping-wing MAVs, however, improvements can be expected when the more advanced manufacturing techniques such as described in this section are used. Especially, the tuning of wing pitching compliance will allow for improvements. Incorporation of fluid–structure interaction modeling may be used to accurately tailor the wing.

## 3.3 Actuators

This section deals with actuator technology applicable to flapping-wing MAVs. Many different actuator technologies exist today and a subset has already been used in flapping-wing MAVs, see Section 3.2. This implies a preselection of tech-

nologies which are applicable to the design of a flapping-wing MAV, either for powering the wing stroke or for control purposes. These possible applications can be directly related to the synchronous and asynchronous muscle types in the insect thorax, see Section 2.2.1. To be more precise in technical terms there might be a need for powerful fast actuators, the equivalent of asynchronous muscle, as well as slower less powerful actuators, equivalent of synchronous muscle, which control wing configurations but not necessarily on a wingbeat-to-wingbeat basis.

### 3.3.1   Actuators types

The possible actuator technologies, potentially suitable to be used as the wing sweeping motion actuator, both linear and rotational, are:

- Piezoelectric actuators (crystalline and polymer)

- ElectroActive Polymer actuators (EAP) which may be subdivided in:

    – Dielectric EAPs
    – Ionic EAPs

- Electromagnetic actuators which may be subdivided in:

    – Linear actuators
    – Rotational actuators

- Shape Memory Alloy actuators (SMAs)

The actuator types will be reviewed on a more detailed level per type in the following sections. Focus is here on the actuator for the flapping motion. Actuators for control are currently not separately reviewed. Several actuator types can be used for both main actuation as well as control purposes.

**Piezoelectric actuators**

There has been extensive research on piezoelectric actuators. Applications include audio drivers and sonar transducers. Due to the trend of miniaturization and the availability of manufacturing techniques, piezoelectrics have been used as actuators for micro devices. One major disadvantage has been that the maximum actuation strain is very small. Solutions have been found in the usage of bi- or unimorphs to increase movement as well as other mechanical amplification structures. Examples can be found in Hall *et al.* [64] who covered bimorphs, Wood *et al.* [141] and Sitti *et al.* [114] also covered bimorphs and more specifically optimized them for low mass applications. Larger amplitude piezo actuators have been developed by Lee *et al.* [79] in the form of the LIPCA actuator. Piezoactuators have been used for micro air vehicle applications, see the projects described in Sections 3.2.1–3.2.10 and the overview provided by Table 3.1. Application

in flapping-wing MAVs is complex due to medium to high voltages needed for actuation, and the corresponding need for high voltage electronics.

### EAP actuators

Bar-Cohen provides a very extensive overview on Electro Active Polymer (EAP) actuators in his textbook [10]. The book covers many aspects of EAP actuators and includes the chemical basis and physical principles as well as the mechanical properties relevant for real applications. EAPs and more specifically the dielectric EAPs which rely on electrostrictive or electrostatic properties of the material for their functioning, seem very promising for application inflapping-wing MAV applications. Their properties include high specific power, high strains and to some degree a large freedom in topology. They have a major drawback, which is shared with piezoelectric actuators, namely the high electric field required for actuation. Typically in the order of 1 V/$\mu$m.

Ionic EAPs, see, for example Shaninpoor [112], rely on an electrophoresis process for the displacement of ions inside the polymer to achieve actuation. The movement of charge induces a different configuration in the polymers chains thereby freeing energy to do work. This change requires the actuator to be immersed in a medium which is capable of facilitating such a change. This immersion can be integrated very effectively in the design of the actuator. Ionic EAPs do not rely on electric field strength for actuation but on low potential. Typically in the order of 1–2 V. Ionic EAPs may produce large forces and strains but have a slow actuation response which may impair functioning in high frequency applications. EAPs have been proposed for usage in flapping-wing MAVs and prototypes have been built, see, for example Park *et al.* [98] and Pelrine *et al.* [100].

### Electromagnetic actuators

Electromagnetic actuators, either in rotational or linear form, have been available for a long time. Rotational electric motors have been the actuator of choice for most MAV and flapping-wing MAV applications for a large scale range. The smaller vehicle applications are possible due to the fact that very small electric motors are available, usually DC-motors. The technology is relatively well developed and easy to access. Small rotational parts, *i.e.* gears, cams and bearings, can be bought off-the-shelf or easily manufactured. The same is true for electronics needed for control. One major drawback of mechanical origin is that rotational electric motors require some sort of conversion from rotational to translational when driving a reciprocating system such as flapping wings. Although this is a drawback when looking at mechanism complexity, the corresponding decoupling between actuator frequency and flapping frequency allows for increased energy density of the actuator.

The use of linear electric motors for driving flapping-wing MAVs wings has not been described in literature. Linear electric motors come in two types. First,

a type that employs a coil and piece of magnetically conductive compound which produces a magnetic field when an electrical current is passed through. The metal is movable and can be used for actuation, known as a solenoid type actuator. The actuation principle is based on the minimization of the potential energy in the magnetic field. The other type is the voice-coil, of which the basics are that of a Lorentz force actuator. The application of these technologies for the actuation of control surfaces is widely used including the field of flapping-wing MAVs.

**SMA actuators**

SMAs are one of the promising technologies for application in flapping-wing MAVs. The actuation principle is the fact that these metals can regain their initial shape by heating after an initial pseudo-elastic deformation. These properties are usually due to a temperature-dependent austenite/martensite phase transformation. To make an actuator, the SMA metal has to be combined with a spring to make a reciprocating system or in an antagonistic setup to make a two way actuator. An introduction to SMA actuators is given in Büttgenbach *et al.* [25]. SMAs show very high power densities but the actuation is slow and might not be applicable for higher frequency applications. SMAs are currently used in flapping-wing MAVs applications, see Friend *et al.* [57], which covers SMA actuation integrated in the wing and Bunget and Seelecke [24] who present bat-inspired SMA driven wings.

### 3.3.2   Actuator selection criteria

In order to choose one actuator technology or another, the actuators have to be checked if they live up to the boundary conditions which are imposed by a flapping-wing MAV. The design of the flapping-wing MAV is highly influenced by the choice of actuator. More realistic is that the actuator choice is an intrinsic part of the development and design of the flapping mechanism, this is illustrated by the variety of designs based on different actuator technologies in Section 3.2.

The most stringent demand on the actuator is the specific power. This requirement is imposed by the mass objective of the overall flying structure. In general, linear actuator technologies have a frequency dependence. Therefore, energy density in linear actuators is limited due to one-to-one coupling between flapping and actuator cycles in this setting of flapping-wing MAVs. The obtainable actuation frequencies are thus a requirement for the actuator. The actuator must be able to function in a regime that is needed for the flapping-wing MAV.

Some control over actuator force, position or velocity has to be possible within the setting of flapping-wing MAVs. This requirement for control measures is highly dependent on the intended design of the flapping-wing MAV. Control at actuator level will be covered in Section 3.3.3 but is mentioned here in order to be able to give an overview.

Typical attainable actuation strain, both in type and magnitude are important. This importance follows from the complexity of the support structures needed to apply the actuator in a flapping-wing MAV. Since wing sweeping motions are inherently of large amplitude, a small actuation strain requires the presence of a resonant or mechanical amplification system. Properties of the actuators are given in Table 3.2, which covers the mentioned: energy density, typical actuation frequency, actuation strain, control complexity and support structure complexity.

The information for this table has been derived from the information published by Kornbluh *et al.* [77] and Langelaar [78]. Note that the energy densities seem low for technologies that are typically listed as high performance, this is due to the previously mentioned frequency dependent output power seen from this low frequency setting. The efficiency is part of the table, however this is the efficiency of the only the active mass of the actuator. Supporting control electronics are not included and have a negative effect on efficiency. For the piezoactuators, electromagnetic actuators and SMA actuators this data is accurate and based on real-life applications. For the EAPs this data has been based on laboratory test and might prove to be different in actual applications. However, since EAPs are not at a well-developed level, improvements may be expected in the coming years.

### 3.3.3 Actuator control

The actuators mentioned above rely on the usage of electric power for actuation. Electric power is at this moment the most convenient option for usage in flapping-wing MAVs, as compared to, for example, chemical energy. When relying on electric power for actuation, the control of the actuator technologies has to be accomplished by the addition of a control circuit. For most flapping-wing MAV implementations control has to be implemented at actuator level to invoke control at system level. For example, amplitude and frequency in linear actuators

**Table 3.2:** *Comparison of different actuator technologies suitable for application in flapping-wing MAVs. Based on aspects which are important for application in the setting of flapping-wing MAVs. Typical mammalian and insect muscle types are included for comparative purposes.*

| Actuator | Energy dens. [J/g] | strain % | frequency [Hz] | Efficiency [%] | Control complexity | Support complexity |
|---|---|---|---|---|---|---|
| Piezoactuators | 0.13 | ~1 | High | High | Low | Low |
| Dielectric EAP | 1–4 | 1–10 | High | High | Medium | Low |
| Ionic EAP | 0.001 | 2 | Low | Low | High | High |
| E. motor rot. | 0.005 | – | High | Med | Low | High |
| E. motor lin. | 0.003 | 50 | High | Med | Low | Low |
| SMA | 15 | 1–8 | Low | Low | High | Low |
| Muscle mammal | 0.07 | 40-50 | Low | Low | – | – |
| Muscle insect | 0.10 | ~5 | Med | Low | – | – |

or frequency in rotational actuators. An overview of control options of diverse actuators is given in Karpelson *et al.* [71].

The control electronics must be used in all cases to regulate the available power and convert it to the control signal that controls the actuator. The system needed will be described here per actuator technology. The actual electronics are not considered here, nor are the sensors. Only the type of response is elaborated upon. The actuators will be reviewed here in the same order as listed above on Page 40 in which the control complexity is also included. The control assumption used here is that there is the need to control the force and position of the actuator.

**Piezoelectric actuators**

Piezoactuators rely on an applied potential to function. For a typical actuator voltages are in the 100–200 V range depending on thickness of the active material layer and intended actuation strain. Piezoactive materials can be controlled by the applied voltage. The response to this voltage is approximately linear with very little hysteresis, as long as the actuation strain is well within the elastic limit of the material. The linear behavior is very interesting for control, however control options are complicated due to high voltages involved. If the actuator is blocked, the blocked force increases linear with applied voltage, which is more important for control purposes. Examples of control using piezo actuators has been shown by, for example, Wood *et al.* [141] for a piezo bending actuator and Hall *et al.* [64] for a combined piezo/electrostrictive monomorph actuator, respectively.

**EAP actuators**

The two EAP actuator varieties require different methods of control. To start with dielectric EAPs: The dielectric properties are in principle linear. However, the material may exhibit geometrically nonlinear properties which contribute to nonlinear terms in the voltage/displacement or voltage/force responses. If the actuator response is approximately linear without any significant hysteresis, the control model can be simple. However, if the material behaves nonlinear, due to, for example, the mentioned geometrically nonlinear effects or hysteresis, the control must be based on more complex models. This is shown by Du *et al.* [38] who employ a Newton method for control of an electrostrictive actuator which also shows piezo and dielectric responses. A revised method is presented by Hu *et al.* [69]. Ionic EAPs require more elaborate control strategies. The magnitude of the activation is time dependent due to ion transport mechanisms that must lead to a new equilibrium state after a voltage increase or decrease. These time dependent effects introduce the need for elaborate control strategies when positioning is required. This has been described by Shaninpoor [112] in 2003.

**Electromagnetic actuators**

Electric motors, rotational and linear, can usually be controlled by simple means when high precision is not a requirement, such as MAV applications. Both electromagnetic actuator types and their control possibilities have been very well developed due to the historically wide range of applications. The electric rotational motor, in the form of a DC-motor, is very simple to control. In most flapping-wing MAV applications only control over rotational speed is required. When looking at brushless technologies, control is more complex. Linear electromagnetic actuators are more difficult to control since they show reciprocating movement and require some degree of control over positioning. The response can however be linearized for simple control. It is possible to use the drive coil as sensor for feedback. For both linear and rotational technologies, implementation of control electronics is straightforward due to the low voltages involved.

**SMA actuators**

SMAs show significant hysteresis in their material properties. The phase change in SMAs, on which SMA actuation is based, introduces significant nonlinearity. SMAs need either complex control or control schemes which employ neural networks, fuzzy logic and genetic algorithms, see, for example [117]. The main focus of many articles is position control. Velocity control is not mentioned since the main focus is on applications where velocity is of lesser importance, for example, surgical instruments. The more complex control types require a learning period to adjust the controller to the nonlinearities of the system.

The other extreme for SMAs is very simple control. Since it can be very hard to control the phase transformation, it is better to accept this as such and use the SMAs as an actuator with an on and off setting. In this case control is very simple and has been used historically for lots of applications such as "muscle wire" (NiTiNol) in radio controlled aircraft which do not employ control and rely on an on-off binary setting. In order to apply this type of control, the design of the structure plays an increasingly dominant role for efficient application of SMA actuators.

### 3.3.4   Feasibility

Due to a number of issues, not all mentioned actuator technologies are equally feasible. Implementation effort for the application of a specific actuator technology depends on the size of the intended flapping-wing MAV. Scaling laws drive the frequency of flapping up when moving to smaller scales. This favors all forms of linear actuators due to increase in actuator power density. While favorable for the actuator itself, the required miniaturization of control electronics introduces new challenges.

Looking at specific aspects that may hinder implementation, per actuator technology a few major issues come forward. One major drawback of dielectric EAPs and piezos is the required significant voltage to operate. This voltage is not readily available on flapping-wing MAVs and requires highly miniaturized high-voltage electronics which are currently of similar weight as the actuator. As can be seen from the projects reviewed in Section 3.2.1 no flapping-wing MAVs exist today which are piezo powered and have onboard electronics. EAPs can in general not be found outside of laboratory environments. Although very promising it seems unlikely that they will be available at a level applicable for flapping-wing MAVs like current electromagnetic and piezo actuators within the near future. This does not mean that any research in to their application in flapping-wing MAVs is pointless. When the required electronics become available, their promised properties will make them very attractive for flapping-wing MAV applications. Rotational electric motors are feasible for current and future, even smaller scale, flapping-wing MAVs. Their application in a resonant setting is less suitable due to mechanical issues. Although, elegant gear-based partially resonant mechanisms are possible. Fully compliant structures are more feasible at insect-scales making the required gears less suitable. Linear electromagnetic actuators are currently available but may be hindered by low specific power density. Currently available actuators are not designed for specific power density. So custom designs may bring improvements. Both linear and rotational technologies are low voltage, allowing for light weight control electronics. SMA actuator technologies are not able to reach the high flapping frequencies of smaller scale flapping-wing MAVs. They may be suited for control purposes.

## 3.4   Control

This section is included to give insight into control possibilities for controlling a flapping-wing MAV. Since control has to be implemented from the initial design phase to avoid less elegant and heavy solutions it is reviewed here. The control of a flapping-wing MAV can be based on the control of insects. Insect control, both for stability and heading, is based on adjustment of wing kinematics and body orientation. Insects possess a very high degree of aerial agility, a flapping-wing MAV does not need to have the same degree flight performance, since their requirements allow them to function successfully at a lower degree of aerial agility. Therefore, control measures can be implemented which are based on smaller control signals. A restriction is placed on the type of control; the focus is on control integrated in the motion of the flapping wings. Other options, such as the addition of a tail section, are less suitable for hovering applications and are not included.

This section assumes that the main wing sweeping motion is a steady-state motion, which corresponds to hovering flight. In addition, most smaller scale flapping-wing MAVs rely on resonant principles and, consequently, significant changes in flapping frequency are not feasible, since they will have detrimen-
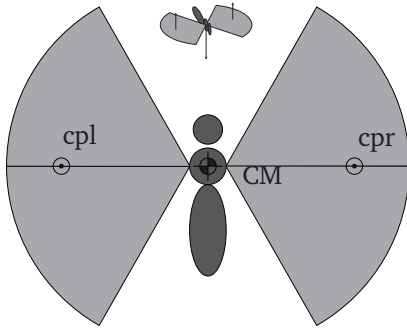
**Figure 3.10:** *Steady-state hovering. Area swept by wing motion is indicated, view is from the top. flapping-wing MAV orientation indicated by the small inset. Effective centers of pressure and center of mass are indicated.*
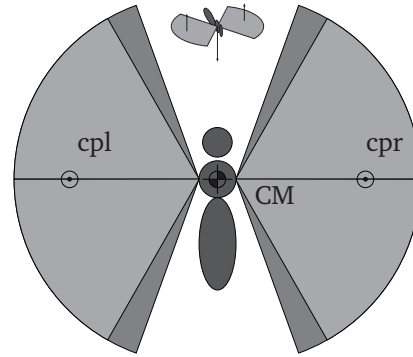
**Figure 3.11:** *Increased wing sweeping stroke, frequency kept constant, resulting in increase in lift. Increased stroke angle indicated in dark grey. Decrease also possible. Effective centers of pressure and center of mass are indicated.*

tal effect on flapping amplitude, see Ellington [49]. When limited to a single wing sweeping frequency different control options exist. In order to maneuver in 3-dimensional space a minimum of set of control possibilities is required.

Starting from steady state hovering flight, which is defined as the reference condition, a number of control possibilities can be proposed. The reference condition is further defined as being a symmetric flapping motion with horizontal flapping plane of a hypothetical 2-winged flapping-wing MAV, shown in Figure 3.10 from [20]. In the current view the wing pitching kinematics are assumed to be passively controlled and that control is accomplished solely by influencing wing sweeping kinematics. The first option for control is the possibility of increasing or decreasing the stroke of the wing sweeping motion. In this manner the lift production can be increased and decreased, resulting in an altitude change.

Figure 3.10 represents the steady state hovering situation, the center of mass (CM) and the effective centers of pressure for left and right wing are indicated (cpr and cpl). In Figure 3.11 an increase in wing sweeping amplitude can be seen, resulting in an increased amount of lift it can be seen that the center position of the resonator for the left and right wing do not shift. A decrease in wing sweeping amplitude is possible, resulting in a decrease in lift production. This can be used to vary the operational flying height of the flapping-wing MAV. If this operation is performed in a nonsymmetric manner a rolling torque will be the result, offering possibility to obtain left-light control.

The second option is a shift of the center position of the wing sweeping motion. This change shifts the position of the effective centers of pressure of the left and right wing which leads to a backwards pitching moment due to the shift
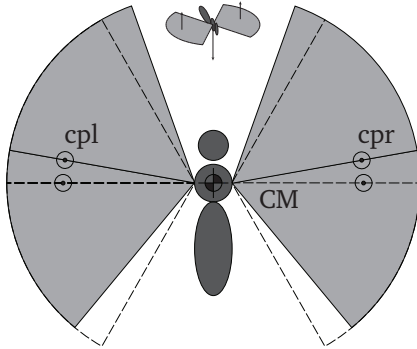
**Figure 3.12:** *Shifted center position of the wing sweeping movement. Outline of the initial wing positions is indicated by dotted lines. The resulting backwards pitching moment can be used to obtain backwards flight. Reverse and nonsymmetric actions are possible. Effective centers of pressure and center of mass are indicated.*

relative to the center-of-mass, seen in Figure 3.12. This shift introduces a pitching torque which may be exploited for obtaining a forward motion. The same shift backwards leads to a forward pitching moment and consequently may be used for obtaining backwards motion. This can be done asymmetrically to explore other control options.

The two methods described, including all nonsymmetric possibilities, yield a set of controls that are sufficient to control the flapping-wing MAV in both altitude and attitude. The only challenge that remains is the yawing motion, since it requires some sort of rowing motion by the wings. Under the current assumptions of passively pitching wings obtaining a yawing torque is not possible. As an alternative a combination of the motions above can be used to make a banked turn. As mentioned before, a flapping-wing MAV with these controls will not be as agile as an insect which do have active control of the wing rotation. The inclusion of active wing rotation is not necessary for controlled flight but probably will be needed if there is a request for very high agility.

### 3.4.1   Control in wings

A very specific method for implementing control is influencing the airflow around the wing. Using this method it is possible to gain a high degree of control due to direct influence on the efficiency and magnitude of lift and drag production. In order to implement this type of control options are required for controlling aspects such as: local wing compliance, curvature, surface roughness and membrane permeability. The possibility of influencing one of these properties, in combination with the methods described above, gives a very elaborate set of controls for a flapping-wing MAV, removing any need for a tail section.

Various options for control in wings have been reviewed in literature, see, for example, Pornsin-Sirirak *et al.* [103, 103] and Ho *et al.* [67] who discussed the usage of implementing electrostatic MEMS vent holes in the wing membrane. If unactuated the vents are open allowing free flow through the membrane. When actuated the vents close, stopping flow through the membrane. In this way there

is active real-time position dependent control over the pressure difference between the trailing and leading surface of the wings and thus significantly influencing aerodynamic performance. In order to successfully control the aerodynamic loads a direct measurement is very valuable. An approach based on the direct measurement of the lift force during flapping flight, by integrating sensors in the wing, has been proposed by Yang *et al.* [145]. In order to implement this solution a wing membrane is constructed from a PVDF (Polyvinylidene fluoride)-Parylene composite. The PVDF functions as a sensor and is applied by means of a MEMS process. The piezoelectric properties of PVDF are used to identify the local loading condition. Using this type of sensors, the wing driving can be controlled in real-time for optimal lift production and the implementation of control.

## 3.5   Functional mechanism requirements

An overview of current and recent projects aimed at the realization of a flapping-wing MAV is presented in this chapter. Various related subjects are also reviewed, such as actuator technology applicable to flapping-wing MAVs, methods of implementing control and constructional principles for flapping-wing MAV wings. This review forms part of the inspirational basis on which the current flapping-wing MAV wing actuation mechanism is seated. The other significant part is extracted from the review of insect anatomy as presented in Chapter 2.

The different projects which are reviewed show a large variance in their intended goals. The starting points of the different projects are also very different since they originate from very different groups, for example, micromechanical, biological, aerospace or space exploration. The run time of the projects, available financial means and experience of the people involved varies greatly. Taking this into account, all flapping-wing MAVs described above have unique and interesting traits which make them interesting as a source of inspiration.

On a higher level, the correlation between complexity of the mechanism, expressed in the number of mechanical links, bearings, hinges and the like, and the success, expressed in successful flight, is undeniable. The aim for low mechanical complexity is not a certified route to success but in general a sound idea due to associated coupling between mass and complexity. The usage of rotational electric motors forces the design of the flapping-wing MAV, in general, towards more standard solutions. Other solutions, more overtly leaning on insect inspiration, employ the usage of linear actuator technologies and compliant mechanisms.

The integration of resonant principles, *i.e.* the incorporation of elastic elements in the structure, is used in many projects. The manner in which this is done varies significantly. From a highly integrated system, in which the actuator doubles as the elastic element, to a modular approach, in which tuned springs are added to a preexisting mechanism, both have their merits. The intention of the integration of an elastic element can be significantly different. Either for resonant amplitude amplification, reduction of inertial cost of wing movement or

a combination of the two. Resonance is particularly interesting in the setting of compliant mechanisms and linear actuators because the combination of the two is well suited implementation in flapping-wing MAVs.

The application of a tail section with control surfaces is commonly used in flapping-wing MAVs. When looking at hovering flight a tail section is less interesting due to the flow required for useful control forces. The added mass of the tail section can be removed by looking for control options with a higher degree of integration. Influencing the resonant state of the flapping-wing MAV offers large possibilities while maintaining a high level of integration. The addition of integrated control has to be done in the early stages of the design process. Other options of control which use actuators in the wings are very promising but are not at application level at the moment.

The selection of the subset of electric powered actuators is a justifiable choice at this moment, based on intended size range and technology development level. The use of linear actuator technologies is almost required when looking at the usage of resonant principles. Choice of actuator is guided by factors as: ease of use and specific power density. For smaller flapping-wing MAVs piezo technologies are the only feasible option, when larger flapping-wing MAVs are reviewed options are extended to include linear electromagnetic actuators. In summary, the choice of actuator should be based on a system view of the actuator and the accompanying control system. This choice is of course restricted by the design of the flapping wing mechanism.

In conclusion, a good option for the design of the wing flapping mechanism is a low complexity compliant mechanism powered by a linear actuator technology. In order to exploit resonance, inspired by insects, an elastic element should be included. Options for control should be thought of and taken into account from the initial design of the mechanism. Wings can be based on current technologies but can be replaced by more advanced designs at a later stage.

# Chapter 4

# Conceptual flapping-wing MAV thorax design

## 4.1 Introduction

The development of the wing action mechanism is the base for the entire flight apparatus of the flapping-wing MAV currently under development. The analysis of both insects in Chapter 2 and current flapping-wing MAVs projects in Chapter 3 has led to a set of functional requirements for the wing actuation mechanism. In essence this mechanism, referred to as thorax in analogy with insect anatomy, is the basis for the flapping-wing MAV and as such the first step in the development. In this chapter focus is purely on the thorax structure itself, wings are not reviewed and assumed given. The division between thorax and wings is artificial and introduced to be able to compartmentalize the development of the functional parts of the flight mechanism. In fact, wings are an integral part of the wing actuation mechanism, especially when the structure has to exploit resonance.

Based on the functional analysis of insects and flapping-wing MAVs projects, the thorax has to function as a structure for elastic energy storage. The storage of elastic energy is intended to introduce a resonant state to the mechanisms. This allows for a reduction of energy required for driving the wings in aerodynamically efficient patterns, as described in Chapter 2 and 3 for insects and flapping-wing MAVs, respectively. In order to couple the wings to the elastic storage unit, an amplitude amplification mechanisms is required. This mechanism can be accomplished in many forms and is an internal part of the thorax development.

This chapter covers the selection of the elastic storage modes and their implementation within the developments of the thorax at a conceptual level. A number of solutions is presented to convert motion of the elastic storage unit to the large

rotation needed to drive the wing base. These solutions are based on the use of compliant mechanisms.

## 4.2    Energy storage

The application of resonance in the wing actuation mechanism for a flapping-wing MAV is based on the storage of potential energy in a deformable structure, *i.e.* the elastic deformation of an amount of material. Four properties are of importance for how the energy storage is accomplished: The material used, the volume of material, the deformation mode and amount of deformation.

### 4.2.1    Deformation mode

The deformation mode used to store potential energy has large influence on the design of the thorax structure. Many different structures can be designed to store mechanical energy. The deformation modes which can be used are compression, tension, bending, torsion and shear of a material which can store energy efficiently, meaning high energy density, see Figure 4.1. Note that extension, compression and bending are essentially the same but are mentioned separately since their application may lead to very different designs. Combinations of deformation modes are possible, the combinations are not reviewed here but may prove to be interesting for more advanced designs and may be exploited for control purposes, especially nonlinear coupling effects between the modes might be of interest.



a)            b)            c)            d)            e)
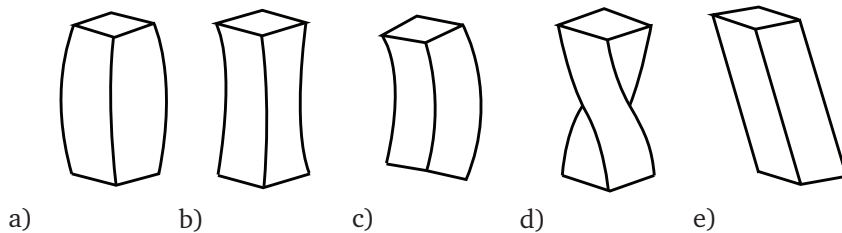
**Figure 4.1:** *Modes of deformation usable for potential energy storage in flapping-wing MAVs, from left to right: a) compression, b) Extension, c) bending, d) torsion and e) shearing.*

In order to classify these modes from the perspective of application in flapping-wing MAVs, they are reviewed in an application matrix, see Table 4.1. The table is based on the assumption that a specific amount of energy needs to be stored using a generic material. This assumption is intended to clarify possibilities of the modes, but not to give direction towards possible application methods. The amount of energy storage represents the maximum value obtained during resonant excitation. Constrained by the flapping-wing MAV setting, the columns in

**Table 4.1:** *Comparison of different deformation modes for application in flapping-wing MAVs. Based on the use of a generic linear elastic material loaded up to the elastic limit for a fixed amount of energy storage.*

| Deformation mode | Loads involved | Support structure | Notes |
|---|---|---|---|
| Compression | High | Heavy | Buckling |
| Extension | High | Heavy | |
| Bending | Low | Light | |
| Torsion | Low | Light | |
| Shearing | High | Heavy | |

Table 4.1 can be explained as follows: First, the loads involved to store the required amount of energy. These loads are highest for tension and compression and moderate for bending, torsion and shearing, depending on material and configuration of the design. The need for support structures can best be explained by means of an example: When a helical spring configuration is chosen it needs to be embedded in a structure to be able to use it. It is this need for surrounding structures that complicates application of some of the modes. The information in Table 4.1 should not be seen in a black and white view but more like a set of guidelines which can be used to review elastic storage possibilities.

The application of the deformation modes as posed above, leads to the conclusion that compression and extension are less suited for application in flapping-wing MAVs. This conclusion cannot be posed with large certainty of general application to resonance based flapping-wing MAVs. This is due to the fact that designs can be devised which do not, or only to a certain extent, rely on extensive support structures. The choice of materials also influences the applicability of the deformation modes. Low Young's modulus materials are applicable in extension and compression, as can be seen in the insect thorax in the form of the drive muscles. However, for technically feasible materials the forces for these deformation modes are generally too high.

Application of technically feasible materials will introduce constraints due to factors such as manufacturing. The material needs to be connected in some way to the rest of the structure and the materials need to offer possibilities to do this. Morphology may be a factor. For some materials certain morphologies cannot be reached either due to material properties or manufacturing possibilities.

## 4.2.2   Material choice

The choice of the material which is used to store energy, is very important. This choice is subject to an important objective which is imposed on the top level of the design, namely the overall mass of the structure. While posed separately here, the material choice is highly coupled with the previous section. However, the

**Table 4.2:** *Specific energy storage of various materials*

| Material | Youngs modulus [GPa] | Strength [MPa] | Density [kg/m$^3$] | specific energy storage [kJ/kg] |
|---|---|---|---|---|
| Spring steel[a] | 210 | 2100 | 7850 | 2.65 |
| UD Carbon[b] | 145 | 2100 | 1500 | 20.25 |
| Nylon(PA-6)[c] | 2.5 | 50 | 1100 | 2.30 |
| Resilin[d] | 0.002 | 4 | 1000 | 8.00 |

*References*: [a]Matbase [86]; [b]van Dijk Pultrusion Products [127]; [c]Matbase [86]; [d]Shewry *et al.* [113].

selection of suitable materials for energy storage in the setting of flapping-wing MAVs the material choice is reviewed separately here. The mass objective imposes bounds on material selection, which is the maximization of the performance index $M$ or specific energy storage, from Ashby [7]:

$$M = \frac{\sigma_f^2}{\rho E} \tag{4.1}$$

In which $\sigma_f$, $\rho$ and $E$ are the strength, Young's modulus and density of the material, respectively. Since this chapter has the intention to portray and explain the basic conceptual design, there is no need to perform a material selection. However, to give an indication of suitable materials a list of materials is given in Table 4.2. This table shows that natural materials exist which have high specific energy density, especially the protein resilin, and therefore are efficient materials for elastic energy storage in resonant mechanisms. In fact, resilin is present in the insect thorax and the wings. Note that carbon fiber materials are suitable for application in flapping-wing MAVs. Indeed for these materials application in extension or compression involve high loads. Application in compression may lead to buckling type behavior which may require design adaptations.

The actual volume of elastic material used depends on the amount of required elastic energy storage. This value is restricted by the elastic limit of the material, which can differ significantly for different materials. Thus the ratio between the specific energy storage and the elastic limit determines how effective the material can be used. This is true for the pure material but the true effectiveness is reduced by the need and presence of support structures.

## 4.3   Towards an actuation mechanism

The generation of concepts for the first actuation mechanisms for the flapping-wing MAV currently under development relies on inspiration obtained from the

insects as discussed in 2 as well as other flapping-wing MAV projects reviewed in Chapters 3. The ideas and inspiration obtained there are supported by knowledge on materials and elastic storage concepts reviewed earlier in this chapter.

In order to put boundaries on the design space a few choices have been made. These choices reflect the knowledge obtained from studying both nature and the man-made flapping-wing MAVs. Four main aspects influence the design and provide design directions.

**Simplicity** Based on the fact that simpler designs seem to be more successful, see Table 3.1, it seems that low complexity designs are usually of low mass and therefore provide better chances of lift-off.

**Resonance** The design has to be based on resonant principles. The design has to fully exploit resonance for maximum reduction of the power expenditure in accelerating and decelerating the wings. The resonance will be used to drive the wing sweeping motion of the wing, the main stroke as described in Section 2.4.

**Passive wing pitching** Mostly inspired by methods of wing pitching in insects, see Chapter 2, the choice has been made to employ passive wing pitching in the design. This is a trade-off between aerodynamic efficiency and a low mass structure. Although actively pitched wings are able to produce more lift, the increase in mechanism complexity leads to an overall increase in mass.

Distilling the most important aspects from this list leads to the conclusion that the overall nature of the wing actuation mechanism has to be of a compliant nature. The use of compliant structures allows for a large design space of resonant mechanisms. The exploitation of resonance is less straightforward in traditional gear-driven flapping-wing MAVs. A second aspect, which will become more important in the future, is the ability to scale down the structure. The absence of gears, bearings and other traditional mechanism construction elements ensures that the design may be scaled down effectively. In addition, the usage of linear actuator technologies are better suited to drive a mechanism which relies on compliant principles, these actuators are better suited for actuation at small scales.

## 4.4 Concepts

The concepts covered in this section provide an introduction on how to store energy in simple structures. Preferably the structures are self-contained, self-containedness is defined as the property of a structure that is able to perform the intended task without the need for support structures. In the ideal case the elastic storage unit should consist entirely out of elastic storage material. This implies, among others, that the elastic unit needs to be self supporting and, for example, be able to guide the intended motion of actuator without exterior means.

These structures are the basis for the resonant structure and will as such be extended and augmented by other structures which include the compliant mechanism used to drive the wing.

### 4.4.1 Spring like structures

As discussed in Section 4.2.1, bending and torsion are the most probable candidates for storing elastic energy in this setting of flapping-wing MAVs. A very simple self-contained version of the use of bending for energy storage is a ring-type structure. This structure, and variations on this concept, will be seen as the basic structure for the wing actuation mechanism. Under the term variations, derivations of the ring should be considered, for example, ellipsoids and half rings. The application of the ring can be seen as the equivalent of a self stabilizing coil spring.

The ring is by no means the only method to use bending but the elegance lies in the fact that the free-vibration modes of the ring can be exploited without the need for support structures. The elegance of the ring is especially pronounced for opposing attachment points which may be placed on the ring and can be used to attach linear actuators and compliant wing driving mechanisms exploiting reciprocal motion. By varying different aspects, such as: material and geometry, the usage of bending can be tailored for to suit a large number of different designs. For clarification purposes the most simple application of the ring is shown in Figure 4.2 in which attachment points for, for example, an actuator are shown.
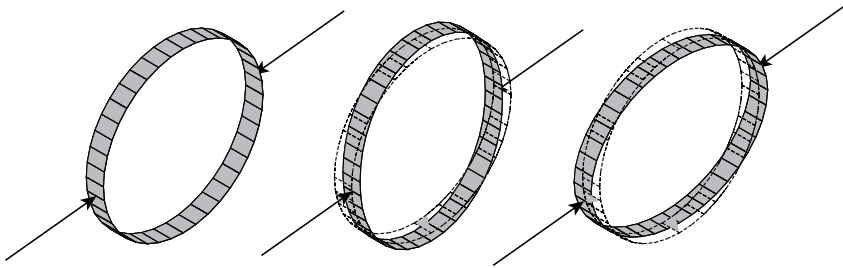


**Figure 4.2:** *A simple application of a ring as a spring, attachment points indicated by arrows, inward and outward deformations can be seen. Various attachment points can be used for both the wings and the actuator, which need not necessarily be at the same position.*

### 4.4.2 Coupling

When focusing on the use of a ring as the basic structure, choices can be made in the coupling of the wing. Two choices can be made [20]. The first is a soft coupling, the second is a stiff coupling by means of a mechanism. In the first

case the wing is driven as a part of the resonating structure and needs to be of material that is able to store elastic energy. The second option is the use of a direct coupling between ring deformation and wing deflection. The wings can then be rigid in bending direction, deformation by torsion can still be significant in the sense of passive wing pitching as discussed in Chapter 2.

In both settings the wings function as a significant source of the equivalent inertia of the resonant system. At this stage it is assumed that the wing rotation can be accomplished by passive means so that only the flapping movement of the wing has to be driven by the thorax structure. The first method of transferring energy from thorax to the wing is to apply a soft coupling to the wing and have this system resonating, see Figure 4.3. The second is to apply a deterministic method of wing coupling, which is to say that the wing position is dictated by the deformation of the ring which is part of the flapping-wing MAV thorax structure, see Figure 4.4. In these figures a dividing line has been drawn to separate the parts internal of the thorax and external of the thorax, *i.e.*, the wing. The wing has its own inertia indicated $m_w$, the equivalent inertia of the moving body parts is indicated by $m_t$. The thorax stiffness is lumped in the generalized thorax stiffness $k_t$. The wing bending stiffness is lumped in $k_w$. The input and output are given by the actuator and aerodynamic force, $F_{act}$ and $F_{aero}$, respectively. Note that the soft coupling introduces one more degree of freedom.
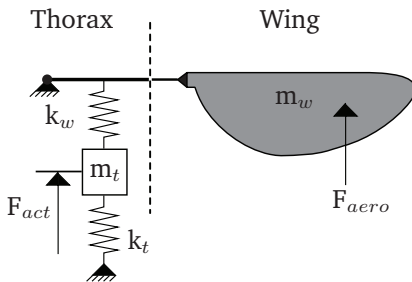


**Figure 4.3:** *Wings as an integral part of the compliant structure, wing bending is exploited for amplitude amplification.*
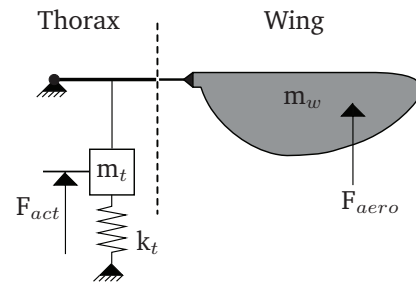
**Figure 4.4:** *Direct wing coupling, deformation is the result of the ring deformation and one-to-one wing coupling.*

## 4.5   Concepts

A number of different concepts are presented. These are all based on the ring type structure which seems most promising for various reasons as discussed in Section 4.4.1. First the basic structures are introduced which will be used to study effectiveness of these building blocks for usage in the current flapping-wing MAV. The focus in this section is on the development of basic concepts and their usability in the wing actuation mechanism for flapping-wing MAVs. Emphasis is

on the ability to function in a setting in which the wings and elastic storage unit are driven as part of a resonant system.

### 4.5.1    Simple ring based structures

The first is a structure which has softly coupled wings. The wings and ring function as a resonator which is aimed at maximum deflection of the wings using resonance, see Figure 4.6, this structure is one of the simplest possible extensions of the ring to include wings, depicted in Figure 4.5. This structure follows the



**Figure 4.5:** *The ring used as the basis for the conceptual structures.*



**Figure 4.6:** *Simple compliant extension of the ring to include wings, the wings are deformable part of the structure.*

wing coupling strategy which can be seen in Figure 4.3. Note that, the analogy in this case is not fully clear, since the structure is not discrete but fully compliant. The structure can be tuned to make sure that the resonance frequency which corresponds to the main wing sweeping motion is exactly at the frequency which is to be determined most efficient for flapping the wings.

When taking the coupling strategy depicted in Figure 4.4 as a basis, an extension of the ring is depicted in Figure 4.7. This simple extension of the previous model introduces struts which couple the deformations of the ring to movement of the wings. The introduction of the two struts introduces the change from a distributed wing hinge to a localized one at the root. This structure is inspired by the resonant structure of Cox *et al.* [29]. The result is a two winged design which uses the ring as a self-supporting spring. This structure can, due to elastic hinges, be used for larger amplitude deflections. An extension of this structure is the extension to four wings, see Figure 4.8, which can be used to obtain a more favorable orientation of the flapping plane for hovering applications. This extension is based on a mirroring of the wing driving mechanism. These basic structures form the basics of the wing actuation mechanisms which are to be developed for driving the wings of the flapping-wing MAV.
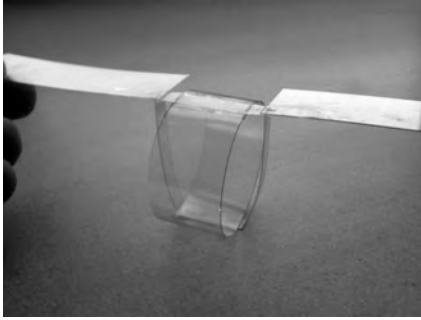
**Figure 4.7:** *Ring based structure using two struts to transform and amplify ring deformation to wing root rotation.*



**Figure 4.8:** *Extension of the two winged concept allowing for a more favorable horizontal flapping plane.*
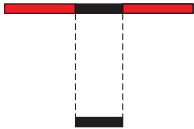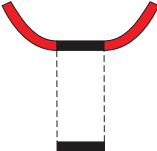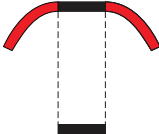
## 4.6   Review of concepts

The conceptual ideas posed in Section 4.5.1 have to be analyzed in order to judge their applicability for usage as the flapping-wing MAV thorax. They have to conform to various criteria, for example, the requirement on the overall project is that the flapping-wing MAV should have the ability to hover. As mentioned in Chapter 2 this does not necessarily require a horizontal flapping plane, therefore two winged concepts are not excluded. The set of models described in Section 4.5.1 is an inspiration for the set of structures proposed in this section.

### 4.6.1   Comparison of mechanisms

To objectively review the different concepts they are placed in a tabular form to compare different aspects. First, the most simple model proposed in Figure 4.6 can be seen in Table 4.3 designated Concept 0. In this table the resting, wings up and wings down positions are depicted reduced to their functional basics. The ring is given as a cross section at the attachment point of the wings. The current model depicts a typical coupling between wing and ring. A phase shift of $\pi$ degrees is equally valid because the structure will still reach maximum deflection at the same time.

The proposed structures, which are based on the usage of a compliant mechanisms using compliant hinges, are given in Table 4.4. In this table Concepts 1 and 2 are introduced in Section 4.5.1. Concept 3 is a simplification of Concept 2 by a reduction of the number of struts. Concepts 4 and 5 do not rely of the usage of struts but introduce the usage of two or more rings to drive the wings, in which Concept 5 is an extension of Concept 4 with two more wings and one ring. The table depicts the simplest functional form of the concepts. The concepts are shown in resting condition and in the wings up and down configurations. The

**Table 4.3:** *Overview of Concept 0 which is a compliant structure to transform and amplify ring deformation to a wing deflection. Wings are indicated in red, ring cross section in black connected by dotted lines. Resting, wings up and wings down position are shown.*

| Concept | Initial | Wings up | Wings down |
|---------|---------|----------|------------|
| 0 | | | |

rings are given as a cross section. All the proposed mechanisms are planar in origin.

Table 4.4 shows the designs on a conceptual level but does not introduce criteria for rating the mechanisms. The final choice will be made by comparing aspects from manufacturing, analysis and convenience. These aspects will be covered in Chapter 5. Table 4.5 gives criteria which can be used to compare the different mechanisms. The number of wings, rings, number of compliant hinges and possible Degrees of freedom are listed. The degrees of freedom are listed because of later possibilities of control.

## 4.7 Extended concepts

A myriad of possibilities exist to combine a set of wings with rings used for elastic energy storage. The ideas posted above are used as candidates for the design of the resonant base for the wing actuation mechanism. Five possible designs are introduced which are all candidates for the final design. Concept 0 is excluded here because it is not based on compliant mechanisms for amplitude amplification. In this section an overview is given on how these mechanisms may look when used to construct a flapping-wing MAV. For this purpose dummy wings are included.

### 4.7.1 Overview of concepts

The first concept, Concept 1, consists of two wings and one ring. The wings are connected by six elastic hinges using a compliant mechanism. The wings flap in the vertical plane depending on orientation of center of mass, see Figure 4.9. This setup has one degree of freedom which might eventually be used for control purposes.

Concept 2 consists of four wings which and one ring. The wings are connected using 12 elastic hinges, as mentioned before an extension of Concept 1. the wings

**Table 4.4:** *Overview of the different concepts which use a compliant mechanism to transform and amplify ring deformation to a wing root rotation. Wings are indicated in red, links in black and compliant hinges in grey. The cross section of the rings are indicated by the black parts connected by the dotted lines. The initial, wings up and wings down positions are shown. Concept 1 is two-winged setup simply exploiting ring motion. Concept 2 is an extension of Concept 1 by mirroring the wing configuration. Concept 3 is a simplification of Concept 2 by removing two struts, thereby adding a degree of freedom. Concepts 4 and 5 use multiple ring and a phase difference in ring motion to drive the wings.*

| Concept | Initial | Wings up | Wings down |
|---------|---------|----------|------------|
| 1 | | | |
| 2 | | | |
| 3 | | | |
| 4 | | | |
| 5 | | | |

**Table 4.5:** *Comparison of the different concepts based on the amount of wings, representing the orientation of the flapping plane, the number of rings required, the minimum number of compliant hinges, the degrees of freedom in the system and the minimum number of actuators required to drive the system.*

| Concept | Wings | Rings | ♯ hinges | DoF | Min. ♯ actuators |
|---------|-------|-------|----------|-----|------------------|
| 1 | 2 | 1 | 6 | 1 | 1 |
| 2 | 4 | 1 | 12 | 1 | 1 |
| 3 | 4 | 1 | 8 | 2 | 1 |
| 4 | 4 | 2 | 4 | 2 | 2 |
| 5 | 2 | 3 | 8 | 3 | 3 |

flap in the horizontal plane, see Figure 4.10. The setup has one degree of freedom which can be used for control purposes.

The third concept is a simplification of the four-winged setup described in Section 4.5.1. It consists of four wings connected to one ring, see Figure 4.11. The simplification is in the number of struts. Resulting in a reduction of the number of compliant hinges. The number of degrees of freedom is increased to two, expanding control possibilities.

The fourth concept is based on two rings, see Figure 4.12. Two wings which flap in the horizontal plane are compliantly connected to two rings. The number of degrees of freedom in the system two. A phase difference in ring motion may be exploited for control purposes.

The last concept is based on Concept 4 but employs three rings driving four wings. No struts are used, control can be implemented by using different amplitude actuation for the different rings, see Figure 4.13. Consequently, it has three degrees of freedom.

## 4.8   Concluding remarks

The conceptual ideas presented in this chapter cover various structures which may be used as the resonant mechanism for driving the wings in the flapping-wing MAV. The inspiration for these mechanisms comes from nature. A direct translation from insect thorax to engineering equivalent is not possible or desired, because technical solutions follow different guidelines and use different materials rather than biological structures. The inspiration from insects is therefore used by distilling valuable guidelines for engineering implementation. This means that at a high level principles are set for overall functioning but local implementation is purely engineering based.

The ring has been proposed to function as the main elastic energy storage unit. By no means is the ring the only structure viable for usage in this manner but it does offer some very specific benefits. First, it can be used as a self-supporting
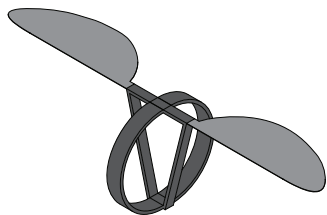
**Figure 4.9:** *Artist impression of Concept 1. The structure is based on amplification of the ring motion by means of a compliant mechanism to drive the wings.*
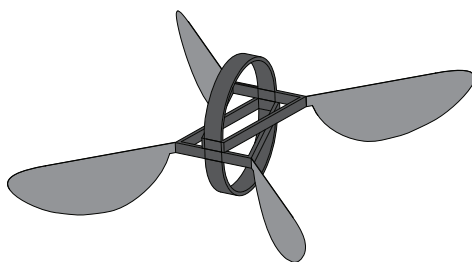


**Figure 4.10:** *Artist impression of Concept 2. The structure is an extension of Concept 1 by mirroring the wing setup. A more favorable, horizontal wing sweeping plane is thus obtained.*
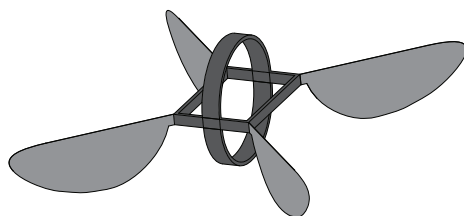


**Figure 4.11:** *Artist impression of Concept 3. Concept 3 is based on Concept 2 and shares the same wing orientation. Simplification is obtained by removing two struts and relocating attachment points of others.*
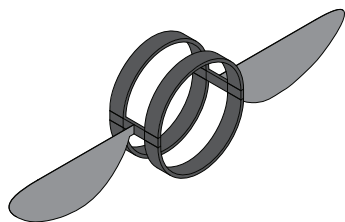


**Figure 4.12:** *Artist impression of Concept 4. Two wings and two rings with a horizontal flapping plane. The use of two rings allows for control of the structure by the possibility of introducing a phase shift between the rings.*
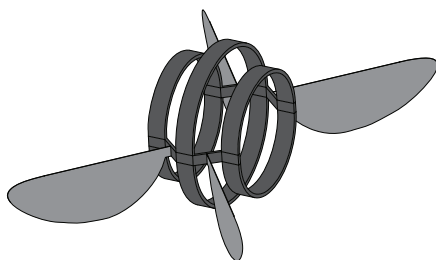


**Figure 4.13:** *Artist impression of Concept 5. Extension of Concept 4 to allow for the use of four wings. Three rings are used to store elastic energy.*

compliant structure. Second, being self contained it offers a multitude of configurations in which the rings can be combined with a compliant mechanism to drive the wings.

Based on the ring, five concepts have been introduced, all of which are candidates for being used as the resonant base for the wing actuation mechanism. The essence of the mechanisms is the combination of one or multiple rings, for elastic energy storage, and compliant mechanisms, to transform and amplify the linear motion of the ring, into a large wing sweeping motion. The design and analysis of the wing will be covered in Chapter 6.

The requirements for the current developments of the wing actuation mechanism for the flapping-wing MAV mentioned in Section 4.3 are geared towards the implementation of resonant principles while maintaining a very simple design. The wing design is effectively decoupled from the thorax design by placing the passive wing pitching mechanism in the wing or wing root. The current, essentially planar, mechanisms comply with all the described boundary conditions. The design specification and detailing of these concepts will be covered in Chapter 5, in which a selection will be made for the most feasible concepts. The chosen concept will be realized and tested.

# Chapter 5

# Analysis

## 5.1 Introduction

The concept of exploiting resonance for the actuation of the wings in a flapping-wing MAV has led to various concepts. These concepts, as proposed in Chapter 4, are all based on a combination of a ring and a compliant mechanism. The ring functions as the elastic energy storage unit while the compliant mechanism is used to transform and amplify the ring deformation to a large rotation. The basic setups have been proposed on a conceptual level. Consequently, they have to be analyzed in more detail before they will be utilized in a prototype. The analysis includes sizing of prototype, choice of materials and development knowledge. This analysis includes the kinematic and dynamic analysis of the structures. Clearly, such a study may lead to improvements of the concept designs as well.

The analysis of the design is performed in two steps. The first step in the design is the development of a basic modeling approach, which is used to gain knowledge on the working principles of the designs [16]. This is basically an exploratory search to gain insight into the possibilities of the currently proposed resonating structures. In addition knowledge on the manufacturing techniques required to realize the proposed concept will be generated, as well as exploring the wealth of materials available and needed for realizing the flapping-wing MAV wing actuation mechanism. The basic modeling strategy is also used for the selection and validation of analysis techniques for the design. The second step is the development of a detailed design of the flapping-wing MAV wing actuation mechanism. This includes the application of analysis tools to characterize and optimize the design [18].

Three different tools are used to characterize and support the design of the flapping-wing MAV thorax. Kinematic analysis is used for obtaining correct dimensions and estimates for the achievable movement range. Dynamic analysis,

65

in the form of rigid body dynamic models, is used to review the resonant state and corresponding movement patterns of the mechanism as well as determination of dimensions. Finally, Finite Element (FE) models are used to gain more detailed insight in the eigenfrequencies and transient behavior of the mechanisms. The initial design is analyzed by all three mentioned analysis tools. The detailed design is not analyzed by rigid body models since this step does not add to the understanding of the functioning. The structure of this chapter follows the path of increasing complexity in both analysis and design.

The wings are included in this chapter as rigid bodies that constitute a moving mass and include a damping factor. Detailed information on the aerodynamics, such as the efficiency of lift production, is not taken into account. This means that for the analysis of the resonant and transient behavior of the structure only the wing drag is taken into account. The structural, kinetic and morphological requirements on the wing follow from the results of this chapter and are used as the basis for the next chapter, *i.e.*, Chapter 6 which covers the analysis and design of the wings. There exists an inherent coupling between this chapter and Chapter 6 described by the fluid–structure interaction which is the basis for correct functioning of the flapping-wing MAV actuation mechanism. This interaction implies that, although separately analyzed, the design choices made, in either the wing or the thorax, will influence the other and thus result in changes of the behavior of the overall structure. It is for this reason that the wings, in simplified form, must be incorporated in the analysis of the flapping-wing MAV thorax.

## 5.2   Choice of concepts

The various concepts presented and conceptually analyzed in Chapter 4 are all possible candidates for the wing actuation mechanism. The concepts offer possibilities for wing actuation and vary in different aspects. In order to make a selection of those to be tested, some concepts can be excluded beforehand. The criteria for these exclusions are based firstly on aspects concerning actuation, and secondly stability requirements posed by later application as a flying platform.

For convenience, the emphasis is placed on concepts which require only a single actuator. Since simplicity is paramount for this stage of the design, which is at proof-of-principle level, multi-actuator concepts are not reviewed. The two concepts which rely on the use of multiple actuators, see Section 4.7.1, Concepts 4 and 5, are thus excluded. In future applications, when more emphasis is placed on possibilities concerning control, these concepts are very promising and should be reviewed extensively.

When looking at the flapping-wing MAV, from a system perspective, an overall requirement is the need for low complexity and power usage. A simple manner of reducing control requirements is by employing a certain level of passive stability into the design. This can be done by positioning the center of gravity significantly below the effective working point of the lift force in order to exploit pendulum

stability. Another option is the use of four wings which, in combination with the above mentioned positioning of the center of gravity, allows for increased levels of passive stability. These four wings should then be positioned at four corners of the design. Although passive stability can be obtained by making use of a two-winged setup, see, for example [138], the correct positioning of the center of gravity is far easier when using four-winged concepts. Based on these criteria Concepts 2–5 are usable. However, in order to gain insight in functioning, the two-winged concepts are included in the current analysis because of their low complexity.

In summary, the concepts which will be reviewed in this early design stage are Concepts 0–3. These concepts were reviewed on a conceptual level in Section 4.5.

## 5.3   Resonance in flapping-wing MAVs

As described in Chapter 2, the insect thorax exhibits resonance during steady state flight or hovering and this helps to reduce the mechanical power required for wing movement. This property is partially or fully exploited in different existing flapping-wing MAVs as described in Chapter 3. Exploitation of resonance seems very promising to reduce power usage within the wing actuation mechanism currently under development. To support the claim of efficient power usage by exploiting resonance a simple but useful approach is presented here.

An abstraction of the thorax-wing system is shown in Figure 5.1. In its simplest
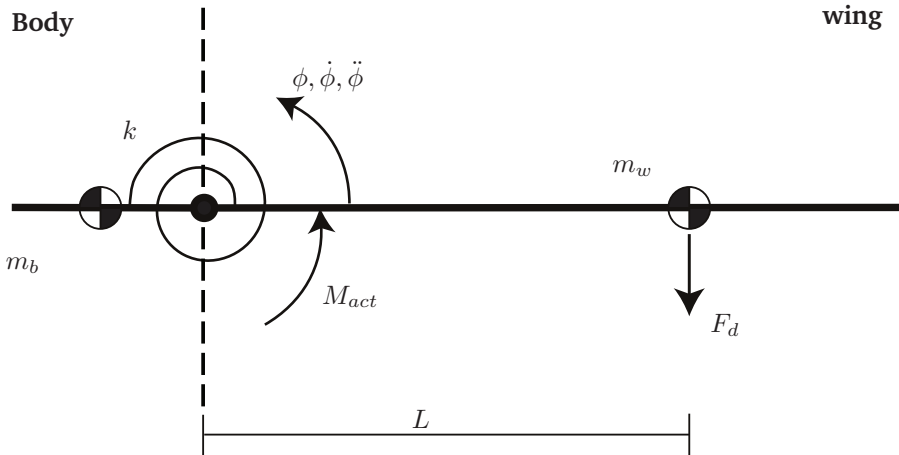


**Figure 5.1:** *Schematic representation of the insect/flapping-wing MAV wing actuation mechanism. The system is reviewed as being single degree of freedom represented by the wing sweeping angle. Separation between wing and body is indicated by the dashed line. Within this model study, the body is assumed significantly heavier than the wing which, body motions are therefore neglected.*

form, the insect thorax or proposed flapping mechanism for the flapping-wing MAV system can be described as a one-dimensional damped system. The single degree of freedom, $\phi$, corresponds to the sweeping angle of the wings as depicted in Figure 5.1. In this simplification the moving mass is lumped in a wing mass and the thorax stiffness collected in the torsion spring. Wing and thorax are separated by a dashed line to indicate the relevant masses of the insect or flapping-wing MAV.

The properties of this representation of the insect flight system can be described by the following properties: $m_w$ and $m_b$ denote the generalized inertia properties of the wings and body, respectively. In general the body does not show significant movement and is assumed stationary here, based on the large difference in mass between $m_w$ and $m_b$ and symmetric wing orientations. The spring constant $k$ reflects the generalized stiffness properties of the system. Inertia $I$ represents the equivalent inertia of the system and includes all wings present. The length $L$ is used to include a measure of size of the system. This length is used to position the attachment point of the aerodynamic forces. The attachment point has a fixed ratio to the wingspan. The aerodynamic drag on the wing is applied to the system by a velocity dependent force on the aerodynamic center of pressure and is depicted in Figure 5.1 by $F_d$. The actuation is applied as a torque at the wing root, designated $M_{act}$. The lift force, $F_l$, is assumed to be orthogonal to the wing velocity at all times and depends solely on the angular wing velocity and acts on the same position as $F_d$. The question is, based on this simple representation, which factors allow for a low mass, efficient system? The objective is to minimize both the mass and power delivered by the actuator.

The basis for the approach is the one-dimensional equation of motion describing the system:

$$I\ddot{\phi} + k\phi = M_{act}(\dot{\phi}) - M_d(\dot{\phi}). \tag{5.1}$$

In order to include the external forces a simplified expression for lift and drag is required. The expressions for the drag torque and lift force are crudely approximated by

$$M_d = C_{d,c} L^3 \dot{\phi}^2 \frac{\dot{\phi}}{\sqrt{\dot{\phi}^2}} \tag{5.2}$$

and

$$F_l = C_{l,c} L^2 \dot{\phi}^2. \tag{5.3}$$

In which the drag force is viewed as a torque on the wing root using the characteristic length of the insect or flapping-wing MAV. Note that the drag force always opposes the velocity. These are simplified expressions and subsequently do not capture the finesses in lift and drag production by insect or flapping-wing MAV wings precisely, therefore $C_{d,c}$ and $C_{l,c}$ are not dimensionless here. The coefficients are defined as $C_{d,c} = \frac{1}{2}C_D S\rho$ and $C_{l,c} = \frac{1}{2}C_L S\rho$, in which $C_D$ and $C_L$ are the dimensionless lift and drag coefficients, $S$ is a measure of wing surface area and $\rho$ is the density of air. However, for the simplified review of the system here

they are adequate. A harmonic forced motion is assumed, $\phi = A\sin\omega t$, based on simple harmonic wing sweeping motions observed in insects. The cycle time $T$ is related to $\omega$ by $T = 2\pi/\omega$. Maximum amplitude $A$ is restricted by the wing setup of the insect or flapping-wing MAV. The required actuator torque can then be written as:

$$M_{act} = (k - m_w L^2 \omega^2) A \sin\omega t + C_{d,c} L^3 A^2 \omega^2 [\tfrac{1}{2}\cos 2\omega t + \tfrac{1}{2}] sgn(\cos\omega t). \quad (5.4)$$

In this description of the actuator torque two contributions can be distinguished. The first term is the torque required to overcome wing inertia. The second term is the torque required to overcome wing drag. Now we use the definition of the natural frequency, $\omega_0^2 = \frac{k}{m_w L^2}$, to highlight the importance of resonance:

$$M_{act} = A m_w L^2 (\omega_0^2 - \omega^2) \sin\omega t + C_{d,c} L^3 A^2 \omega^2 [\tfrac{1}{2}\cos 2\omega t + \tfrac{1}{2}] sgn(\cos\omega t). \quad (5.5)$$

So far there is no link to the lift force required to keep the system hovering. Since hovering is one of the most energy demanding states it is used in this model study. In order to incorporate the minimum average lift requirements imposed by vehicle mass a constraint on lift generation has to be defined. Starting from average lift:

$$\bar{F}_l = \frac{1}{T} \int_t^{t+T} F_l \, dt, \quad (5.6)$$

which, using Equation (5.3), results in the expression

$$\bar{F}_l = \tfrac{1}{2} C_{l,c} L^2 A^2 \omega^2. \quad (5.7)$$

And can be used to introduce a minimum lift constraint to the system. For a given average lift generation we have the design requirement:

$$A\omega = \sqrt{\frac{\bar{F}_l}{\tfrac{1}{2} C_{l,c} L^2}}. \quad (5.8)$$

As mentioned, flapping amplitude $A$ is fixed by the design and thus the only parameters which can change are the wing size and flapping frequency. The minimum average lift required to sustain hovering flight is determined by the total mass of the vehicle, body and wing, given by:

$$\bar{F}_l = m_{tot} g, \quad (5.9)$$

in which $g$ is the gravitational acceleration and $m_{tot} = m_b + m_w$. Equations (5.8) and Equation (5.9) are substituted in Equation (5.5) in order to gain the following expression for the actuator torque:

$$M_{act} = A m_w L^2 (\omega_0^2 - \omega^2) \sin\omega t + 2\frac{C_{d,c}}{C_{l,c}} L(m_{tot}) g [\tfrac{1}{2}\cos 2\omega t + \tfrac{1}{2}] sgn(\cos\omega t) \quad (5.10)$$

It can be noted that a phase shift exist between the damping force and inertia forces. The lift coefficient for flapping wings is significantly larger than the drag coefficient. The ratio between the two is typically in the range $0.1 \leq \frac{C_D}{C_L} \leq 0.25$, see Ellington [46]. This ratio only describes efficiency of lift production and does not influence conclusions which can be drawn from this system.

When looking at Equation (5.10) a number of aspects come forward. These aspects are generally valid for flapping-wing MAVs without making very large assumptions with respect to scaling and frequencies. These aspects are:

- The first aspect which can be noticed, when looking at the first term, is that driving the system outside the natural frequency will require a larger actuation torque. When looking at this setting of flapping-wing MAVs, a larger actuation torque requires a more powerful and heavier actuator. The addition of mass is undesirable and should be avoided. From this view exploitation of resonance is desirable.

- The aerodynamic force requirements are determined by the overall mass of the system. There is no obvious way to reduce energy expenditure here, besides the reduction of overall system mass.

- The ratio between inertial and aerodynamic forces can be used to tune the amount of resonant amplitude amplification of the system. As well as to tune the sensitivity of the system to frequency changes.

- A special case exists when the aerodynamic forces, the second term, are significantly larger than the inertial forces. This can come forward in flapping-wing MAVs which have extremely light weight wings, or wings which are large and slow moving compared to the overall mass of the structure. When this is true exploiting resonance does not yield significant energy reduction.

- These conclusions are valid for wing motions which are not purely sinusoidal. A wave form which is not sinusoidal will introduce extra terms but the minimum in actuator force remains close to the resonant frequency, slightly shifted depending on magnitude of the damping.

In summary; the flapping-wing MAV thorax should be driven in resonant frequency of the system. The total system should be designed such that the resonant frequency is optimal for the aerodynamics of lift generation and that the overall mass of the system is low.

## 5.4   Initial design

Based on the ring concept, various options exist to mount the wings. As the deformation of the ring is small when compared to deflections of the wing, the way

in which the wings are kinematically connected to the ring determines the amplitude amplification which can be reached. Two different connections can be distinguished: the connection can be very compliant, implying the wings can be seen as a deforming part of the resonating structure and thereby provide amplitude amplification. Or as a compliant mechanism, in which comparatively rigid structures are coupled by elastic hinges, implying the structure uses mechanical amplification to provide amplitude amplification, both have been discussed in Section 4.4.2.

In this section, four concepts are studied to explore the possibilities of the application of ring type resonators in flapping-wing MAV flight. These structures are studied first numerically, later they are realized and tested. The four concepts are explained in Section 5.4.2.

### 5.4.1 Materials

In order to be able to quantify the dynamic behavior of the concepts a selection of materials has to be made which will be used to build prototypes. In this exploratory phase, mass is not of major concern since focus is on the performance evaluation of resonant principles, not on absolute performance. The selection of the materials which is used to create the prototypes that are to be tested is based on various criteria which vary for the different parts of the design. For example the ring, the material has to have excellent elastic properties and low hysteresis. Besides specific criteria for the individual parts the materials should be readily available and relatively easy to use since multiple prototypes have to be made. The material types used in the realization of the prototypes are equal for all concepts in this section.

The materials for the thorax include: spring steel for the ring and the elastic

**Table 5.1:** *Materials used to realize the initial concepts. The material used are selected based on functional requirements, such as specific energy storage, not strictly on mass based requirements. Note that the table describes the cross sectional properties of the material. This due to the fact that various lengths will be used for the different designs.*

| Material | Part | Width [mm] | Thickness [mm] | Young's modulus [GPa] | Density [kg m$^{-3}$] |
|----------|------|-----------|----------------|-----------------------|----------------------|
| Spring steel | Ring | 12.5 | 0.05 | 210 | 7850 |
| | Hinges | 2 | 0.05 | 210 | 7850 |
| UD carbon | Struts | 2 | 0.4 | 145 | 1500 |
| | wingspar | 2 | 0.4 | 145 | 1500 |
| PET | Wingmembrane | ~12 | 0.1 | 2-4 | 1100 |

hinges. Spring steel is also used for the wings in Concept 0. Unidirectional carbon is used for the rods for the struts. The materials are listed in Table 5.1 which shows thicknesses, widths and physical aspects. Most parts, except for the wing membrane, are strip based. For realization shorter pieces will be used.

**Wings**

In order to include some form of aerodynamic damping in the experiments the prototypes are equipped with very simple wings. These wings serve no other function than to act as surfaces on which an aerodynamic drag force acts. As such, the wings do not possess the possibility to express a pitching motion and therefore cannot generate lift. In a later stage the wings should be replaced by aerodynamically efficient wings in order to produce lift. The wings are constructed from a relatively stiff Polyethylene TerephThalate (PET) membrane which is partially supported by a length of unidirectional carbon fiber spar as listed in Table 5.1.

**Actuation**

The actuation of the model during tests will be performed by a solenoid actuator. This type of actuator possesses low specific power density, see Table 3.2. Expected actuation frequencies between 20-40Hz are feasible using solenoid type actuators. Since solenoid actuators are usually very powerful, maximum actuation force is limited by the structure not the actuator. The chosen actuator is a small COTS pull-type solenoid actuator, Dialight BLP Ltd. type 45-120-610-620, typically actuated on 12V. The actuator is used slightly beyond specified stroke length by extending the stroke to 6 mm.

## 5.4.2   Kinematic and dynamic analysis

**Rigid body modeling**

The analysis of both the kinematic and dynamic behavior is based on a two-dimensional multi-body representation. This analysis is chosen based on the assumption that, while elastic hinges are used, their effects are very local and thus rigid body theory may be used, known as pseudo rigid-body assumption. The elastic hinges are implemented using equivalent elastic models based on pseudo rigid-body theory from Howell [68]. The chosen approach for the dynamic analysis is Newton-Euler with constraints. The equations of motion are derived by making use of the principle of virtual power while the constraints are incorporated in to the virtual power balance by using Lagrange multipliers, see van der Linde and Schwab [126]. The resulting system of Differential Algebraic Equations (DAEs) is integrated over time by making use of the fourth-order Runge-Kutta method with fixed time step. In order compensate for drift a constraint projection step is

used to stabilize the results, see Eich-Soellner and Führer [41]. The models are numerically analyzed in the Matlab® environment.

**Overview of concepts**

The basic conceptual structures are presented and discussed in Chapter 4. The concepts are discusses here on a functional level to explain if the modeling strategy is appropriate for each concept.

**Concept 0**    The first design is the simplest possible extension of the ring to include flapping wings. The wings are included as a deformable part of the resonator in the form of a bending beam, which is rigidly coupled to the ring at the center position. The main mode of amplitude amplification is the bending of the wings. This feature is not found in insects but still interesting to test as an engineering solution. The structure is driven by a linear actuator inside the ring, which is coupled to the ring in such a way that its direction of actuation is perpendicular to the wingspan. The multi-body equivalent model is shown in Figure 5.2. Note that in this case wing bending deformation is lumped into the torsional spring at the wing base.

**Concept 1**    The second design exploits a compliant mechanism for mechanical amplification. The wings are elastically connected to a side of the ring. Struts are in place, which connect the opposite side of the ring to the wing. By these means the linear motion of the ring is converted into a large rotation at the wing base. The wing connection setup is inspired by the work done by Cox *et al.* [29]. All compliant connections are flexure hinges. The actuator is connected in the same manner as described in Section 5.2. The main mode of amplitude amplification is now carried by the compliant mechanism, note that the wings do not store elastic energy in this design, as they are modeled as being rigid. This design is better suited for a pseudo-rigid-body representation then Concept 0, see Figure 5.3.

**Concept 2**    The third design is, in essence, an extension of the second concept. The number of wings is doubled to four. A major benefit of this setup is the positioning of the wings. Their stroke plane, as compared to the center of mass, is far better suited to support hovering flight. The struts now interfere with each other, meaning that the realization has to include a small offset. The pseudo-rigid-body representation is shown in Figure 5.4.

**Concept 3**    The fourth design is a simplification of the third, that is, two struts have been removed. The side of the remaining struts which was coupled to the ring is now coupled to the wing at the same position as the other side. This is primarily for weight reduction. The benefits with respect to the orientation of the
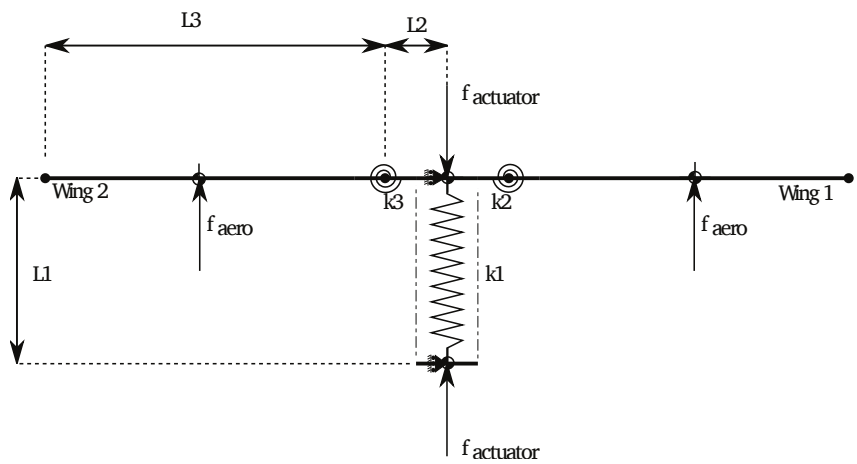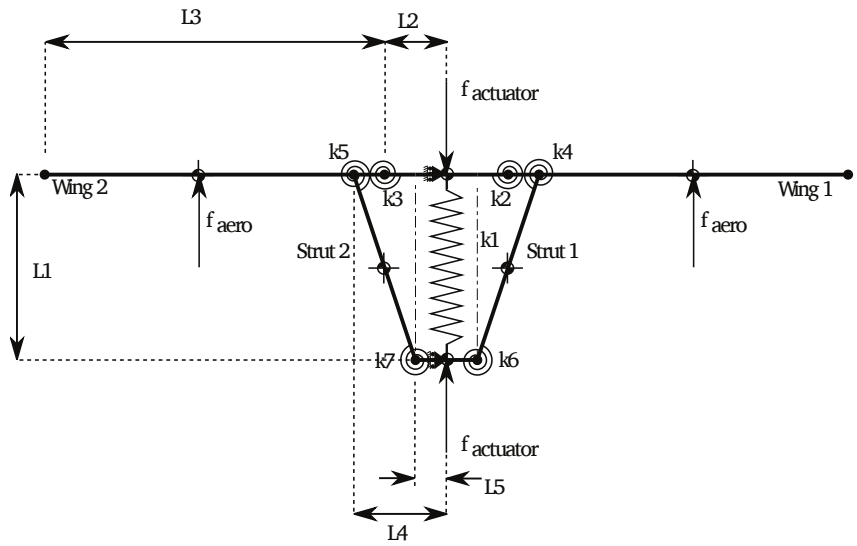
**Figure 5.2:** *Rigid-body model for Concept 0*



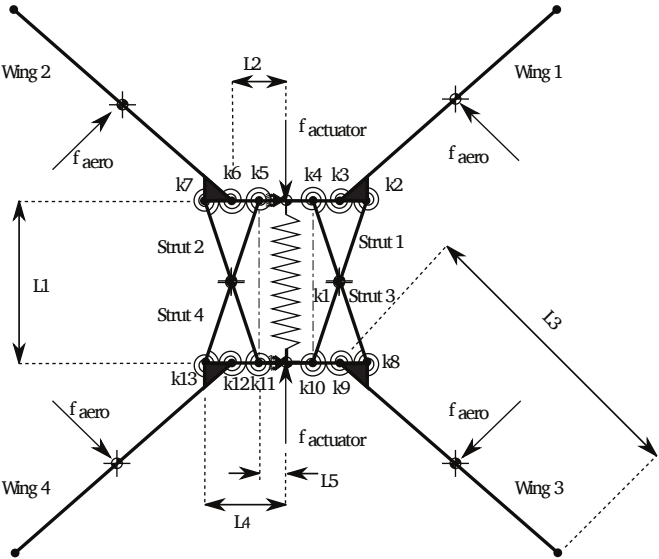**Figure 5.3:** *Rigid-body model for Concept 1*

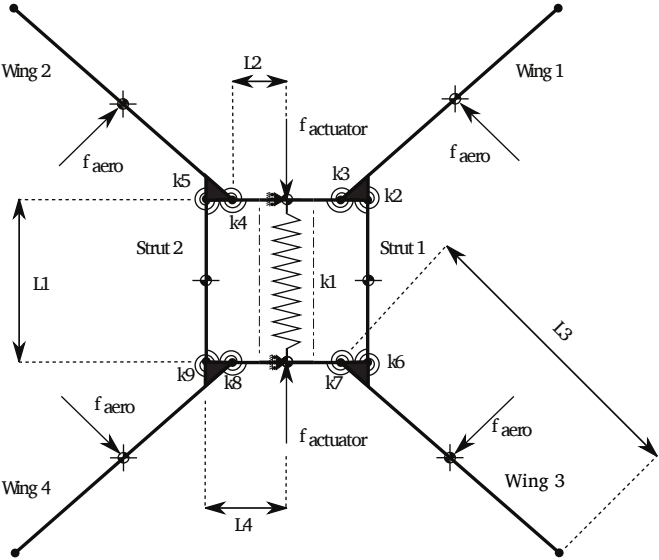**Figure 5.4:** *Rigid-body model for Concept 2*



**Figure 5.5:** *Rigid-body model for Concept 3*

stroke plane are also valid for this setup. The pseudo-rigid-body representation is depicted in Figure 5.5.

**Dimensioning**

The first step is the kinematic analysis of the models. Setting up the multibody model involves the creation of constraint equations. These constraint equations can be used for performing kinematic analysis. As mentioned before this is an explorative setting, accuracy is therefore of lesser importance. The kinematic requirements are used to size the initial designs mostly based on the dimensions and stroke of the actuator. In this way the length of the links and ring diameter have been determined. These dimensions determine the amplification factor of the mechanism. The maximum stroke of the concepts is kinematically restricted. The mechanism proposed for the two winged models is restricted to 120°. The usage four wings in the same plane restricts the maximum stroke to 90°The usable actuator stroke is 6 mm. The actuator determines the dimensions of the ring since it has to be placed inside, for all models a diameter of 28 mm. To create a large safety margin, and to avoid overloading the structure, the current amplification ratio is chosen conservatively. Focus is on obtaining a resonant state while large amplitude wing sweeping motions will be obtained in more advanced models.

Based on these input constraints, the mechanism dimensions which give the correct, but conservative, amplification ratio are given in Table 5.2. These values have been determined by a non automated analysis process of the constraint equations set up for the multibody dynamic analysis. The definitions of these di-

**Table 5.2:** *Dimensioning of initial designs. Lengths are with reference to the pseudo rigid-body models described in Section* 5.4.2.

| Concept | L1 [mm] | L2 [mm] | L3 [mm] | L4 [mm] | L5 [mm] |
|---------|---------|---------|---------|---------|---------|
| 0 | 28 | 10 | 50 | - | - |
| 1 | 28 | 10 | 50 | 13.5 | 6.75 |
| 2 | 28 | 8.5 | 50 | 12.5 | 6.75 |
| 3 | 28 | 7.5 | 50 | 10 | - |

mensions can be found in Figures 5.2–5.5. The dimensions of the model are based strictly on idealized assumptions with respect to the kinematics and function as a basis for the dynamic analysis which includes material densities and stiffnesses.

**Dynamic analysis**

After the initial scaling of the concepts has been completed, the dynamic behavior of the models has to be studied. In order to get some insight in real-live behavior

both actuation and aerodynamic damping have to be included, whereas the lift components are not included. The lift, and effectively also the drag, are dependent on the wing kinematics. Since the analysis is currently two dimensional, only the drag part of the aerodynamics is included in the form of a viscous damping force on the wing in the center of mass. This drag force is determined such that it the energy expenditure corresponds to the drag force generated by a generic wing of the same size. The force is determined from the aerodynamic model presented by Deng *et al.* [34] and is applied such that at mid stroke, when velocities are highest, it gives the most accurate results. This approach is well suited for the current exploratory setting and used by Tantanawat and Kota [122], among others.

The actuation is implemented by applying a sinusoidal force at the intended position of the actuator. The multi-body representation of the four models is depicted in Figures 5.2–5.5 in which the attachment positions of the actuation and aerodynamic forces can be seen. Besides the aforementioned assumptions with respect to actuation and aerodynamics, there have been assumptions on the representation of the mass and stiffness properties of the ring and hinges. The mass distribution of the ring is assumed lumped in two bodies for all models. The force of the actuator acts on these bodies and the mass of the actuator is also lumped here. The actuator mass is much larger than the mass of the ring indicating that the simple interpolation function chosen to lump the mass of the ring has a small influence on the results.

The elastic behavior of the ring is assumed to be linear in the deformation range imposed by the maximum stroke of the actuator. Stiffening effects will occur if the ring is deformed too extensively, resulting in an increased resonant frequency for very large amplitude resonance. To increase predictability of the system nonlinear stiffening effects are avoided by limiting ring deformation. The equivalent spring constant of the ring is determined by the ring diameter, width and thickness as well as the material. The equivalent ring stiffness of the currently used steel ring is 206 N/m for linear deformations.

The torsional spring constant for the flexure hinges is determined by inspecting the pseudo rigid-body equivalent [68]. In this manner the equivalent torsional spring constant is determined for all flexure hinges. The hinges used share the same length and as such share the same equivalent spring constant which can then be used in the rigid body analysis. The equivalent spring constant is $1.1 \times 10^{-3}$ Nm/rad.

The path followed is to first determine the resonant frequency. This frequency is determined in an unactuated fashion. The frequency which is determined is then used as the driving frequency in the model which is actuated. The actuation force is adjusted such that the amplitude of the wings then corresponds to the desired value.
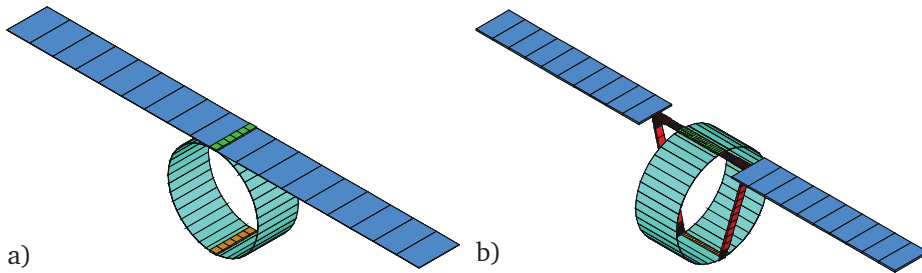
**Figure 5.6:** *FE-models of Concept 0, see a), and Concept 1, see b). The models consist of beam elements. The local cross-sectional areas and colors have been used to indicate materials used for the different parts.*
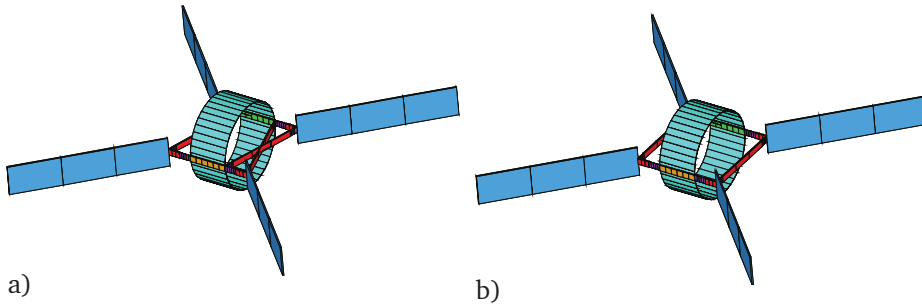


**Figure 5.7:** *FE-models of Concept 2, see a), and Concept 3, see b). The models consist of beam elements. The local cross-sectional areas and colors have been used to indicate materials used for the different parts.*

**Finite element modeling**

In order to study, in a more accurate manner, the behavior of the different concepts a FE-modeling procedure is used. The FE-analysis is performed to gain insight in how the designs, found by the multibody analysis, react to large amplitude resonance. The FE-models are parameterized to be able to easily implement parameter changes. Parameters from the multi-body analysis are thus easily implemented. As described earlier, the structures are composed of strips and struts and elastic hinges. Two options exist for modeling these structures, shell and beam elements. Since focus is on speed and flexibility in the analysis the choice for the simplest version is made. Thus, beams are chosen to discretize the structures. Beams are well suited for representing the bending aspects of the anticipated deformations, and although shells are the obvious choice for the wings, as no wing deformation of the wing membrane has to be modeled beams are also a valid choice for the wings. The concepts are modeled using a commercial FE-code, namely Ansys®.

The FE analysis has two stages: First a modal analysis is performed to find the

eigenfrequencies of the designs, more specifically the eigenfrequency of interest, which at this time, is the one that corresponds to hovering flight. The frequencies so determined are used as the actuation frequency in a nonlinear transient analysis to simulate the responses due to the actuation at resonance. Two factors exist which influence the resonant response when deflections become large. First, geometrically nonlinear behavior, especially of the ring in case of large deformations, and second, the magnitude of the damping which, when the value is large, influences the resonant behavior. The value of the damping is chosen such that the energy expenditure corresponds to that of a typical aerodynamic loading case.

The damping is implemented by applying rotational viscous dampers at the wing root, this assumption is valid for Concepts 1, 2 and 3, which have relatively stiff wings. For Concept 0 linear dampers have been used which attach to the aerodynamic center of pressure, which is a reasonable assumption for small and intermediate wing deflections. As in the multi-body analysis, the damping value is chosen such that it represents the drag force of the aerodynamics. Actuation is implemented by applying sinusoidal force on the intended position of the actuator, similar to the multi-body analysis. The force of actuation is adjusted such that the flapping angles obtained are equal to those used as input for the kinematic analysis, see Section 5.4.2. Boundary conditions are applied such that they represent the conditions in free flight. The models are fixed in lateral, vertical and rotational directions at the actuator attachment points and free in the flapping plane. No net movement will result because the actuator force is applied symmetrically. The material properties and topology used in the FE models represents the real material properties and topology, which are later used to realize the structures.

The FE-models for all concepts are shown in Figures 5.6 and 5.7. The results of the analysis are given in Table 5.3 on Page 85.

### 5.4.3   Realization

In order to review the value of the predictive capabilities of modeling methods presented and to view how the concepts perform, prototype structures have been built and tested in a laboratory setup. The first part is the realization of the models. The materials that are used to build the models are listed in Table 5.1. The construction principles are discussed in this section.

The main part of the designs is the ring. The ring is constructed from spring steel starting from a strip of material. The ring is formed by using spot welds to attach the ends to each other. The resulting ring has a small overlapping section. The hinges are formed by cutting the required sections from spring steel sheet. These sections are bent into shape and spot welded to the ring. The struts are attached to the hinges by cyanoacrylate glue. This glue is again used in the manufacture of the wings in which the PET sheet is attached to the main wing spar. The actuator is placed inside the rings by attaching the endpoints to the ring by
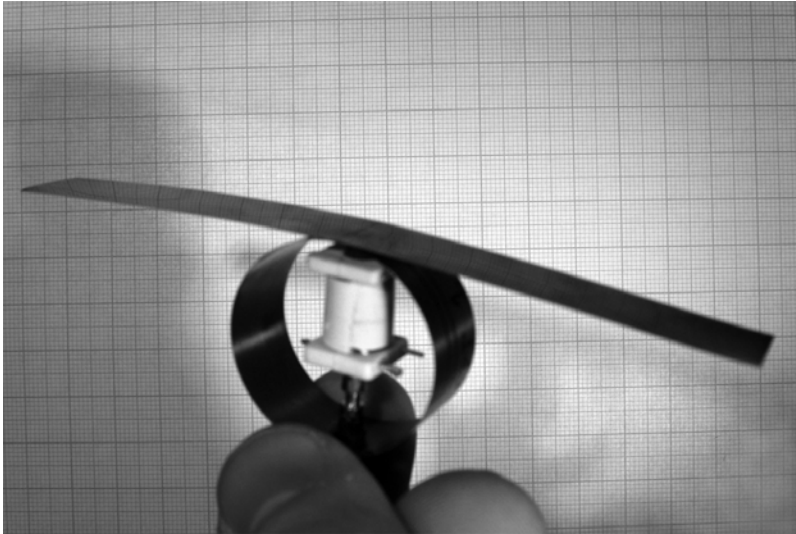
**Figure 5.8:** *Concept 0: Two winged design, amplitude amplification by resonance of compliant structure. Wings are part of the system used to store potential energy.*
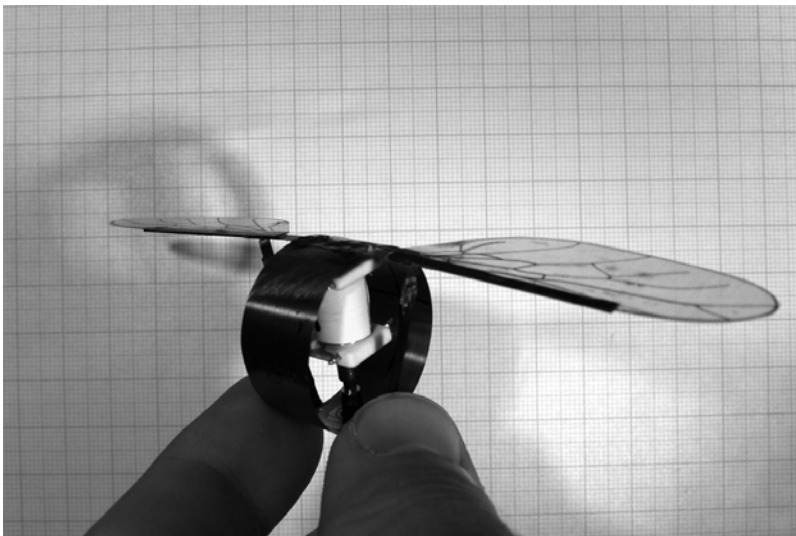


**Figure 5.9:** *Concept 1: Two winged design, amplitude amplification based on a compliant mechanism.*
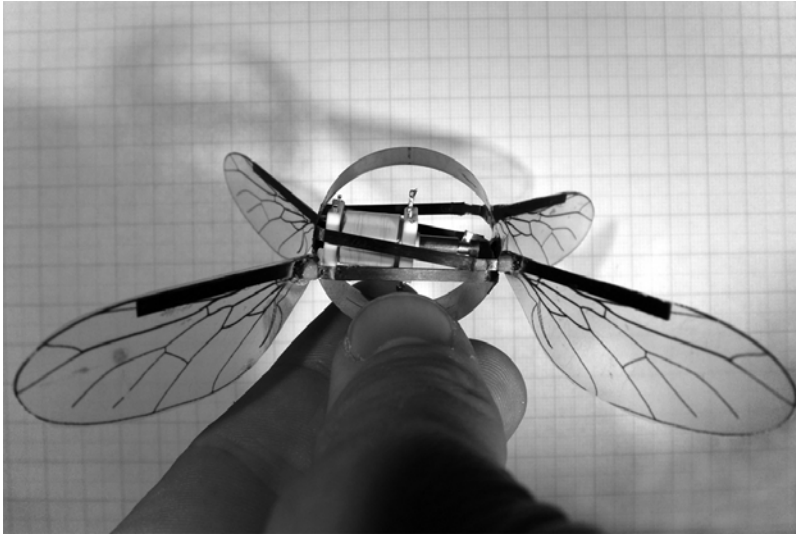
**Figure 5.10:** *Concept 2: Four winged design, extension of Concept 1. Horizontal flapping plane.*
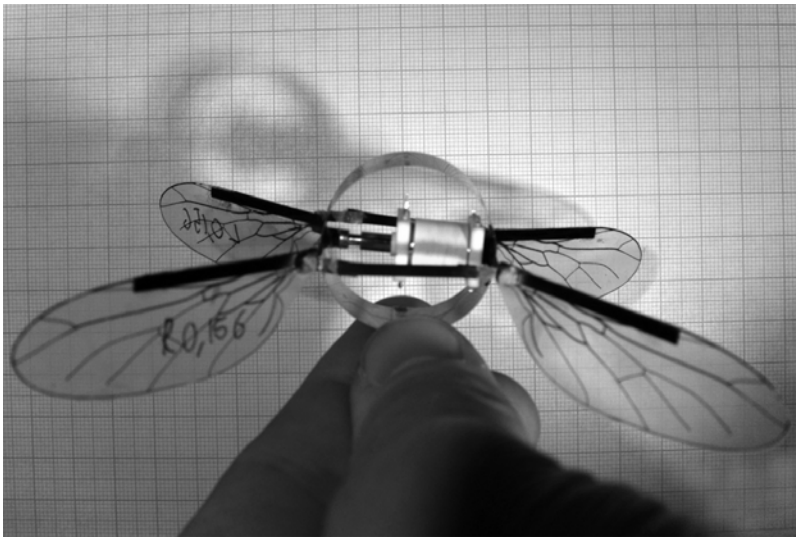


**Figure 5.11:** *Concept 3: Four winged design, simplification of Concept 2. Horizontal flapping plane.*

small circular rubber pieces. These pieces have negligible mass as compared to the rest of the structure. The models are shown in Figures 5.8–5.11.

### 5.4.4   Experiments

The prototypes are tested in an experimental test setup. In this setup the proto-types are suspended from the power leads in order to make photographs of the actuated models. The suspension is such that the prototypes are able to resonate freely but not move in horizontal or vertical direction, see Figure 5.12. The model is placed in front of a wall on which a grid is placed to allow for making judgment on basis of photographs. Visual inspection is used to estimate the maximum
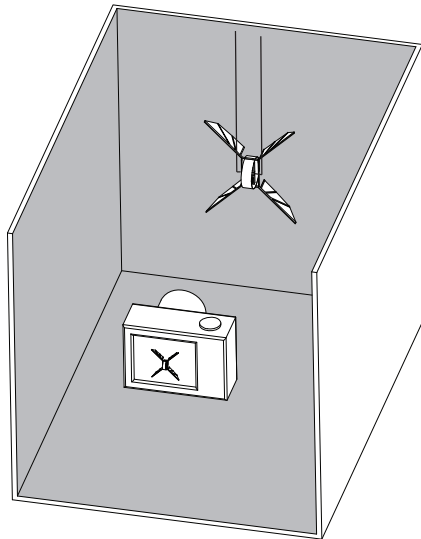


**Figure 5.12:** *Test setup to review resonant frequency and wing sweeping amplitude, showing suspended model and camera. The model is suspended from the power leads, significant movement is not expected due to the absence of lift production.*

deflection of the wings to search for resonance. This process is supported and guided by results from the numerical modeling. As in the numerical modeling, only the eigenfrequency that corresponds to flapping flight is of interest, this is not necessarily the first eigenfrequency. Photographs are made using a shutter time which is significantly larger than the cycle time at resonance. Amplitudes can be obtained from the photographs.

The results of the numerical modeling, finite element and multi-body dynamics, and the testing of the prototypes are all important for the review of the designs. Early indications from results of Concept 0 indicate that this concept is not able to convey enough power from the actuator to the wings while maintaining
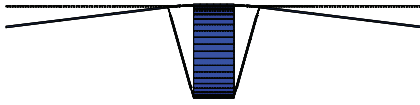
**Figure 5.13:** *Concept 1: FE-model showing showing the resonant mode. Initial configuration shown.*
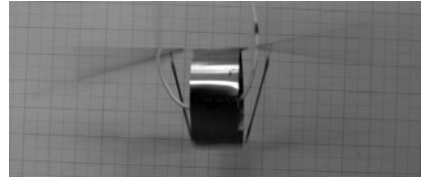


**Figure 5.14:** *Concept 1: Realized model showing the resonant mode.*
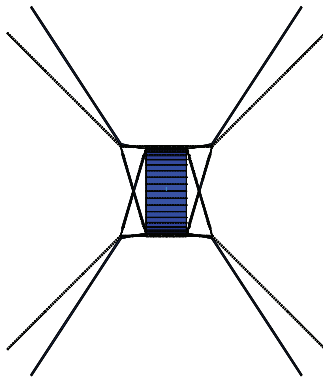


**Figure 5.15:** *Concept 2: FE-model showing showing the resonant mode. Initial configuration shown.*
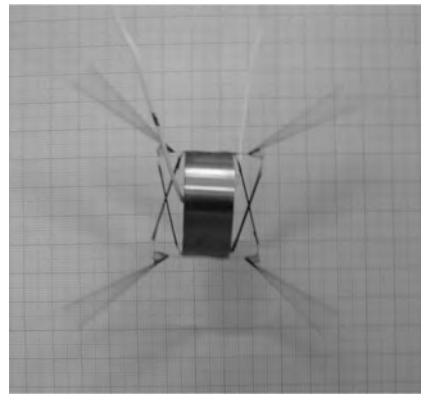


**Figure 5.16:** *Concept 2: Realized model showing the resonant mode.*
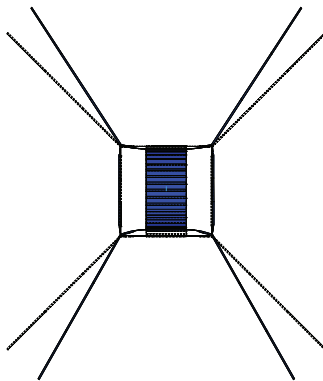


**Figure 5.17:** *Concept 3: FE-model showing showing first resonant mode. Initial configuration shown.*
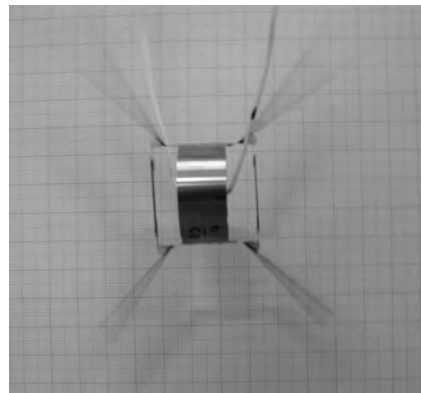


**Figure 5.18:** *Concept 3: Realized model showing the resonant mode.*

a large amplitude wing stroke. The predicted eigenfrequencies are low, using the current actuation and realization, the model could not produce large deflections. We will therefore focus on Concepts 1, 2 and 3.

The results of the transient analysis in the FE-models shows that the concepts are able to produce large deflections while being actuated at resonance. The deflections of the models are shown in Figure 5.13–5.17, superimposed on the undeformed configuration.

Using the described laboratory setup, the models can be measured. The designs are actuated at their resonant frequency. This frequency has been previously found by sweeping through the expected range around the intended eigenfrequency from the FE-analysis. Photographs of the concepts, actuated at resonance, are shown in Figure 5.14, 5.16 and 5.18, for Concepts 1, 2 and 3, respectively.

Both the results from the numerical modeling and the realized designs are encouraging for the use of rings as the main energy storage in flapping-wing MAVs. There are differences between the FE-models and the laboratory tests. First, large deflections are easily obtained by the FE-models. For the laboratory tests it proved more difficult to obtain large amplitude amplification. Second, the eigenfrequencies from the FE-models and the test are given in Table 5.3, which shows the difference between the two. Large differences exist, but these results still show for the predictive value of the FE-modeling. These differences arise from both modeling errors and errors in the realization.

Concept 1 should be studied more to investigate other configurations and parameters which might improve performance. Aim here is at hovering flight, which makes this design less suitable. The positioning of the wings makes it difficult to have a horizontal flapping plane. This problem does not exist for Concept 2 and 3. The configuration with four wings is well suited for a hovering platform. Both designs are able to function with large amplitude deflections. The differences in strut topology makes their functioning different. When general dimensions are the same, then the wings in Concept 3 move half that of those in Concept 2 with identical ring deformation. They are both usable when dimensions, of hinges and struts and their attachment points are further optimized. FE simulations have shown that Concept 3 has eigenmodes around the main flapping eigenmode which might be interesting for control purposes, this feature is open for further study. However, at this point in the design having two adjacent eigenfrequencies might have negative influence, due to mode switching issues.

## 5.5   Discussion initial design

It can be concluded that both the multi-body approach and the FE approach, are suited for the analysis and pre-design of the structures studied here. Depending on the type of information required, a choice between the two has to be made. The multi-body approach is more suited for parameter estimations. Its strength is in the low number of degrees of freedom and thus computational efficiency.

**Table 5.3:** *Comparison of the numerical test and results from the laboratory testing*

|           | Frequency FE-model [Hz] | Frequency Test [Hz] | Difference [%] |
|-----------|-------------------------|---------------------|----------------|
| Concept 1 | 22.58                   | 26±0.5              | 15             |
| Concept 2 | 21.88                   | 28±0.5              | 28             |
| Concept 3 | 26.26                   | 24±0.5              | 9              |

The nonlinear transient FE-analysis is well suited for analysis of compliance and compliant structures for resonant systems.

As can be seen from the results, there is a mismatch between computational and tested eigenfrequencies. This is predominantly caused by the manufacturing tolerances, which are very high in the current prototyping setting. This is especially true for the flexure hinges.

The representation of free flight conditions in the numerical model does more accurately represent real free flight conditions than the suspension in the laboratory tests. The lead wires, which are relatively stiff compared to the involved forces, introduce disturbances in the mass and stiffness distribution of the system. For further testing, more compliant and lightweight, mounting methods have to be introduced. To get better correspondence the FE-models should be expended to include the suspension.

The use of solenoids is well suited for the current exploratory setting. Off-the-shelf actuators carry much excess mass and the low specific power of electromagnetic actuators in general, is not suited for low mass applications such as in flapping-wing MAVs. For real flight at this scale custom electromagnetic actuators could provide enough power. When scaling down the engineer should look at other actuator technologies due to less favorable scaling of electromagnetic actuators.

The wings used currently are too stiff to be deformed by the applied aerodynamic forces. In order to produce lift wings have to be attached, which have a tailored stiffness. In larger insects, *i.e.* with a size comparable with the present design, there is considerable torsional deformation of the wings. Bending of the wing in chord direction or along the span is small. In insects a large part of wing rotation has its source in the compliance of the wing joint. In flapping-wing MAVs a similar system has to be introduced, a combination of wing torsion and compliant hinge at the wing root.

## 5.6   Detailed design

Following the initial design exploration in the previous section and building on these results a framework is set for a more advanced design. This design is aimed at a more advanced version of the flapping-wing MAV wing actuation mechanism. The constructional principles used are, although with different materials and small adjustments, comparable to the initial design. A stricter selection has been made towards the actual application and less towards unbounded design domain exploration. Bounded by these restrictions the two-winged designs are excluded, predominantly due to difficulties in obtaining the required hovering state. Two four-winged concepts will be analyzed and the design specified.

First an overview of mechanism topology is given and the overall dimensions are determined via a kinematic analysis. The required materials are determined next. The required wing stiffness is then determined in order to specify the total design. The resulting design is then analyzed using FE-analysis. The chosen design will be realized and analyzed in a test setup.

### 5.6.1   Mechanism topology

A set of suitable compliant mechanical amplification mechanisms has been proposed to function in cooperation with the ring. These mechanisms can be used to tune the system by altering the transmission ratio between linear motion at the ring and the rotational motion at the wing base. Two four-winged mechanisms which fulfill this task, shown in Figure 5.19, have been analyzed in the initial design stage. Both mechanisms consist of a system of struts to transfer linear motion to one side of the ring. The first system uses has effectively twice the amplification ratio compared to the second. Both mechanisms imply a four winged setup to ensure symmetry of the wings with respect to the center of mass. All four wings flap in the horizontal plane, to ensure that the steady state flapping motion corresponds to a hovering state. The analysis of the transmission mechanism is done by defining the transmission ratio in analogy with a gear ratio, see [137]:

$$T = \frac{\phi}{u} \tag{5.11}$$

Here $\phi$ is the output angle at the wing base in rad and $u$ is the input which is obtained from the deflection of the ring in m, see Figure 5.19 for definitions. The mechanism is analyzed using a kinematic description which gives input-output relationship dependent on parameters $L_1$ and $L_2$, which are defined as the effective centers of the compliant links based on pseudo-rigid body assumptions for compliant hinges, see [68]. This analysis is less rigorous than the kinematic analysis used in Section 5.4 but since more focus is on FE-modeling it is sufficient for obtaining initial values for the mechanism dimensions. The analysis is the same for both systems except that Concept 2 uses the ring deflection two times, which effectively doubles the transmission ratio compared to Concept 3. This assumption
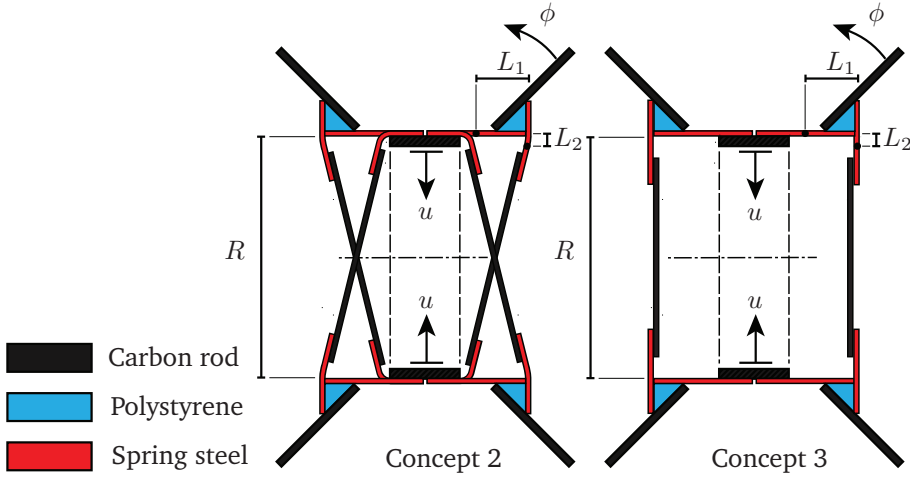
**Figure 5.19:** *Overview of Concepts 2 and 3. Dimensions required to determine the amplification ratio are indicated.*

is based on the relatively shallow angle of the struts in Concept 2 and justified in this design setting. The input–output relationship is given by:

$$\varphi = \arcsin\left(\frac{2u + L_2}{\sqrt{L_1^2 + L_2^2}}\right) - \arcsin\left(\frac{L_2}{\sqrt{L_1^2 + L_2^2}}\right) \tag{5.12}$$

For design purposes only $L_1$ is of influence on the transmission ratio for the whole system, under the assumption that $L_2$ is sufficiently small, effectively half the length of the compliant link. This is due to two reasons: The first is the required symmetric input-output relationship to ensure smooth resonant properties. The second is the loading conditions for the link corresponding to length $L_2$, which are partly in compression and therefore might induce buckling if $L_2$ is chosen to large. A safe length for the link is 1 mm which gives $L_2$ a value of 0.5 mm. The value of $L_1$ has to be chosen such that the output has a peak-to-peak value of around 90°, which is close to the morphological constraint imposed by using four wings in one plane using the current setup. The input is constrained by the maximum stroke of the actuator, in this case ∼6 mm which was determined earlier. Using these parameters an average transmission ratio of 260 rad/m would be required for concept 2 and 540 rad/m for Concept 3. The current choice of parameters yields an approximately constant amplification factor over the stroke.

The values of $L_1$ that give a transmission ratio such that output angle corresponds to the required values, using Equation (5.12), are given in Table 5.4. These values are later used in the modeling and realization of the structures. As can be seen from Figure 5.20 there is approximately a factor two difference between the two mechanisms using optimized link lengths, which was to be ex-

**Table 5.4:** *Dimensions which yield the required amplification ratio for the mechanisms. The factor of two difference is explained by the similarities in mechanism topology.*

|            | $L_1$[mm] | $L_2$ [mm] |
|------------|-----------|------------|
| Concept 2  | 4.5       | 0.5        |
| Concept 3  | 2.2       | 0.5        |

pected from the mechanism topology. The input–output relationship for both mechanisms is linear for a large part of the stroke. Towards the end, especially at the positive side, it can be seen that the relationship becomes nonlinear. This implies that when deflections become large, nonlinearity in the input-output relationship might degrade the sinusoidal motion of the wing sweep. This sinusoidal motion is important to ensure symmetric aerodynamic force generation. It is assumed that for the current setting this is a safe starting point. In a later stage the coupling behavior could be used to tune wing kinematics. This issue is open for further investigation. In several insects the wing sweeping motion was found to be close to sinusoidal, which is one of the early indications that the insect thorax functions as a resonator.

### 5.6.2   Materials

The overall topology of the design is known. Therefore the material selection is placed at the beginning of the design. The materials used for the detailed design are chosen based on experience with the initial models described earlier in this chapter. Other criteria include an overall reduction of mass. Naturally different criteria are in place for the different parts. For example the hinges, which should

**Table 5.5:** *Materials used for realization of the detailed design.*

| Material | Part | Width [mm] | Thickness [mm] | Young's modulus [GPa] | Density [kg/m$^3$] |
|----------|------|------------|----------------|-----------------------|--------------------|
| Spring steel[a] | Hinges | 2 | 0.03 | 210 | 7850 |
| Unidirectional carbon fiber[b] | Ring 1 | 3 | 0.13 | 145 | 1500 |
| | Ring 2 | 2 | 0.13 | 145 | 1500 |
| | Ring 3 | 2 | 0.1 | 145 | 1500 |
| | Struts | 2 | 0.4 | 145 | 1500 |
| Polystyrene[a] | Wingmounting | 2 | 2 | 2-4 | 1100 |

*References*: [a]Matbase [86]; [b]van Dijk Pultrusion Products [127].
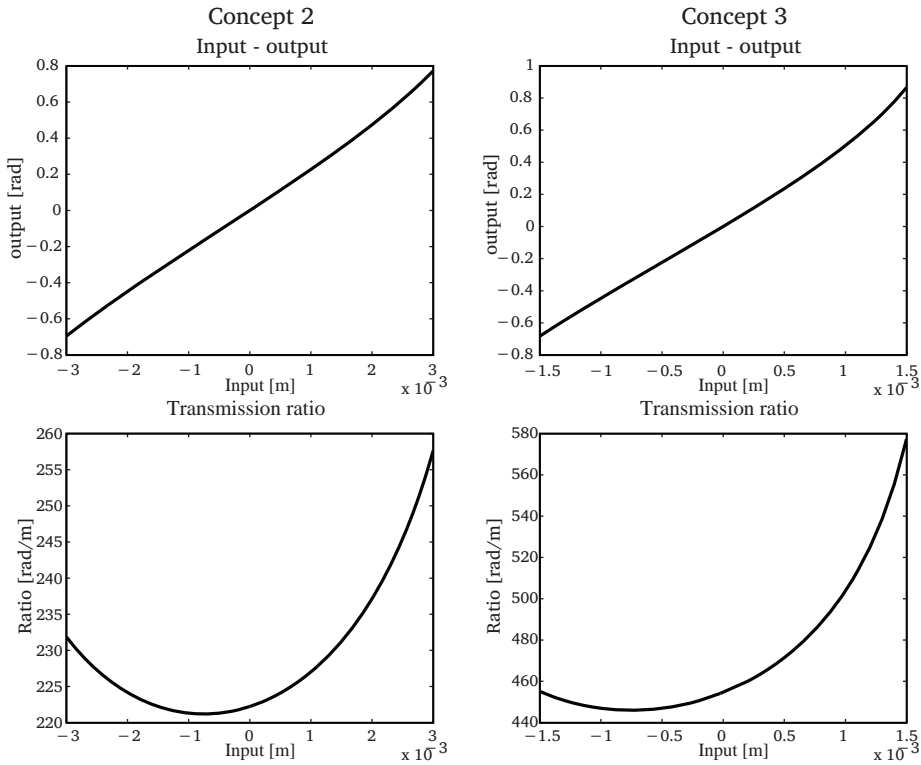
**Figure 5.20:** *Transfer functions of the two mechanisms relating input to output and amplification factor.*

be as light as possible while retaining enough lateral stiffness. The struts should be as light as possible but must be able to resist compressive loading. The ring is perhaps the most interesting part since it is a larger factor in the overall behavior of the system. Multiple rings may be used to obtain the required stiffness. The material for the ring is based on the criteria discussed in Section 4.2.2. The materials used are listed in Table 5.5.

### 5.6.3   Wings

The wings that will be used to generate lift in a later phase have a large influence on the effective mass properties of the system. They especially influence the resonant frequency because the wings are the structures that have the highest velocities and accelerations. As such, the inertial properties of the wings have to be used here in order to reach appropriate ring stiffness to obtain desired resonant frequencies.

**Table 5.6:** *Wing inertia properties*

| Wing | m[kg] | $I_{wingroot}$ $[\mathrm{kg\,m^2}]$ |
|---|---|---|
| Initial | $6.599 \times 10^{-5}$ | $4.947 \times 10^{-8}$ |
| Adjusted | $6.664 \times 10^{-5}$ | $4.945 \times 10^{-8}$ |

The mass properties are dependent on the design of the wing. The detailed design of the wings is discussed in Chapter 6. This design will be adjusted to optimize lift generation. The proposed design does not significantly change the inertial properties of the wing. As such the inertial properties of the baseline wing can be used here safely to analyze the thorax structure. The design of the wing is given in Figure 6.2. The moments of inertia of the wing with respect to the wing root are given in Table 5.6 for the initial and adjusted wing design, respectively. The values in this table are obtained using the Solidworks® CAD software. Since they are almost identical, other factors have more influence. Therefore the value of $4.947 \times 10^{-8}$ $\mathrm{kg\,m^2}$ can be safely used in design equations.

### 5.6.4 Ring sizing

Using the wings described above, the actuator described in Section 5.4.1 and the dimensions determined in Section 5.6.1, the remaining factor of significant influence on the resonant frequency is the ring stiffness. An estimate of the required ring stiffness can be obtained by using the definition of the resonant frequency in which the whole system is seen as a single degree of freedom rotational system. In order to do so, the components which exhibit only linear movement are incorporated by making use of the transmission ratio determined in Section 5.6.1 to find their rotational equivalent. Besides the stiffness contribution of the ring, the hinges also add effective stiffness and have to be incorporated since they experience the same rotation as the wing itself. Note that besides the transmission factor of the mechanisms, the analysis is the same for concepts 2 and 3 and the resulting ring stiffness is also equal.

The desired resonant frequency lies in the range of 25–30 Hz, which is based on the experience from the realization of the initial models. A higher frequency will lead to more lift production but will also induce higher loading on the structure and may lead to premature failure.

The required ring stiffness is obtained by making use of:

$$f = \frac{1}{2\pi} \sqrt{\frac{I_e}{k_e}}. \tag{5.13}$$

In which $I_e$ and $k_e$ are the equivalent moment of inertia and torsional stiffness representing the whole structure. In Tables 5.7 and 5.8 the contributions to

**Table 5.7:** *Contributions to the equivalent inertia properties of the system*

| Part | Mass [kg] | Moment of Inertia [kg m$^2$] | Quantity | Equivalent inertia [kg m$^2$] |
|---|---|---|---|---|
| Actuator 1 | 0.9×10$^{-3}$ | | 1 | 1.2×10$^{-8}$ |
| Actuator 2 | 6.3×10$^{-3}$ | | 1 | 1.2×10$^{-8}$ |
| Wing | 6.6×10$^{-5}$ | 4.9×10$^{-8}$ | 4 | 2.0×10$^{-7}$ |
| Miscellaneous | 0.5×10$^{-3}$ | | 8 | 7.4×10$^{-9}$ |

**Table 5.8:** *Contributions to the equivalent stiffness properties of the system*

| Part | linear stiffness [N/m] | torsion stiffness [Nm/rad] | Quantity | Equivalent stiffness [Nm/rad] |
|---|---|---|---|---|
| Hinge | | 7.0×10$^{-5}$ | 8 | 5.6×10$^{-5}$ |
| Ring | 400 | | 1 | 5.9×10$^{-3}$ |

the resonant system of the individual parts are given. The following parts contribute to the equivalent moment of inertia: the two parts of the actuator (scaled by their relative motion based on mass), the wings and miscellaneous parts of the structure, which have very low impact due to low mass and relatively small movements. These contributions are made to the stiffness: the hinges and the ring In the Table 5.8 a ring stiffness of 400 N/m is included which leads, using Equation (5.13), to a resonant frequency of 26.7 Hz and may be seen as a good baseline for the design. The actuator used is the same as used for the initial design, see Section 5.4.1.

Two system properties need further attention (Table 5.7 and Table 5.8). First, the equivalent inertia is dominated by the wings. This means changes in wing moment of inertia will be most effective in influencing the resonant frequency. Second, the equivalent stiffness is dominated by the contributions made by the ring and consequently changes here are most effective.

The effects of added mass have not been taken into account. Added mass would effectively increase the effective mass and thereby decrease resonant frequencies. The effect of added mass on a slice of wing is given by [39]:

$$dm = \frac{\pi \rho}{4} c(r)^2 \, dr \tag{5.14}$$

in which $\rho$ is the density of air and $r$ is the spanwise coordinate. The chord length of an insect wing, along the radius, can be described by a half-ellipse [12, 134]:

$$c(r) = \frac{4\bar{c}}{\pi} \sqrt{1 - \frac{r^2}{R^2}}. \tag{5.15}$$

in which $\bar{c}$ and $R$ are the mean chord and length of one wing respectively. This description can be used to express the added mass in terms of the moment of inertia with respect to a rotation around the wing base [137]:

$$I_{air} = \iiint_V r^2 dm = \frac{\pi \rho}{4} \int_0^R c(r)^2 x^2 \, dr. \tag{5.16}$$

Combining yields:

$$I_{air} = \frac{8}{15} \frac{\bar{c}^2}{\pi} R^2. \tag{5.17}$$

The proposed wings cannot be described by a smooth function as Equation (5.15), a simple numerical approach to this integral leads to a moment of inertia for the current wings of $7.65 \times 10^{-9} \mathrm{kg\,m^2}$. When this value is compared to the moment of inertia of the structural part of the wing, as listed in Table 5.7, it can be seen that the added mass contribution is approximately 5–10 times smaller. This property will not be taken into account in the following analysis but a general lowering of resonant frequencies is expected. As an example the value for Hawkmoth wings is given here for comparison. The morphological data is obtained from [12, 135, 136]. Using the values, $\rho=1.2041$ kg/m$^3$, $\bar{c}=18.26$ mm and $R=51.9$ mm, the moment of inertia of the added mass effect is $9.53 \times 10^{-9} \mathrm{kg\,m^2}$ for one wing. Hawkmoth wings are comparable in size to the wings proposed for use in this flapping-wing MAV, see Section 5.6.3. However, due to the significantly larger surface the added mass is also significantly larger.

In Table 5.5 various options are listed of materials which can be used for the ring. These materials are in fact all the same carbon fiber composite but the cross-sectional area and corresponding area moment of inertia vary. A selection has to be made on which combination of ring materials yields an overall stiffness close to the 400 N/m that was determined earlier. The diameter of the ring is assumed fixed at 28 mm due to restrictions imposed by actuator placement. The ring combination options which are possible are presented in Table 5.9. We se-

**Table 5.9:** *Ring combinations which yield the required stiffness values.*

| Ring Material | Number of rings | Effective stiffness [N/m] |
|---|---|---|
| 1 | 2 | 381.1 |
| 2 | 3 | 381.1 |
| 3 | 7 | 403.4 |

lected the combination of two rings of 3 mm × 0.13 mm cross section, based on the use of two rings to obtain the required stiffness. In order to make the required 28 mm diameter rings, a length of the material is taken of which the ends

are glued together with a 4 mm overlap. Besides local stiffening effects due to the overlap two factors are of relevance for the application of the ring. First: the stress state introduced by making the ring from a straight strip is purely a moment and therefore hardly influences the eigenfrequencies of the system. Secondly: the dependence of the effective linear spring constant of the magnitude of ring deformation. Because the ring deformation is substantial, *i.e.* a inward and outward 3 mm deflection relative to a 28 mm ring, the effective spring constant will probably not be constant over this range due to geometrically nonlinear effects. The result of these geometrically nonlinear effects is that the effective stiffness of the ring will experience a stiffening effect both on the inward and outward deflection. This effect will be more pronounced on the outward deflection since the ring will start to behave more like the limit case. In the limit case the ring is fully extended and the effective ring stiffness is equal to the extensional stiffness of the rod which is used to make the ring.

### 5.6.5   Detailed design

The two rings, which function in parallel, are connected by a unidirectional carbon fiber crossbar of 0.4 mm ×2 mm cross section. The mechanical amplification mechanism is made from unidirectional carbon fiber struts, with 0.4 mm ×2 mm cross section and compliant hinges, which are made from 0.03 mm thick, 2 mm wide spring steel. The wing attachment point is a triangular piece of polystyrene which is also used to attach the compliant hinges. Due to previous peeling problems in the glue connection between the spring steel and other parts, the need arose to secure these connections using nylon bond wires. The structures with both the two rings, the amplification mechanism but without actuator are shown in Figures 5.21 and 5.21. It should be noted that the wings which are shown in these figures include the passive wing pitching mechanism which will be described in Chapter 6.

### 5.6.6   Finite element modeling

In order to evaluate the performance of the detailed designed structures they are modeled using finite element analysis. To get insight in the performance of the actuated structures most aspects of later realization are incorporated in the models. The actuator is included by two point masses and the actuation forces. Two rings are used with an offset, as determined in the previous section, primarily to fit the desired stiffness values while the spacing allows for simple actuator placement. The analysis is performed in two steps. First an eigenvalue analysis is performed to estimate the eigenfrequency of the structures, confirming correct stiffness values. These eigenfrequencies are then used as the driving frequency in the second step of the analysis, a transient analysis. In order to simulate more realistic conditions, dampers are attached to the wings to simulate aerodynamic
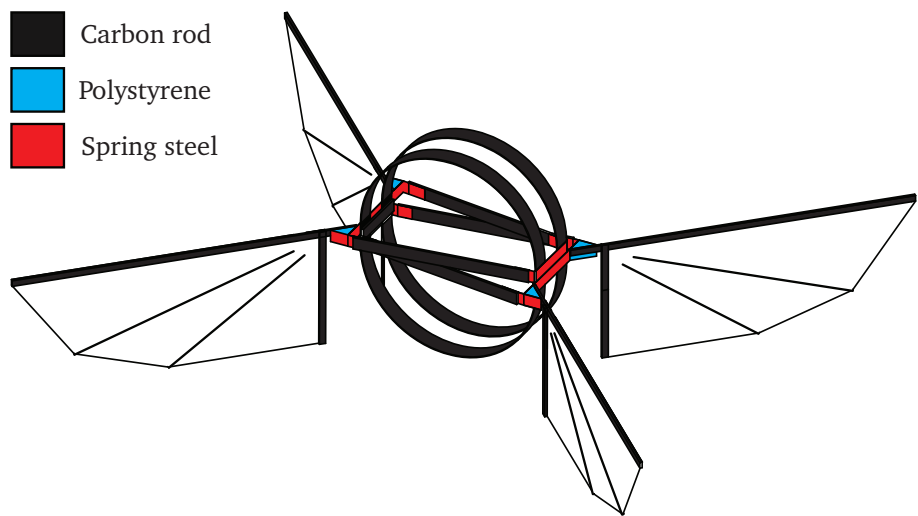
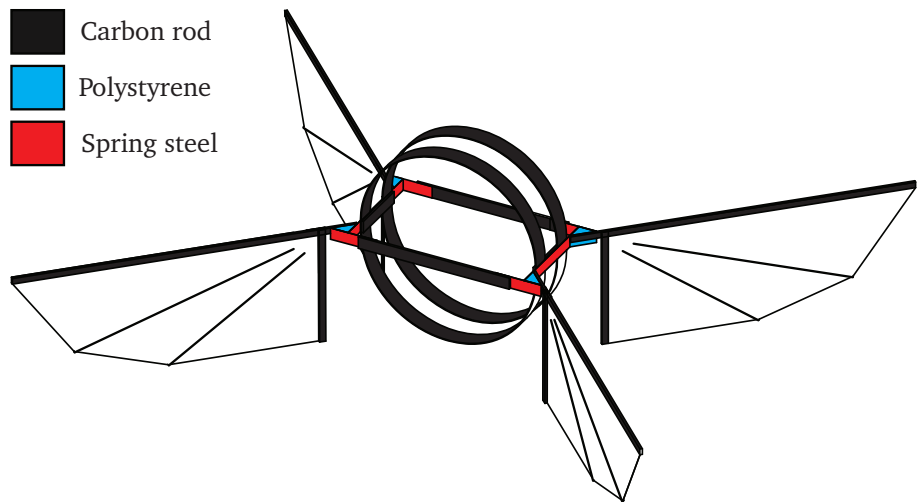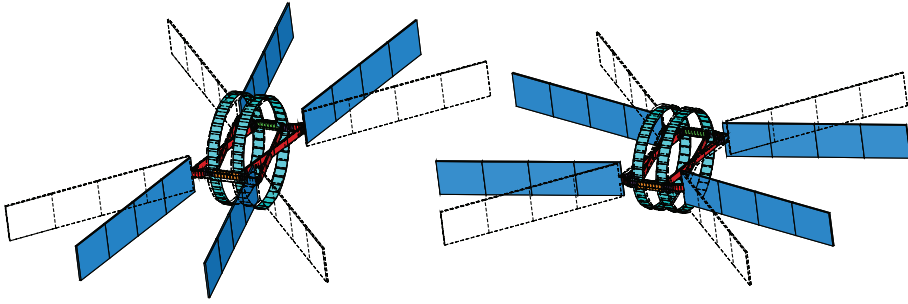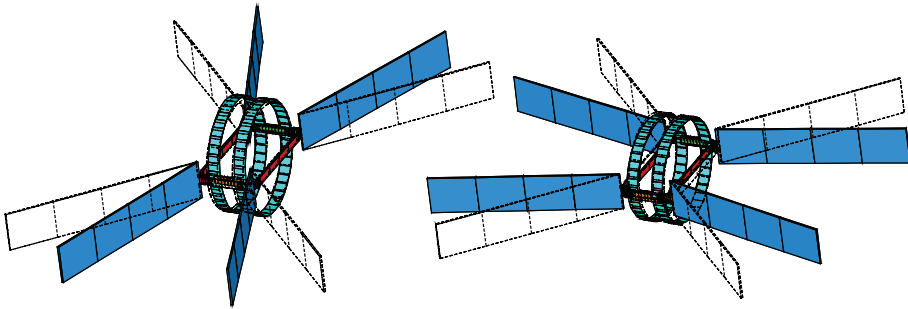**Figure 5.21:** *Detailed design for Concept 2*



**Figure 5.22:** *Detailed design for Concept 3*

**Figure 5.23:** *FE-model of Concept 2 showing minimum and maximum deflections. The different parts are indicated by the different colors.*



**Figure 5.24:** *FE-model of Concept 3 showing minimum and maximum deflections. The different parts are indicated by the different colors.*

loading. The damping value has been estimated using quasi-steady aerodynamic models [12]. Actuation force is adjusted to match performance of the chosen actuator.

The calculated eigenfrequencies are ∼27 Hz for Concept 2, which is shown in Figure 5.21, and ∼29 Hz for Concept 3, shown in Figure 5.22. These eigenfrequencies are later used to evaluate the performance of the realized models. An interesting observation is that the main flapping motion is not the lowest eigenfrequency in Concept 3. This could be expected based on the degrees of freedom of the model, which shows a mode which has the same equivalent moving mass but less equivalent stiffness.

Damping is large in these models due to aerodynamic loading. The calculated eigenfrequencies used to drive the structures in the second step might therefore not correspond perfectly to the large amplitude resonant frequency. The transient analysis is started by applying a sinusoidal force which represents the actuator. The magnitude of this force is adjusted such that the structure reaches the required amplitude. A soft start is implemented to avoid convergence issues. The large amplitude deflections can be seen in Figures 5.23 and 5.24. The stiffness

of the structure is mainly determined by the two rings. The compliant links add stiffness but this is minor compared to the ring stiffness. The aerodynamic loading is only the drag part; incorporating lift forces will add mechanical loads to the model. How these out of plane loads will influence performance will have to be studied.

The mass of the ring has very little effect on the eigenfrequency of the structure. The moment of inertia of the wings is the largest factor in the effective mass of the system. Yet, due to actuator mass the assumption for insects that almost all the effective mass of the resonant system is in the wings does not hold for this design. Therefore, both changes in actuator and wing mass will have effects on the resonant frequency. When driven in the large amplitude resonant state the nonlinear stiffening of the equivalent stiffness of the ring is observed numerically. Although present, the effects are currently small.

## 5.7   Realization and testing

The intent of this section is to present the realization of the models and show results of the testing of the kinematic requirements. Only if the required deflection is reached, can the aerodynamically efficient wings be effectively driven. First a notice on which concepts are to be realized and tested experimentally, the mechanism dimensions which are necessary to realize Concept 3 are very difficult to realize using the current manufacturing process and materials. The glue connections will fail prematurely when actuated at the resonant frequency due to peeling. This is based on the experience obtained with the previous models and prototype structures. These facts lead to the conclusion that realizing Concept 3 will not lead to successful prototypes, and so only Concept 2 is realized and tested. This limitation does not impair the validity of this study. The possibility of generating lift by exploiting the resonant state of a compliant mechanism can be fully explored by looking only at Concept 2.

### 5.7.1   Realization of the detailed design

The realization of Concept 2 is conform the description and sizing of the parts above. In general all glue connections are realized by using medium fill power Cyanoacrylate. The actuator remains unchanged with respect to the initial models. In order to ensure longevity of the glue connection between the spring steel and other parts, the need arose to secure these connections using nylon bond wires. The completed structure is shown in Figure 5.25, a zoom in on the amplification mechanism and the actuator is shown in Figure 5.26

**Figure 5.25:** *The center of Concept 2 ready for testing, including actuator, power leads and wings.*
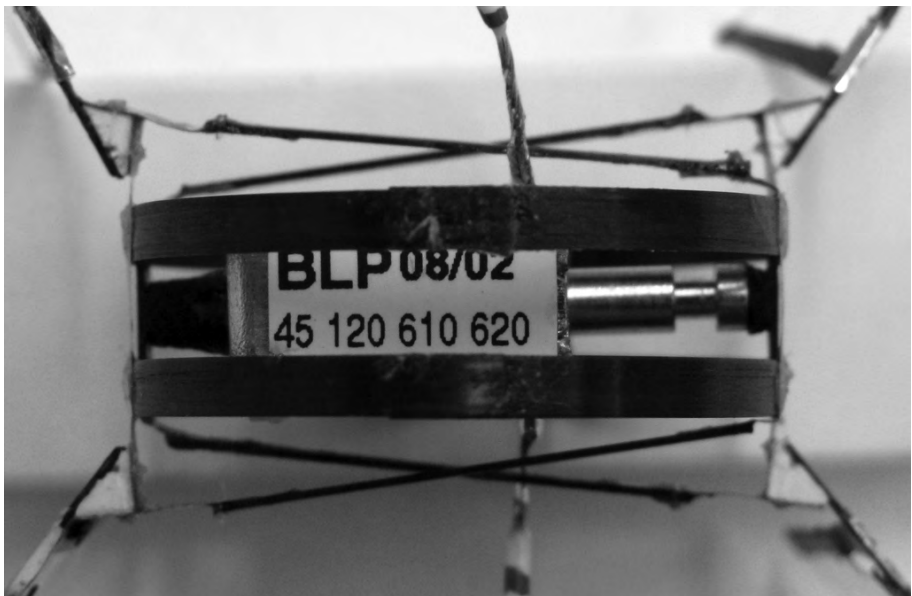


**Figure 5.26:** *Zoom of the thorax area of Concept 2.*

### 5.7.2   Testing of wing deflection

The realized mechanism is tested for two aspects: first, the resonant frequency of the structure and second, the wing sweeping deflection at resonance. The test setup used to test the structure consists of a signal generator and an amplifier to drive the actuator. For visual inspection a second signal generator is used which triggers a strobe light. Resonance is determined by visual inspection augmented by the strobe light. The prototypes are suspended just above the table surface and a camera is positioned such that one wing can be photographed using long a shutter time.

The first aspect tested is the resonant frequency. The frequency at which the wing deflection was largest for constant signal amplitude was $28\pm0.5$ Hz. This frequency is close to the predicted frequency of 27 Hz. The second aspect tested is the wing sweeping deflection at resonance. The obtained value for deflection angle at peak of resonance is close to $68\pm4°$, as is designated by $\phi$ in Figure 5.27.
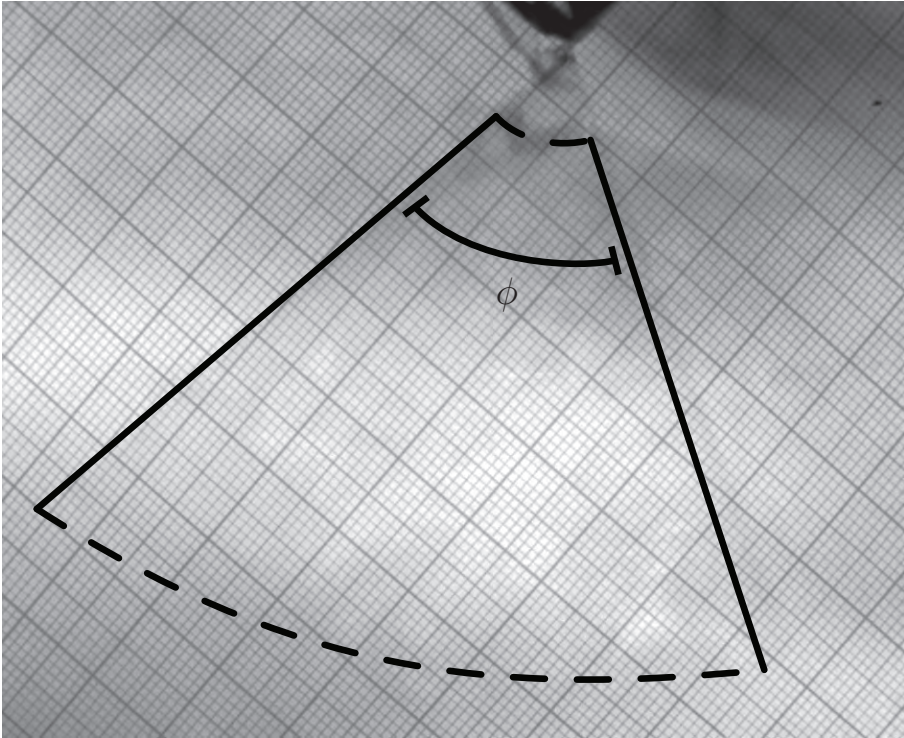


**Figure 5.27:** *Movement range of one wing when driven in resonance. The movement range is indicated by $\phi$ and corresponds to the wing sweeping motion. The extend of the wing sweeping motion is outlined for determining the amplitude.*

The wing edges are outlined for clarification purposes.

## 5.8   Concluding remarks

Rings are a very suitable structure to function as the elastic storage unit in a resonance based flapping-wing MAV. Exploiting deformation of the ring combined with a compliant stroke amplification mechanism in a resonant fashion leads to very positive results concerning wing actuation. Significant stroke angles can be obtained while the frequency is close to the predicted frequency. This indicates that the chosen modeling strategy can be used for further studies in which lift generation is included. The materials and constructional principles used in the realization of the prototypes are very suitable for this type of construction. It allows for rapid assembly of the prototypes but is limited in precision. Further prototypes will also be constructed in this fashion.

The dummy wings used in this study will be replaced by aerodynamically efficient wings. The current structure will then be used to generate lift. Objective is that wing pitching can be obtained in a compliant passive fashion to maintain the compliant nature of the design. The current actuator has a low specific power density value, in order to increase chances of lift-off an actuator has to be designed which suits the requirements better. Concept 3, which was not tested, can be used for control purposes due to the extra degrees of freedom present, which may prove very promising in the future when free flying control of the structures is required. Concept 3 can, using a multi degree of freedom actuator, be used for control by means of influencing the resonant state to introduce asymmetry in the lift production.

# Chapter 6

# Wings and wing hinge

## 6.1 Introduction

The wings are a very important part of the flapping-wing MAV. Perhaps even the most crucial since lift production, and therefore lift-off and flight performance, are dictated by the wings. The wings form the interface between the mechanical and aerodynamical domain. This fluid–structure coupling has to enable efficient lift production in the resonant setting of the development of the current flapping-wing MAV. The wing kinematics dictate the production of lift by enabling the different aerodynamic mechanisms present in insect scale flight as described in Section 2.5. Focus here is on the correct reproduction of insect wing kinematics.

Following from studies which focus on insect anatomy, power usage and wing kinematics, for an overview see Chapter 2, it was found that insects rely on a combination of active and passive means to generate the wing kinematics required for efficient flight. The main sweeping motion is the result of resonant motion in the thorax–wing system, it is via this motion that power is conveyed into the wing. This sweeping motion is the driver for the lift production, whereas the wing pitching motion determines the actual lift production. Both timing and amplitude of the pitching motion have significant effect on lift production. The pitching motion of the wing is accomplished by passive means in the steady state flying motion, as indicated by recent findings, see Bergou *et al.* [11], and therefore dependent on the state of the insect wing root joint and the main sweeping motion.

In order to achieve wing pitching by passive means there has to be a correct balance in the loads on the wing. In insects the wing root joint functions as an elastic hinge with tunable stiffness, which, together with the inertial and aerodynamic loading, makes it possible for the wing to follow an aerodynamically efficient kinematic pattern when driven in a resonant fashion. In a simplified view, the wing root functions as a torsion spring which is only coupled with the

pitching degree of freedom of the wing. The origin of the heaving motion lies in the complexity of the wing root joint. The currently proposed wing actuation mechanism does not offer this degree of freedom, therefore for simplicity the wing heaving motion is currently not reviewed.

The intention of this chapter is to review and analyze options for the application of this elegant method of achieving correct wing pitching kinematics in a passive manner, based on developments presented in Bolsman *et al.* [17]. The design of the wing has to be done in combination with the design of the ring-based resonant structure, which will drive the wings of the flapping-wing MAV developed and analyzed in Chapters 4 and 5. Many wing designs exist which find application in the setting of flapping-wing MAVs, reviewed in Section 3.2.13. An engineering implementation of the tuned wing pitching hinge has to be designed. Many types of elastic hinges exist but only a subset is applicable for integration in the wings of flapping-wing MAVs. The application of an elastic hinge within the setting of flapping-wing MAVs imposes boundary conditions and constraints from the preexisting thorax design. The constraints are both on kinematic requirements, which follow from the resonant wing sweeping motion, as well as the overall mass of the design.

The approach followed in this chapter is based on reviewing options for the application of an elastic hinge in or at the base of the wing. Augmented by the choice of the wing design itself. A preliminary design is chosen and analyzed for the performance and applicability within the current setting. This analysis is based on the choice and usage of an aerodynamic model for determination of the aerodynamic loading on the wing. Coupled to the aerodynamic model is a dynamics model which will be used to represent the motion and state of the wing. The wing sweeping input used originates from analysis of the ring-based structure, see Chapter 5. After the properties of the elastic hinge are determined and optimized, the wing design is realized and tested for performance before integration with the flapping-wing MAV thorax design proposed in Chapters 4 and 5. The resulting wings with tuned elastic properties are implemented with the design of the resonant base in Chapter 7.

## 6.2   Kinematics

The kinematics of insect wings have been qualitatively described in Section 2.4. In this chapter a quantitative measure of insect wing kinematics is required to be able to implement a modeling strategy which will be used for optimizing wing pitching stiffness. The description used in this chapter is based on the assumption that the wing will behave approximately as a rigid body.

The kinematic setting within which the wing is to function is subject to two restrictions from two different origins. The first of which originates from the thorax system which forms the basis of the resonant thorax wing system. The resulting flapping kinematics are now used as boundary condition for the wing

development. These kinematics consist of the flapping frequency, wing sweeping amplitude and shape of the motion, *i.e.*, sinusoidal. The second condition is based on the implementation of a method of passive wing pitching. This choice has been proposed in Chapter 4. The currently proposed wing actuation mechanisms provide an essentially planar motion. Therefore, the motion of the wing is restricted at the wing root to sweeping and pitching. Heaving motion of the wing can, in this setting, only be the result of deformations of the wing itself, which depends on the wing design that is to be implemented.

### 6.2.1   Kinematic description

The kinematic description used here is based on the description used by Berman and Wang [12]. The version used here is simplified due to restrictions imposed by usage of the wing within the proposed resonant setting. For clarification purposes the three angles which determine the wing state are given in Figure 6.1.

The three angles which describe the wing are $\phi$, $\theta$ and $\eta$ for the wing sweeping, wing heaving and wing pitching, respectively. The description of the wing
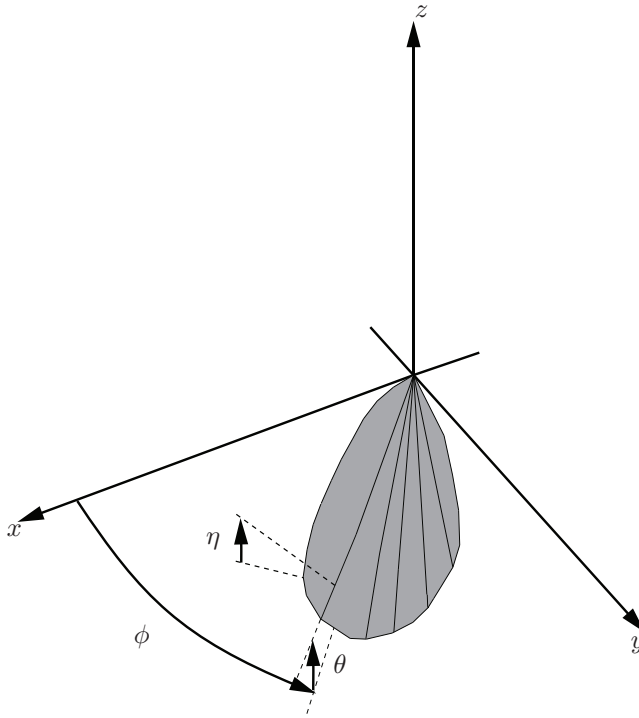


**Figure 6.1:** *The wing orientation, defined by three angles. Respectively, the wing sweeping motion, designated $\phi$, the wing heaving motion $\theta$ and the wing pitching motion defined by $\eta$.*

kinematic can be best be described and understood when referring to the cans-in-series approach as proposed by Schwab and Meijaard [110]. The wing sweeping motion, $\phi$, consists of a rotation around the z-axis. The heaving, $\theta$, is then described by a rotation around the rotated y-axis. Wing pitching, $\eta$, is finally described by a third rotation around the main spar of the wing.

The kinematics are based on harmonic description of both the wing pitching and wing sweeping. For the sweeping this assumption is valid due to the resonant origin, for the pitching motion this is a starting assumption. This assumes that wing motions are symmetric for the up- and downstroke. Wing heaving description is included to make the current approach suitable for future studies which may include this motion. Due to the previously mentioned restrictions, the wing heaving motion amplitude is always zero in the present description. The kinematic description is simplified from [12] to include only the sinusoidal part and becomes:

$$\phi(t) = \phi_m \, sin(2\pi ft), \tag{6.1}$$

$$\theta(t) = \theta_m \, cos(2\pi Nft + \Phi_\theta) + \theta_0, \tag{6.2}$$

$$\eta(t) = \eta_m \, sin(2\pi ft + \Phi_\eta) + \eta_0. \tag{6.3}$$

In which $\phi_m$, $\theta_m$ and $\eta_m$ are the amplitude of the three wing motions. $\Phi_\theta$ and $\Phi_\eta$ are used to describe the phase shift of heaving and pitching with respect to the sweeping motion. $\theta_0$ and $\eta_0$ are used to describe initial offsets in the motion and are not used here due to the assumption of symmetric flapping. $N$ refers to the parameter which determines the nature of the heaving motion. $N = 1$ yields a banana type motion, see Figure 2.9 while $N = 2$ adds an extra heaving cycle which results in a figure-of-eight type motion, see Figure 2.9. The absence of the heaving motion results in basic sinusoidal kinematics given by Figure 2.8.

## 6.3    Wing design

Wings currently used in flapping-wing MAVs usually rely on deformation of a membrane like structure to achieve wing pitching deflections. Generally, these type of wings do not provide enough compliance in pitching direction to exhibit insect like wing kinematics. Generally, a more flexible design is needed to be able to more accurately reproduce the wing kinematics as they are exhibited by insects. This flexibility can be obtained by introducing an extra flexible element in the root of the wing. With this modification it should be possible to obtain, in a passive manner, the simplified insect wing kinematics for lift production.

The introduction of compliance in the wing root of the flapping-wing MAV can be achieved in at least two ways: First, the elastic tailoring of the entire wing to reach a design that is similar to that of insects, see, for example Combes and
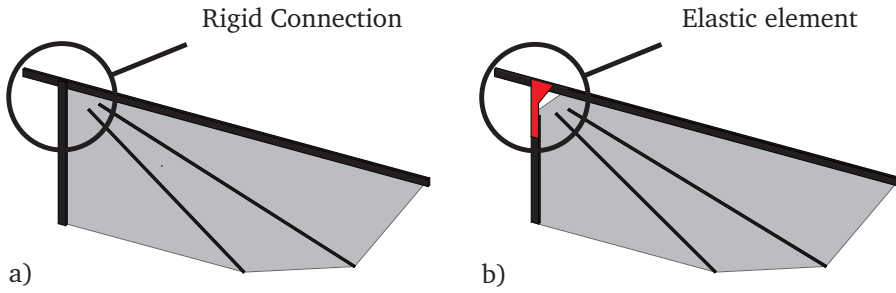
**Figure 6.2:** *a) The basic wing design. b) The modified design which includes an elastic element at the wing root.*

Daniel [27] and Wootton *et al.* [143]. This can be accomplished by designing a structure which effectively decouples the wing bending and torsion. This design will allow for considerable torsional deformation during flapping, thereby reaching the large pitching deflections needed for lift generation. Second, the introduction of an elastic element close to or in the wing root, which introduces flexibility in pitching direction while not greatly influencing bending stiffness of
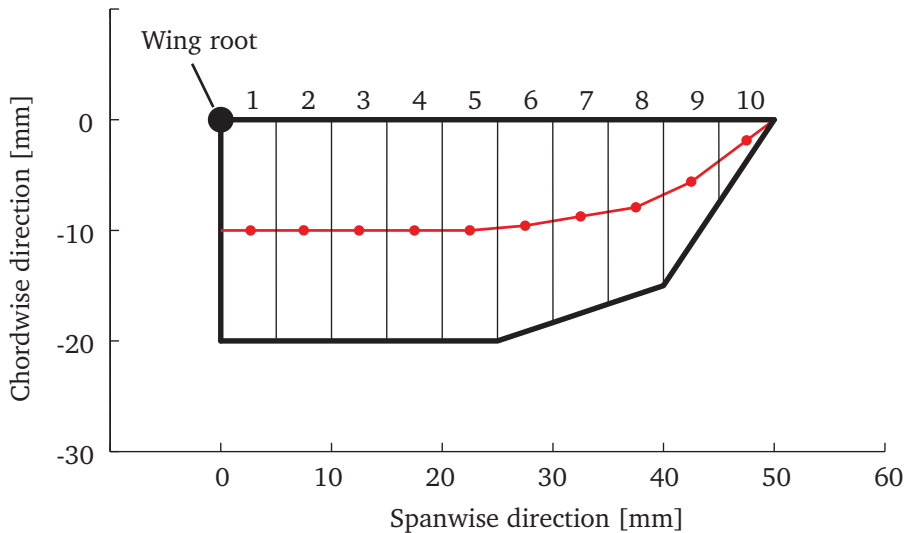


**Figure 6.3:** *Planform of the wing, indicated are 10 strips used for the calculation of the quasi-steady aerodynamic loads as well as the geometric centers of the chordwise strips on which the loads are applied, indicated in red.*

the wing, see, for example Wood [137]. The second option is used here because it allows for the simple construction principles commonly used in flapping-wing MAVs, for example, carbon fiber spars which span a PET membrane, as described in Section 3.2.13.

Two methods of introducing a localized passive degree of freedom for wing pitching can be distinguished. The first is the combination of an elastic hinge with hard or soft deflection limiters which are used to constrain the maximum pitching deflection of the wing during the entire stroke. In this method the wing hinge compliance is to be such that the wing will be deflected by the combination of inertial and aerodynamic loading. The wing hinge should be tuned such that the eigenfrequency of the wing pitching motion is significantly lower than the flapping frequency. The second method consists of just the elastic hinge without limiters. The hinge acts as an elastic element, which allows for pitching movement and limits deflections by the balance between inertial, aerodynamic and elastic loads. In this approach the hinge stiffness has to be carefully tuned.

The option without deflection limiters is used here. Although both options provide equally valid solutions for achieving passive wing pitching, the absence of deflection limiters leads to a more smooth motion which is desirable in the current resonant setting. Even at this small scale the deflection limiters might introduce high loads due to contact which might require sturdier, heavier implementation. Besides the expected sturdier implementation, the deflection limiters also introduce extra mass.

Many types of compliant hinges exist which are more or less suitable for usage in this large displacement setting, see, for example, Trease *et al.* [123], who provide an overview of large displacement compliant hinges. The proposed design of the wing with a flexible element is based on a design commonly used in flapping-wing MAVs and is chosen mainly for simplicity. The flexible element is incorporated by adding a piece of spring steel which provides both the hinge action and the elastic properties needed to tailor the total wing pitching stiffness.

The original design and the design with the added flexible hinge element are shown in Figure 6.2. The design consists of a 1 mm x 0.4 mm cross section unidirectional carbon main and base spar. The membrane is spanned by two 0.28 mm diameter unidirectional carbon spars. The membrane is 5 $\mu$m thick PET sheet. The dimensions of the spring steel hinge are determined by the tuning process described in this chapter. The incorporation of the hinge does not alter the mass of the wing significantly. The planform of the wing is based on that of the Hummingbird and is common among flapping-wing MAVs. The span of one wing is 50 mm and its maximum chord length is 20 mm, primarily determined and constraint by the overall design requirements of the resonant wing actuation mechanism. Other wings planforms may be used as long as the inertia with respect to the wing root remains constant, which may indicate a different combination of length, chord and mass distribution. The detailed wing planform is shown in Figure 6.3.

## 6.4 Modeling

In order to analyze the proposed design and, in a later stage implement an optimization procedure, a modeling strategy has to be chosen. The selection process of suitable models relies heavily on the requirement of simplicity. The current level of the design process favors adaptability and quickness over accuracy. This is supported by the amount of unknowns in the current design setting as well as the state of the art in aerodynamic models available for the analysis of flapping wing flight.

For successful modeling of the wing two physical domains need to be coupled, the structural domain and the fluid domain which constitutes the moving environment of the wing. Since the wing is assumed to be rigid it can be modeled simply. For the model which is to be determined to obtain the aerodynamic loads more options exist, and the choice herein will have to be made. The choices made in the modeling procedures are partially based on the subsequent implementation of an optimization procedure.

In this section focus is on the selection of the aerodynamic and mechanical models which will be used for the tuning of the wing pitching hinge. The aerodynamic model will be selected based on a review of possible models. The mechanical model selection is more straightforward due to rigid body assumptions.

### 6.4.1 Mechanical model

In order to analyze and optimize the hinge stiffness the wing is modeled as a single rigid body in the Simmechanics environment which is part of the Mathworks Simulink® environment. The choice for a single rigid body is based on the assumption that all the wing pitching is due to hinge action and that wing deformations do not contribute to pitching. The inertia properties and center of mass of the wing are obtained from a CAD package, in this case Dassault Systèmes Solidworks®. The aerodynamic loads are implemented by user-defined functions, which relate the current state of the wing (positions, velocities) to the aerodynamic loading condition and will be applied as mechanical loads on the wing. The mechanical model for the wing including the elastic element is given in Figure 6.4.

Since the chosen wing implementation is not infinitely stiff, membrane deformation will also lead to effective pitching deformation. The current assumption that the dominant share of the wing pitching deflection originates in the spring steel hinge is used to justify the usage of rigid body description of the wing. In order to fully integrate the wing deformation, the rigid body description should, in a later stage, be replaced by a model that incorporates elastic deformation of the wing, *e.g.*, by making use of multiple rigid bodies or FE models.

**Figure 6.4:** *Schematic mechanical equivalent of the wing design shown in Figure 6.2b, the torsion spring is the equivalent of the elastic element proposed to obtain passive wing pitching. Inertia and mass properties are obtained using from CAD package. Resting position of the wing is the support spar parallel to the z-axis, torsion spring is shown in deformed position.*
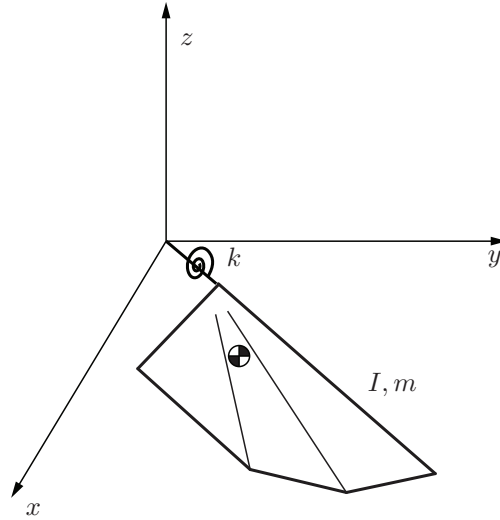
### 6.4.2   Aerodynamic models

In order to be able to implement the current wing design, the aerodynamic loading condition has to be determined during the flapping cycle. A number of different methods exist in literature, which have all been used in the setting of analysis of flapping-wing propulsion. The usage of the models has mainly been focused on the analysis of flight of insects and small birds but can be used equally valid for design and analysis of flapping flight in MAVs.

The existing aerodynamic models vary largely in their type of approach, intended range of validity and accuracy. A list of current aerodynamic modeling methods is given here, ordered by accuracy: Reynolds averaged Navier-Stokes methods, unsteady methods, panel methods, quasi-steady methods and steady-state methods. This classification and overview are based mainly on Ansari *et al.* [6]. In the following paragraphs a short overview is given on the listed methods.

The application of Reynolds averaged Navier-Stokes (RANS) methods is popular for modeling the important flow structures in insect flight, see, for example, Sun and Tang [119] and Ramamurti and Sandberg [105]. The discretization of the fluid domain involved in the application of these methods is very cumbersome. The flow is inherently unstable and vortical which makes solving the equations difficult. The inherently large wing movements involved in small scale flapping flight require a method that is able to handle large mesh deformations, see, for example, Bos [21]. The wings are usually assumed to be rigid with simplified geometry to ease mesh requirements. The implementation of a compliant wing requires the implementation of an efficient fluid–structure coupling. Concluding, these methods are able to give accurate results but computational effort and implementation issues make these methods very time consuming.

Unsteady methods is a broad term used by Ansari *et al.* [6] to give a classification to a group of method which focus on unsteady aerodynamics. The aspects of the flow around the wings on which these models focus are the two flow separations at the leading and trailing edge and the wake. The twin separations have to conform to the Kutta-Joukowski condition. The most current and advanced method in this class is the method proposed by Ansari *et al.* [6] and is in essence the combination of a couple of preexisting unsteady aerodynamic models. Two quasi-steady components, free stream and unsteady motion, and two unsteady components, the leading edge vortex and the trailing-edge wake. The method is two dimensional in origin and total loads on the wing are obtained by integration over the span width. The method has been shown to provide accurate results on both flow structure shape and intensity as well as aerodynamic loads on the wing.

The aerodynamic modeling methods known as the panel methods, are based on a non-viscous flow assumption. Panel methods rely on dividing the wing surface in a two-dimensional or three-dimensional description in a series of uncurved panels. The panels can be considered as boundary elements, these element are then combined with vortex sheets which are placed on each panel. A boundary condition, Kutta-condition, is then imposed on the total circulation of the summed vortex sheets. These type of methods are usually not able to model viscous drag, vortices and flow separation which are important in insect flight. Panel methods are efficient since only the surface of the wing needs to be meshed. Large motions pose no problem and wing wake effects are automatically included. Panel methods have been used for analysis of insect flight by, for example, Smith *et al.* [115]. Wing flexibility can be easily integrated.

Quasi-steady methods use momentum description to model the aerodynamic forces on a moving object in a fluid. These methods are now rarely used but have led to the methods described as the empirically corrected quasi-steady methods. The quasi-steady and empirically corrected quasi-steady methods rely on the same aerodynamic assumptions but their lift and drag coefficient functions are usually obtained from different sources. Empirically corrected quasi-steady methods rely on fitting data of kinematically scaled wings in test setups, for example, Sane and Dickinson [109]. In these methods the resulting loads are usable but no information on flow structures is available. These methods are two dimensional but usually the blade element theory is used to obtain a quasi three-dimensional model. Implementation of these methods is very fast but loads may not be very accurate. The lift and drag coefficients are obtained from measurements, their validity range is therefore limited by these measurements. Usage of these models outside this range requires extrapolation of the measurement data. Many implementations of these models exist for different applications, for example, falling plates [5].

Steady-state methods are the simplest methods used in the description of flapping wing flight. These methods are directly based on momentum jet theory used for helicopters or propellers. The methods are usable for calculating energy requirements for hovering flight. The benefit is that this can be done without

detailed knowledge on wing kinematics and flow structures involved. This is also the major drawback since obtaining knowledge on local wing loading conditions is essential in designing a wing. Ellington [45] proposed the usage of the insect wing sweeping disk to include the effects of wing stroke amplitude and flapping frequency.

The different models are included in Table 6.1 and compared on the factors which are important for usage in this setting of preliminary wing design. These factors are:

- The accuracy of the model

- The computational effort required for one flapping cycle, this is very relevant when optimization is to be performed.

- The implementation effort of the model has to correspond to the intended usage, again adaptability and quickness are more important than accuracy.

- In order to include future possibilities of the effects of wing deformation the model has to be able to be used for the effects of using a non-rigid wing description.

Based on the comparison of the models the choice has been made to implement a quasi-steady aerodynamic model with empirical corrections. It is the current view that the quasi-steady models provide the best balance between accuracy and quick adaptability. The current application will involve an optimization strategy which will require many analyses of the wing movement, even with very few design parameters. In a later stage a more detailed structural design of the wing

**Table 6.1:** *Comparison of the different aerodynamic models suitable for implementation in the setting of flapping wings.*

| Model | Accuracy | Comp. Effort | Implement. effort | Non-rigid wing |
|---|---|---|---|---|
| Reynolds averaged Navier-Stokes | High | Large | High | Yes |
| Unsteady methods | High | Large | High | Yes |
| Panel methods | Medium | Medium | High | Yes |
| Quasi-steady methods | Medium | Small | Medium | Yes |
| Steady-state methods | low | Small | Low | No |

might require an aerodynamic modeling method which is better able to provide local aerodynamic loading conditions. The choice for the quasi-steady model requires a selection from different implementations of this type of models provides by several authors in literature.

The empirically corrected quasi-steady method presented by Sane and Dickinson [109] is corrected using measurements on the Robofly [35] and can accurately predict the unsteady additions to the aerodynamic forces. This research was focused on the fruitfly *Drosophila melanogaster* and is therefore less suitable for application in the current size range for the flapping-wing MAV that is under development. This model has been used in the development of the control setting for the MFI, see Section 3.2.3 and Deng *et al.* [34].

Another well developed quasi-steady model has first been developed for two dimensional analysis of free falling paper, see Pesavento and Wang [101]. The model was later adapted for use in a flapping wing setting: first, to find energy minimizing kinematics for hovering insect flight, see Berman and Wang [12], and second, more important for this work, the passive wing pitch reversal in insect flight [11]. Especially [12] includes a review of the performance of the model in comparison to a CFD solution, see Sun and Du [118], who show that the model is suitable for application to analyze hawkmoth-size wings. The current implementation of the flapping-wing MAV is based on wings that share similar kinematics and dimensions with hawkmoths. It is therefore that this model is chosen in the current setting.

### 6.4.3   Quasi-steady model

The quasi-steady model used is a two-dimensional model used for flapping wings by making use of blade element theory. This results in a three-dimensional model used to determine the loads and torques on the entire wing. The loads on the wing are obtained dividing the wing into a set of infinitesimal chordwise strips. As a consequence there is no span wise component of the flow, this drawback is, however, reduced by using the semi-empirical corrections for lift and drag coefficients.

The infinitesimal loads and torque on a strip of the wing, with infinitesimal width $dr$ in span-wise direction are calculated using the quasi-steady theory. A typical wing strip is depicted in Figure 6.5a, which shows the strip at distance $r$ from the wing root. The surface in which the slice moves is used as the two-dimensional space for the quasi-steady model. It can be seen that the strip is in fact curved which is neglected here and in most quasi-steady approaches. The surface in which the strip is defined is commonly used to depict the movement of the wing in two dimensions.

In this two-dimensional space the loads and torques on the wing strip are defined in Figure 6.5b. Length $l$ defines the geometric center of the wing strip with respect to the leading edge of the wing, in this setting the leading edge always corresponds to the main spar of the wing, see Figure 6.2b. The wing coordinate
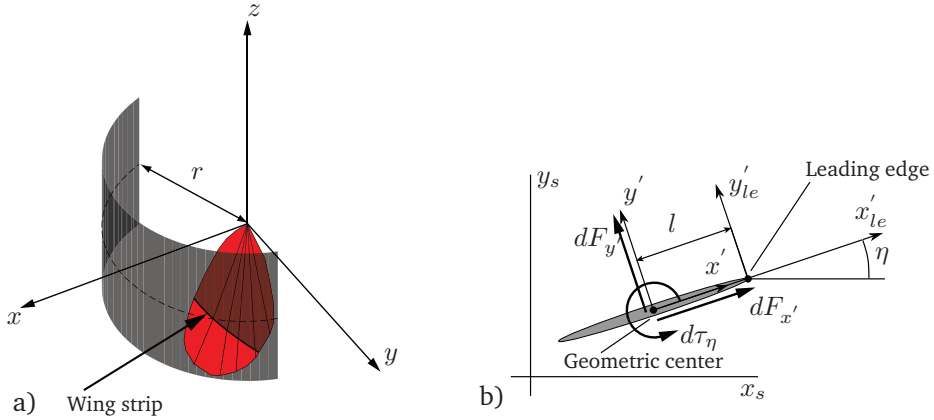
**Figure 6.5:** *a) Surface used for mapping three dimensions to two dimensions for wing movement and implementation of the quasi-steady model. b) Local coordinate system of the wing strip, showing the loads and torque on the infinitesimal strip acting in the geometric center of the wing strip. Axes are indicated by subscript $s$ to differentiate from the wing coordinate system.*

system is defined by the coordinate system $x_s$–$y_s$ which is the equivalent of the surface in Figure 6.5a used for mapping the two-dimensional movement of the wing strips. In this analog it should be noted that in the analysis of the current design the leading edge will always be in the $x$–$y$ plane due to the absence of out of plane motion of the wing.

In order to apply the quasi-steady model, the velocities and accelerations of the geometric center of the wing strip are required. The framework setup by Berman and Wang is used as a guideline. The current framework differs in the sense that the geometric center of the wing is offset by a length $l$, see Figure 6.5. This length introduces an extra velocity component normal to the wing. In the current wing design the position of the leading edge is described by $\phi(t)$, $\theta(t)$ and $\eta(t)$. The position of a typical point on the leading edge is then given by

$$\begin{bmatrix} x \\ y \\ z \end{bmatrix} = \mathbf{R}(\phi)\mathbf{R}(\theta)\mathbf{R}(\eta) \begin{bmatrix} r \\ 0 \\ 0 \end{bmatrix}, \tag{6.4}$$

in which the rotation matrices are defined as:

$$\mathbf{R}\phi = \begin{bmatrix} \cos\phi & -\sin\phi & 0 \\ \sin\phi & \cos\phi & 0 \\ 0 & 0 & 1 \end{bmatrix}, \mathbf{R}(\theta) = \begin{bmatrix} \cos\theta & 0 & -\sin\theta \\ 0 & 1 & 0 \\ \sin\theta & 0 & \cos\theta \end{bmatrix},$$

$$\mathbf{R}(\eta) = \begin{bmatrix} 1 & 0 & 0 \\ 0 & \cos\eta & -\sin\eta \\ 0 & \sin\eta & \cos\eta \end{bmatrix} \tag{6.5}$$

The velocities of this point at distance $r$ from the origin are then given by [110]:

$$\begin{bmatrix} v_x \\ v_y \\ v_z \end{bmatrix} = \left[ \dot{\mathbf{R}}(\phi)\mathbf{R}(\theta)\mathbf{R}(\eta) + \mathbf{R}(\phi)\dot{\mathbf{R}}(\theta)\mathbf{R}(\eta) + \mathbf{R}(\phi)\mathbf{R}(\theta)\dot{\mathbf{R}}(\eta) \right] \begin{bmatrix} r \\ 0 \\ 0 \end{bmatrix}, \qquad (6.6)$$

The velocities in the co-rotating coordinate system positioned at the wing leading edge are then given by, using subscript addition $le$. This coordinate system is an intermediate step towards the two-dimensional wing coordinate system.

$$\begin{bmatrix} v_{x,le} \\ v_{y,le} \\ v_{z,le} \end{bmatrix} = \mathbf{R}^{\mathrm{T}}(\phi)\mathbf{R}^{\mathrm{T}}(\theta)\mathbf{R}^{\mathrm{T}}(\eta) \begin{bmatrix} v_x \\ v_y \\ v_z \end{bmatrix}. \qquad (6.7)$$

Since there is no spanwise velocity, the first term of this vector is zero. The resulting velocities in the two-dimensional coordinate system co-rotating with the leading edge of the wing, $x'_{le}$–$y'_{le}$ , are given by:

$$\begin{bmatrix} v_{x'_{le}} \\ v_{y'_{le}} \end{bmatrix} = \begin{bmatrix} r\left( \cos\theta\dot{\phi}\cos\eta + \sin\eta\dot{\theta} \right) \\ -r\left( \sin\eta\dot{\phi}\cos\theta - \cos\eta\dot{\theta} \right) \end{bmatrix}. \qquad (6.8)$$

The velocities in the geometric center fixed co-rotating coordinate system can be determined by the added term due to shifted pitching axis of the wing:

$$\begin{bmatrix} v_{x'} \\ v_{y'} \end{bmatrix} = \begin{bmatrix} r\left( \cos\theta\dot{\phi}\cos\eta + \sin\eta\dot{\theta} \right) \\ -r\left( \sin\eta\dot{\phi}\cos\theta - \cos\eta\dot{\theta} \right) + l\dot{\eta} \end{bmatrix}. \qquad (6.9)$$

While the velocities can be obtained in this manner the accelerations are not as straightforward from a mechanical viewpoint. The origin of the quasi-steady aerodynamic models lies in the work by Sedov [111]. This introduces a change in approach for the accelerations. The mechanical definition of the accelerations would be to take Equation (6.6) and take the time derivative. In this setting the required accelerations are obtained by looking at the time derivatives of the velocities in Equation (6.9). This in order to satisfy requirements imposed by using added mass as done in this model. The accelerations are then given by:

$$\begin{bmatrix} a_{x'} \\ a_{y'} \end{bmatrix} = \begin{bmatrix} r\left[ \left( \ddot{\phi}\cos\theta + \dot{\theta}\left( \dot{\eta} - \dot{\phi}\sin\theta \right) \right)\cos\eta + \left( \ddot{\theta} - \dot{\eta}\dot{\phi}\cos\theta \right)\sin\eta \right] \\ r\left[ \left( \dot{\theta}\left( \dot{\eta} - \dot{\phi}\sin\theta \right) - \ddot{\phi}\cos\theta \right)\sin\eta + \left( \ddot{\theta} - \dot{\eta}\dot{\phi}\cos\theta \right)\cos\eta \right] + l\ddot{\eta} \end{bmatrix}. \qquad (6.10)$$

The expressions Equation (6.9) and (6.10) are used to couple the mechanical model described in Section 6.4.1 to the quasi-steady aerodynamic model here. These quantities are easily accessible in the mechanical modeling setting used here.

The quasi-steady model is then defined as follows: The infinitesimal loads on the geometric center of an infinitesimal strip of wing are defined in the two-dimensional space from Figure 6.5b. The forces and torques reviewed are due to aerodynamic loads only. Berman and Wang [12] include the infinitesimal mass of the slice, in this approach inertia properties are treated separately in the mechanical model described in Section 6.4.1. Starting from the loads on the wing slice:

$$dF_{x'} = \left[ m_{22} v_{y'} \dot{\eta} - \rho \Gamma v_{y'} - m_{11} a_{x'} \right] dr - dF_{x'}^{\nu}, \tag{6.11}$$

$$dF_{y'} = \left[ -m_{11} v_{x'} \dot{\eta} + \rho \Gamma v_{x'} - m_{11} a_{y'} \right] dr - dF_{y'}^{\nu}. \tag{6.12}$$

In these expressions the first term corresponds to the added mass, see Section 2.5, of the wing which is treated as real mass. The second term corresponds to the circulation around the wing and is related to the density of the air. The third term is strictly the inertial force which corresponds to the acceleration of the added mass of the wing. The last term is a dissipative term based on viscous loads. Torques on the infinitesimal wing slice are obtained from:

$$d\tau_\eta = \left[ (m_{11} - m_{22}) v_{x'} v_{y'} - I_a \ddot{\eta} \right] dr - d\tau^{\nu}. \tag{6.13}$$

In this equation the first two terms are due to added mass effects. The last term is due to viscous forces induced by wing rotation.

The circulation, which is required to determine the loads on the infinitesimal slice of wing in Equations (6.11) and (6.12), is determined by:

$$\Gamma = -\frac{1}{2} C_T c(r) |\mathbf{v}| \sin 2\alpha + \frac{1}{2} C_R c^2(r) \dot{\eta}. \tag{6.14}$$

In which $C_T$, $C_R$ are the translational and rotational coefficients, $c(r)$ is the chord length at distance $r$ from the origin and $\alpha$ is the angle of attack.

The dissipative terms required for Equations (6.11) and (6.12) are given by:

$$dF_{x'}^{\nu} = \frac{1}{2} \rho c(r) \left[ C_D(0) \cos^2 \alpha + C_D(\pi/2) \sin^2 \alpha \right] |\mathbf{v}| v_{x'} dr, \tag{6.15}$$

$$dF_{y'}^{\nu} = \frac{1}{2} \rho c(r) \left[ C_D(0) \cos^2 \alpha + C_D(\pi/2) \sin^2 \alpha \right] |\mathbf{v}| v_{y'} dr. \tag{6.16}$$

In which $C_D$ is the drag coefficient and $\rho$ is the density of the air. The coefficients used in Equations (6.14),(6.15) and (6.15) are experimentally obtained and constitute correction factors required for improved accuracy of the model. The last dissipative term is only influenced by rotational motion of the wing and flapping frequency and given by

$$d\tau^{\nu} = \frac{1}{16} \pi \rho c^4(r) \left[ \mu_1 f + \mu_2 |\dot{\eta}| \right] \dot{\eta} dr. \tag{6.17}$$

The dimensionless viscosity coefficients used are given by $\mu_1$ and $\mu_2$ and the flapping frequency by $f$. The added mass terms also required for Equations (6.11), (6.12) and (6.13), are based on the assumption that the wing is modeled as a very thin ellipsoid, this assumption is commonly used in quasi-steady models. The added mass terms are then given by defined by:

$$m_{11} = \frac{1}{4}\pi\rho b^2, \tag{6.18}$$

$$m_{22} = \frac{1}{4}\pi\rho c^2(r), \tag{6.19}$$

and

$$I_a = \frac{1}{128}\pi\rho[c^2(r) + b^2]. \tag{6.20}$$

Which are purely determined by the geometry of the wing slice.

The model is implemented by assigning 10 equally spaced strips of constant width in span wise direction over the wing, see Figure 6.3. On these strips the aerodynamic loads are calculated. Velocities and accelerations of the geometric center of the wing, needed above for the calculation of the aerodynamic forces, are obtained from the mechanical model.

### 6.4.4 Implementation

Both the mechanical and aerodynamical model are implemented in the Mathworks Simmechanics environment. The combined model is solved for a given time period using fixed time steps. The Simmechanics implementation is coupled to the Matlab workspace to be able to control the kinematic input by scripts or implement an optimization procedure. The current implementation allows for easy implementation of different wing geometries and input kinematics.

### 6.4.5 Validation

In order to use the described quasi-steady aerodynamic model the current implementation has to be checked for validity. Since the model will be used to test wings of proprietary design, a benchmark case has to be selected to objectively judge performance. The current implementation is compared to the implementation by Berman and Wang [12]. The wing designs that will be tested are very close to Hawkmoth wings from both a kinematic and morphological perspective. It is therefore that the model parameters can be used for the proposed wing designs.

The test case uses the morphological and kinematic data from a Hawkmoth from Willmott and Ellington [135, 136]. Berman and Wang used the kinematics from Sun and Du [118] and compared with the same study, which is based on solving the Reynolds averaged Navier-Stokes equations. The current implementation will be tested using the same set of morphological and kinematic parameters.

The test case consists of three parts: The morphology of the wing, *i.e.*, the planform, the aerodynamic parameters and the kinematic pattern.

The wing morphology is described by a simple elliptic description [12], based on the ellipsoidal description given by Weis-Fogh [134]. This description relies on two parameters: $\bar{c}$ and $R$, *i.e.* average chord length and wing length, respectively. Based on these parameters the wing chord is defined as a function of the wing length:

$$c(r) = \frac{4\bar{c}}{\pi}\sqrt{1 - \frac{r^2}{R^2}} \tag{6.21}$$

The morphological parameter values used are identical to those used by [12] for the Hawkmoth case, in which $\bar{c}$ is 18.26 mm and $R$ is equal to 51.9 mm.

The aerodynamic parameters used are based on Hawkmoth measurements. The values used are: $C_T$ and $C_D$ from [12] obtained from Usherwood and Ellington [124] valued $C_T = 1.678$, $C_D(0)$ and $C_D(\pi/2)$ are 0.07 an 3.06, respectively. $C_R$ is set to be equal to $\pi$, obtained from Andersen *et al.* [5]. Viscous torque parameters $\mu_1$ and $\mu_2$ are taken to be 0.2, from Andersen *et al.* [4]. Density of air $\rho$ is 1.29 $\mathrm{kg\,m^{-3}}$.

The kinematic parameters used are based on the simplified kinematic description of the wing movement given by Equations 6.1, 6.2 and 6.3. The parameters are $f$=26.3 Hz, $\phi_m$=1.05 rad, $\theta_m$=0 rad, $\eta_m$=0.55 rad, $\theta_0$=0 rad, $\eta_0$=0 rad, $\Phi_\theta$=0 rad and $\Phi_\eta$=-0.29 rad. The usage of simplified kinematics, especially in the description of the wing pitching timing, will introduce some discrepancies between this implementation and the reference model.

The lift production of the model is taken as the reference. The average lift production is compared. The lift produced by the model by Berman and Wang [12] is $9.26\times10^{-3}$ N, the lift produced by the current implementation is $9.26\times10^{-3}$ N. It can be seen that there are small discrepancies between the current implementation and the reference implementation by Berman and Wang [12]. Discrepancies are explained by the usage of a smaller number of wing strips and the afore mentioned simplification in the wing kinematics description.

## 6.5   Optimization

The wing design with the addition of the compliant element has to generate lift in a passive manner. In order to do so, it has to be able to reproduce a desired wing pitching motion when the only input is the wing sweeping motion. The wing sweeping motion is the driving output of the resonant wing–thorax system. To have a set point for the required wing pitching output, a desirable wing kinematic description has to be defined which is to be used as the reference.

In order to tune the passive hinge a reference motion has to be defined. The kinematic description presented in Section 6.2 is used. In this selection a number of kinematic parameters are predefined, namely, the frequency and wing sweeping amplitude which are the resultant of the analysis the wing-thorax resonant

system in Section 6.2. The parameters concerning heaving motion of the wing are constricted to zero by the thorax design. Since symmetric flapping is assumed, the pitching offset is zero. The remaining parameters are the wing pitching amplitude and wing pitching phase shift. Thus, two values have to be determined to fully define the reference motion.

Since the goal of this study is to determine the possibility to tune an elastic wing to exploit passive wing pitching for reproducing wing kinematics, a conservative starting point for pitching kinematics has to be chosen. Inspiration for these values lies in insects of similar size and experimental experience with the wing design. The amplitude of the wing pitching motion has been chosen to be 45°, this value is larger than for Hawkmoths but considered a safe value in the current setting and not uncommon among insects. The pitching phase shift is chosen to be -0.5$\pi$ rad and is considered a conservative value when looking at Hawkmoth kinematics. As an overview, the kinematic values which shall be used as the reference are given in Table 6.2.

**Table 6.2:** *Kinematic parameters which are used as the reference model. The proposed wing design should be tuned such that they represent these kinematics while relying on the exploitation of passive wing pitching. The motivation of these values lies in the previously developed resonant structure and partially in insect wing kinematics.*

| Parameter | Value |
| --- | --- |
| f[Hz] | 27 |
| $\phi_m$[rad] | 0.66 |
| $\theta_m$[rad] | 0 |
| $\eta_m$[rad] | $0.25\pi$ |
| $\theta_0$[rad] | 0 |
| $\eta_0$[rad] | 0 |
| $\Phi_\theta$[rad] | 0 |
| $\Phi_\eta$[rad] | -0.5$\pi$ |
| N | 1 |

### 6.5.1 Approach

In order to be able to passively reproduce the desired wing kinematics an elastic element was introduced, see Figure 6.4. The only degree of freedom of this system is the pitching motion. The other kinematic properties, $\eta$ and $\theta$, are fully defined. The pitching motion is determined by the inertial- and aerodynamic loads and the torque introduced by the rotational spring which represents the elastic element. The properties of this spring have to be determined and these properties are the only tunable parameters of this system.

The spring torque required to sustain the dynamic equilibrium of the wing

pitching motion is not known. Consequently, a spring is defined which includes both a linear and nonlinear component to be able to cover a wide range of possible rotation-torque relationships. The spring which provides the pitching restoring torque is taken as:

$$k = k_1 \eta + k_2 \eta^3. \tag{6.22}$$

This spring shows symmetric behavior around the centered position. This is supported by the assumption of a symmetric pitching motion. The two spring constants are the tunable parameters of the system. A flowchart of the approach used to determine optimal wing pitching hinge stiffness is given in Figure 6.6

The process described in this flowchart is centered around the coupled mechanical and aerodynamical models. The tunable mechanical model has one degree of freedom, namely, the wing pitching. The wing sweeping and heaving motion are fully described. The input parameters are the spring constants which determine the spring constant of the spring, $k_1$ and $k_2$. The objective is to minimize the difference between the desired pitching kinematics, $\eta_{ref}$, and the pitching kinematics obtained from the simulation, $\eta$.

The comparison of the wing pitching motion has to be done over time. To obtain accurate results, *i.e.*, reduce the influence of startup effect, the model simulation time is set to 0.2 s, significantly longer than the flapping cycle time. The tunable model is given an initial pitching deflection, equal to desired mid-stroke value, again to reduce calculation time. Many options exist to compare the desired and simulated pitching kinematics. A simple approach is used here based on expressing the pitching motion as a vector over time, designated $\boldsymbol{\eta}_{cycle}$, and defined as $\boldsymbol{\eta}_{cycle}^{\mathrm{T}} = [\eta_{t_n}, \eta_{t_{n+1}}, \ldots, \eta_{t_{n+T}}]$. The norm of the difference between the two pitching vectors is used as the objective. The flapping cycle used for comparison is taken at the end of the simulation time to exclude startup effects. This can be expressed as follows depending only on parameters $k_1$ and $k_2$:

$$f(k_1, k_2) = \frac{||\boldsymbol{\eta}_{ref,cycle} - \boldsymbol{\eta}_{cycle}(k_1, k_2)||}{n_T} \tag{6.23}$$

The objective is scaled with the number of time steps in one flapping cycle, $n_T$, in order to be able to compare results with different time steps and flapping frequencies. The spring constants, $k_1$ and $k_2$ have to be bounded to exclude unfeasible solutions and speed up the tuning process.

## 6.5.2   Tuning

Initial investigation has shown that the problem is subject to local minima and therefore considerable effort has been put into finding bounds within which the optimal value for the spring constants can be found. This initial exploration of the domain has brought forward that very valuable results can be obtained while looking only at $k_1$ and keeping $k_2$ zero. The initial values of $k_1$ between which an optimal value can be found, are in the stiffness range $1.0 \times 10^{-4}$ Nm/rad to

$5.0 \times 10^{-4}$ Nm/rad. Outside this range the model quickly loses convergent properties. As an example, the response for two different starting conditions are shown in Figure 6.7 for $1.5 \times 10^{-4}$ Nm/rad and $4.0 \times 10^{-4}$ Nm/rad. It can be seen that for the lower value, there is significant overshoot of the pitching deflection. For the higher value the deflection is too small, indicating too rigid a wing hinge. In both cases startup irregularities can be seen.
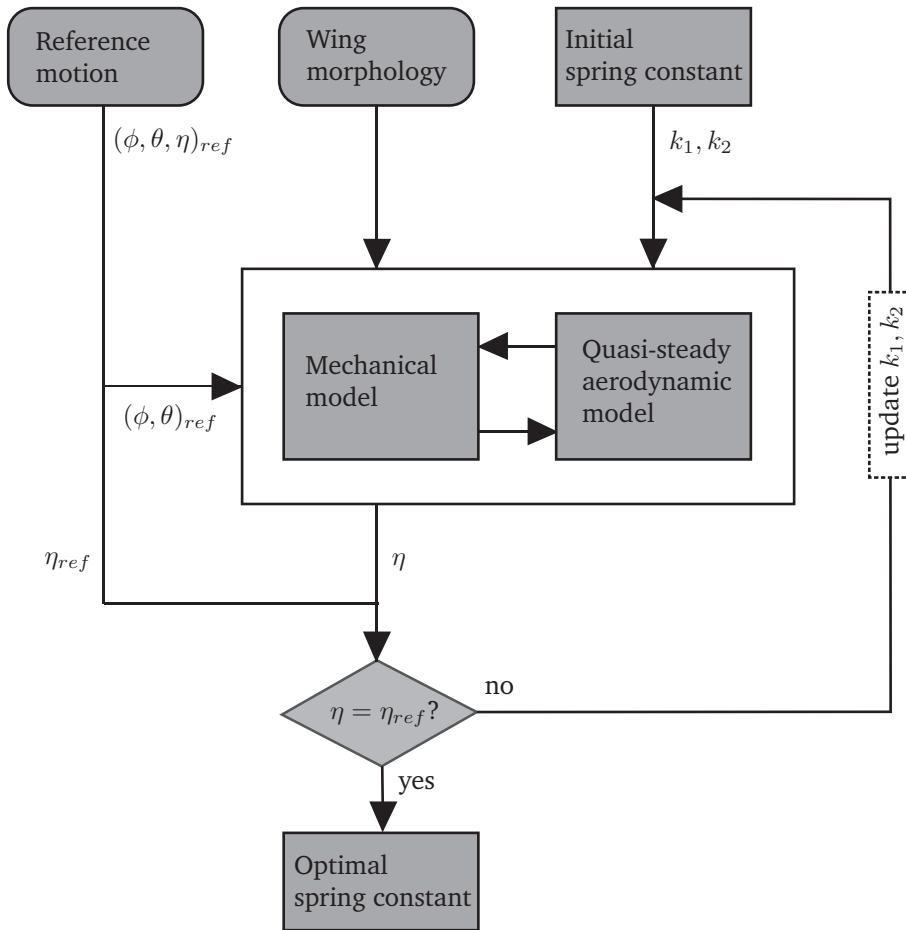


**Figure 6.6:** *Flowchart used to tune the spring which provides the restoring torque required to obtain passive pitching. The goal is to accurately reproduce the reference wing motion. The center of the flowchart is the coupled mechanical–aerodynamical model. In this setting the only output of this model which is used is the pitching motion. This pitching motion is compared to the desired pitching motion. Spring constants $k_1$ and $k_2$ are the tunable parameters. Inputs are the desired wing kinematics and wing morphology.*
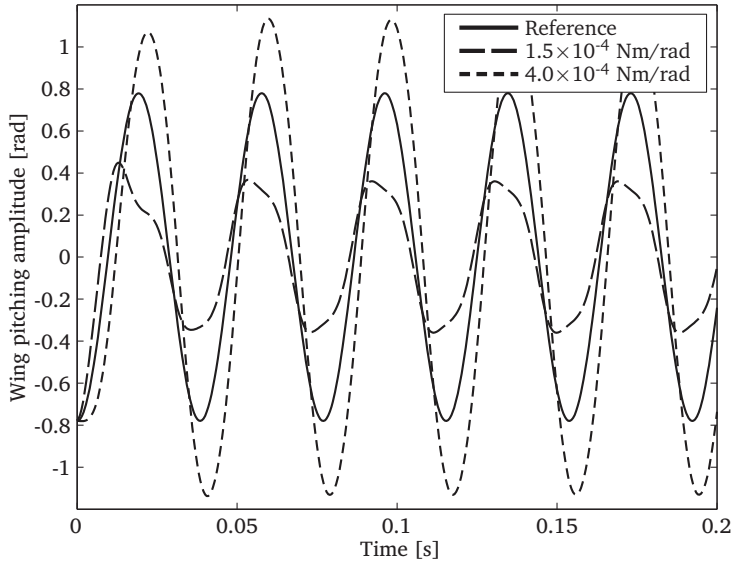
**Figure 6.7:** *Wing pitching response for 2 different hinge stiffness values, $1.5\times10^{-4}$ Nm/rad and $4.0\times10^{-4}$ Nm/rad as compared to desired wing pitching response of the reference.*
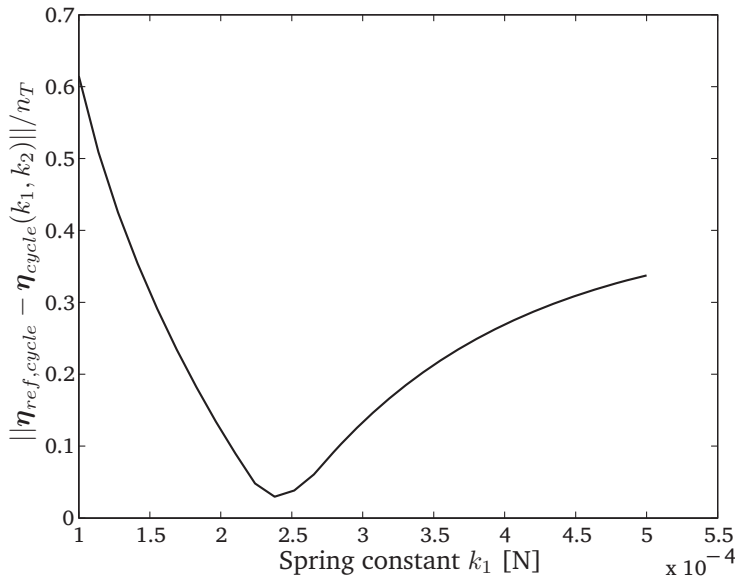


**Figure 6.8:** *Objective of Equation* (6.23) *for the $k_1$ range $1.0\times10^{-4}$ Nm/rad to $5.0\times10^{-4}$ Nm/rad showing presence of a minimum. The objective is scaled with the number of time steps in one flapping cycle, $n_T$.*
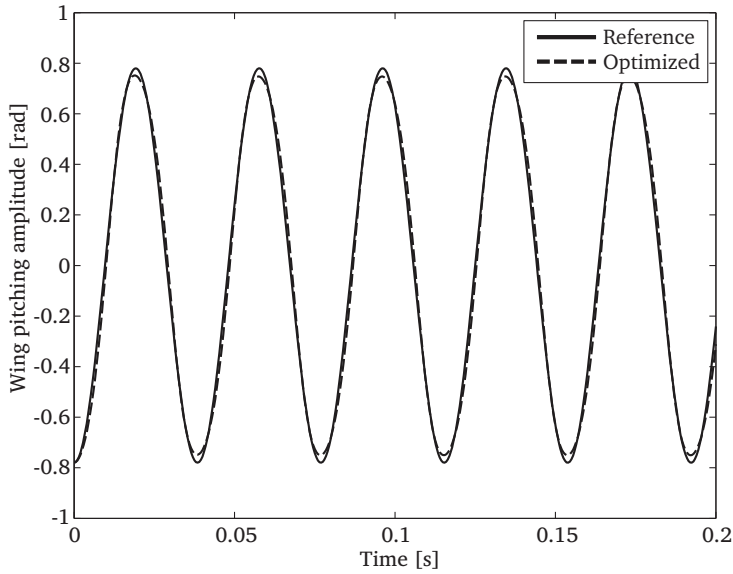
**Figure 6.9:** *Reference and system wing pitching response for the optimized stiffness value of $2.38 \times 10^{-4}$ Nm/rad. The optimized model shows a good fit, most discrepancies are found in the maximum positions.*

The objective function is plotted in Figure 6.8 for the spring constant range indicated above. The optimum can be determined by visual means but a line-search procedure is implemented which allows for an automated procedure in case of small changes in kinematics or wing morphology. The optimum stiffness value is determined at $2.38 \times 10^{-4}$ Nm/rad. The wing pitching response for the optimum value of the wing hinge stiffness is shown in Figure 6.9 and compared to the reference pitching response. The value found is now ready to be tested for performance, real wings will have to be manufactured and tested in a test setup to experimentally check the results. The will be done in the next section.

## 6.6 Realization and Testing

The optimized value for the wing hinge has to be implemented in the proposed wing design. The elastic element is essentially a compliant hinge and effective stiffness can therefore be approximated by [68]:

$$k_{hinge} = EI/l_{hinge} \tag{6.24}$$

In which $E$, $I$ and $l_{hinge}$ are the Young's modulus, second moment of area and length of the hinge, respectively. Using the proposed spring steel sheet, 0.03 mm
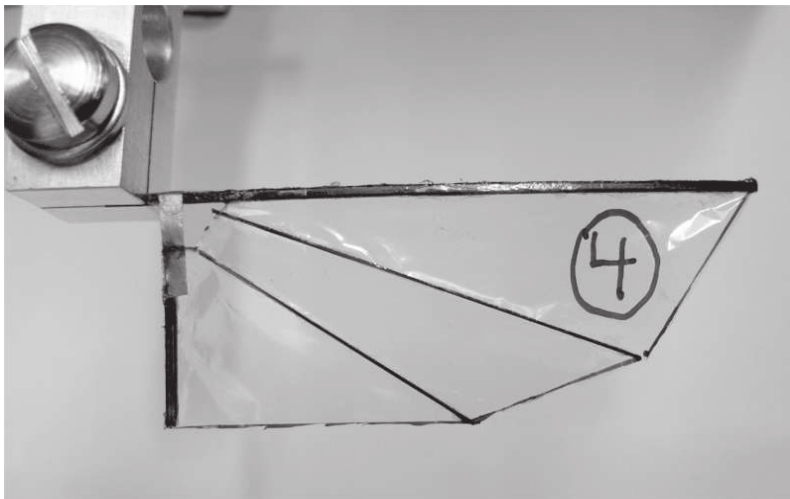
**Figure 6.10:** *The realized wing, showing the elastic element positioned near the wing root, mounted in the clamp for actuation in the test setup.*
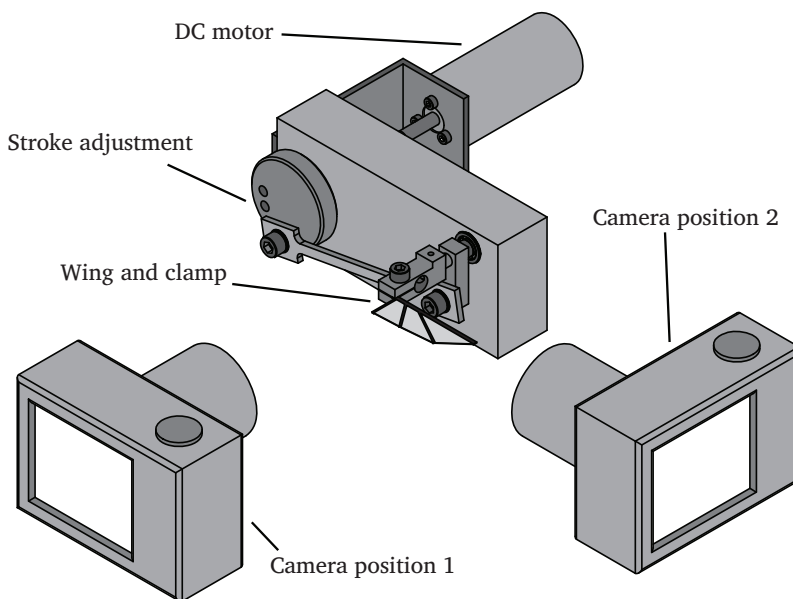


**Figure 6.11:** *Test setup used to independently test the wings. Linkage system is used to transform the DC motor output to a sinusoidal wing sweeping motion. Various sweeping amplitudes can be chosen as well as actuation frequency. Two camera positions are indicated: 1. To review pitching behavior and 2. to capture mid-stroke pitching motion.*

thickness, and choosing a link length of 3.5 mm leads to a link width of 1.8 mm. The rest of the wing is constructed using materials and dimensions as described in Section 6.3. The completed wing is shown in Figure 6.10.

Before the wings are attached to the resonant mechanism they are tested in an experimental setup. This setup uses a DC motor to drive a mechanism that converts rotation into reciprocal wing motion found at the wing root. The mechanisms is adjusted such that the wing sweeping range corresponds to the range obtained using the resonant mechanism. Only wing sweeping is actuated. Actuation frequencies are obtained by means of an encoder present on the electric motor. The test setup is shown in Figure 6.11. This setup does not provide an exact simple harmonic motion. The harmonic motion provided is close enough to simple harmonic for the intended purpose.

Wing movements are captured on video using a camera augmented by a strobe light to visualize the motion, exploiting the harmonic nature of the movement to slow down the motion. Two different camera positions are used, shown in Figure 6.11, the first position is chosen such that the entire flapping motions can be captured by positioning the camera such that the wing sweeping can be caught. Using this setup the dynamic response of the wing can be classified. The second position is chosen such that the pitching deflection at the center of the sweeping stroke can be imaged. This is done by placing the camera such that the viewing direction is coincident with the main spar of the wing during wing sweeping stroke.

### 6.6.1 Testing

The wing is tested using the described setup and settings imposed by later usage as part of the resonant mechanism, *i.e.* a flapping frequency of 27 Hz and wing sweeping motion with an amplitude of ~37.5°. A sequence of one wing flap is shown in Figure 6.13.

The mid stroke wing deflections on both sides of the wing sweeping stroke are shown in Figure 6.12. Analysis has shown that the real wing deflection at the base does not reach the intended 45° at the base of the wing, it is more close to 37±2° on both the upstroke and downstroke, shown by $\eta$ in Figure 6.12a and b. Small differences exist between the up and downstroke, as can be seen in Figure 6.12. Part of the explanation for this phenomenon is the construction of the wing, which has a mass distribution which is not symmetric with respect to the membrane. The test setup drive mechanism introduces an asymmetry in the wing sweeping motion and might therefore also be a factor in the asymmetry of the wing pitching. Further along the wing, towards the tip, considerable increased rotation indicates that the rigid plate assumption taken during modeling is questionable at the least.
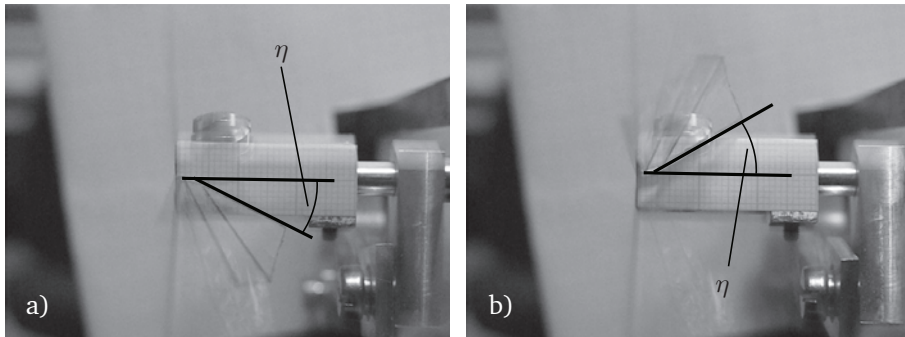
**Figure 6.12:** *Mid-stroke pitching deflections for the upstroke in a) and the downstroke in b). Pitching deflection indicated by η.*

## 6.7   Concluding remarks

The proposed solution of adding an elastic element to an existing wing design for flapping-wing MAV wings has the possibility of offering a very simple modification which makes it possible to achieve passive wing rotation. The tailoring of the stiffness of the elastic element can be accomplished using currently available quasi-steady aerodynamic models. The tailored wings are able to accurately reproduce insect wing kinematics when wing sweeping input is a harmonic signal.

Discrepancies exist between predicted and realized response and can be partially explained by to manufacturing tolerances. The currently used quasi-steady model might not capture the complete behavior of the wing due to membrane deformations. Consequently, fine tuning of the wing stiffness has to be done based on experimental techniques, *e.g.,* optimization using a design of experiments approach.

The predicted wing pitching deflections are not reached by elastic hinge action alone. Membrane deflections are present and increase total deflections increasingly towards the tip of the wing. The combination of these two effects leads to more beneficial effective pitching deflections towards the wing tip. Further tailoring of the wing stiffness can be expanded by including a simplified model of the membrane stiffness which can be tuned for aerodynamic efficiency by a modification of the current setting.

The wings and tuned wing pitching hinge will be coupled to the resonant ring type structure analyzed in Chapter 7. When combined, this system should provide efficient lift production by means of accurate reproduction of insect wing motion, both in sweeping and pitching. Further weight reduction of the other parts of the system: ring, wing coupling mechanism and actuator should lead to a system capable of producing lift in the same order as the total mass.

The current wing shape is a starting point, inspired by other flapping-wing
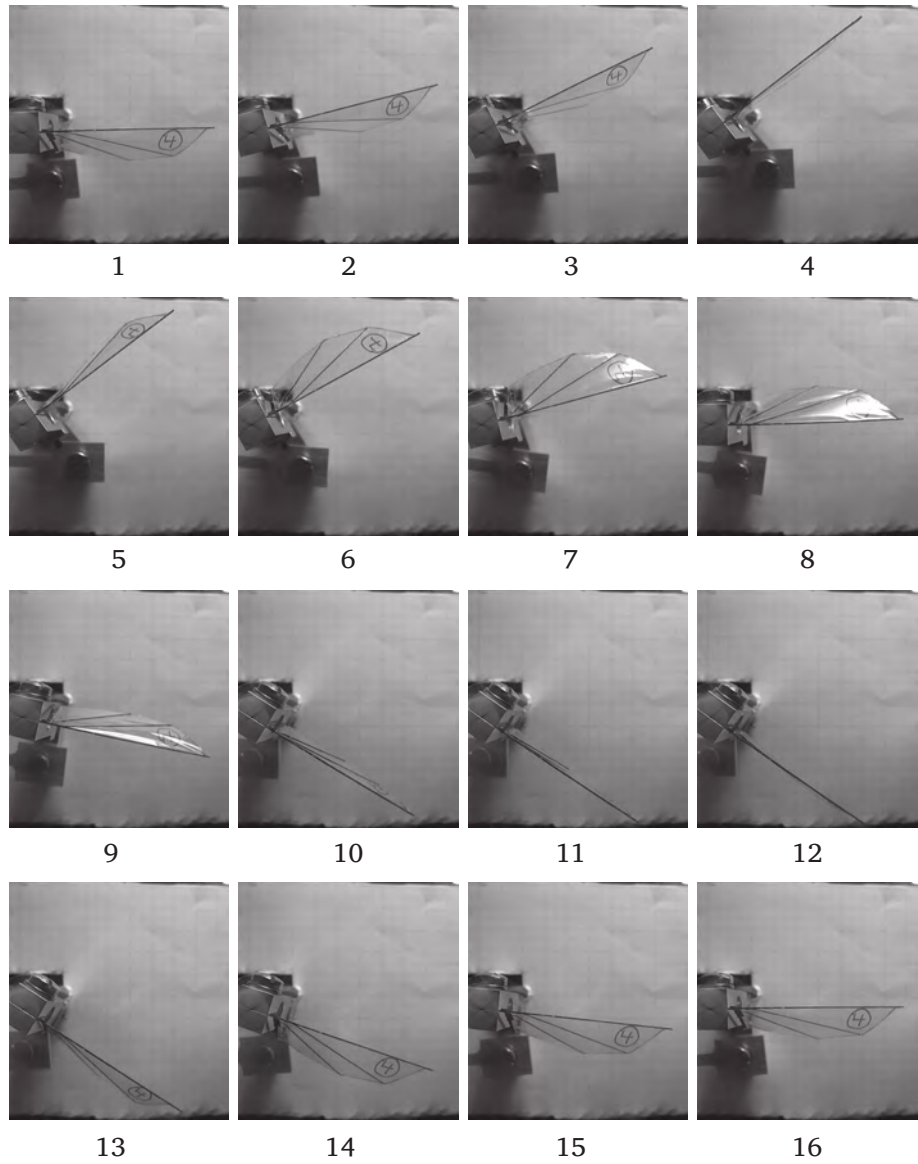
**Figure 6.13:** *Sequence of consecutive steps of the wing flapping motion for one flapping cycle, clearly showing passive wing pitching*

MAV designs. Improvements in the lift production can be expected by tuning the shape of the wing. The usage of a localized hinge to accomplish passive wing pitching leads to an accurate reproduction of wing motion. Improvements, in aerodynamic efficiency, are expected when a more insect inspired design route is chosen, for example, the introduction of a bending torsion coupling.

# Chapter 7

# Integration and experiments

## 7.1 Introduction

The focus of this chapter is on the integration and testing of the different aspects of the flapping-wing MAV. The different resonant thorax concepts, which were proposed on a conceptual level in Chapter 4 and analyzed and preselected in Chapter 5, need to be combined with the wings which were analyzed and tuned in Chapter 6. The resulting combination of a resonant base and passively pitching wings needs to be realized and tested to evaluate performance and to provide recommendations for improvements. The first step towards testing is the integration of the wings and thorax structure [19] in to prototype structures. These prototypes should conform to the most basic requirement on the flapping-wing MAV, namely the striving for low mass structures.

In order to thoroughly evaluate the performance of the prototype it is necessary to look at specific aspects. Many different performance metrics can be used to judge performance of the prototypes. In fact the simplest performance index would be the successful lift-off of the prototype. However, due to the usage of an actuator with low specific power density, stable flight or even unstable lift-off are not to be expected. Therefore, a more structured method of testing performance should be used.

The first aspect to be tested is the production of lift. The amount of lift is a valuable index for performance of the prototype. A suitable test setup should be able to provide information on the amount of lift which is produced. The second aspect is the correct reproduction of intended motion in the resonant state, consisting of: wing movement angles and flapping frequency. With these two aspects known performance of the prototype can be judged in order to gain insight into options for performance improvement. One possible manner of the measurement of kinematic patterns requires the possibility to have a series of images

127

or videos which can be analyzed. These images or the videos can be obtained by various means. Options include: visualization by means of a high speed video camera, making pictures using a conventional camera using a short exposure time or slowing the visible motion of the prototype down by optical means exploiting the harmonic nature of the movement.

This chapter discusses the manufacture of the prototypes, the aspects of the prototype that are to be tested and the design of the test bed. The two aforementioned aspects are tested; lift production and reproduction of motion, leading to a review of the overall performance of the design.

## 7.2   Realization

The integration of the resonant base and the passively pitching wings consists of combining the designs of the two individually analyzed parts. In the detailed analysis of the concepts non lift producing wings were already included (see Section 5.6). The newly designed wings (see Chapter 6) share the same attachment points as the non lift producing wings and can therefore be easily combined with the resonant base.

The materials and manufacturing methods, as well as dimensions, used for the design have been described in Section 5.7 for the thorax and Section 6.6 for the wings, respectively. The detailed design consisting of the resonant thorax and the passively pitching wings is shown in Figure 7.1. The different parts are indicated by numbers. The mass of the prototype without actuator is approximately 0.6 g. The realized prototype, including actuator, is depicted in Figure 7.2.

## 7.3   Design of experiments

The performance of the prototype is judged based on two separate aspects. The first aspect is the correct reproduction of the intended wing motion. The second aspect is the lift production. Both aspects of the design, the generation of correct wing motion and the generation of lift, require the model to be driven at resonance. This is accomplished using a frequency generator and signal amplifier to drive the solenoid actuator. Resonance is observed by visual means.

### 7.3.1   Test setups

The measurement of lift generation of the prototype requires a setup which is capable of measuring the lift force while the prototype is driven at resonance. Since the signal wires, which are used for suspending the prototype, are connected to the actuator, they are inherently coupled to the resonant motion of the prototype. Consequently, the intended test setup has to be able to identify the lift from the total signal either by filtering or mechanical isolation. Focus is on simplicity of the
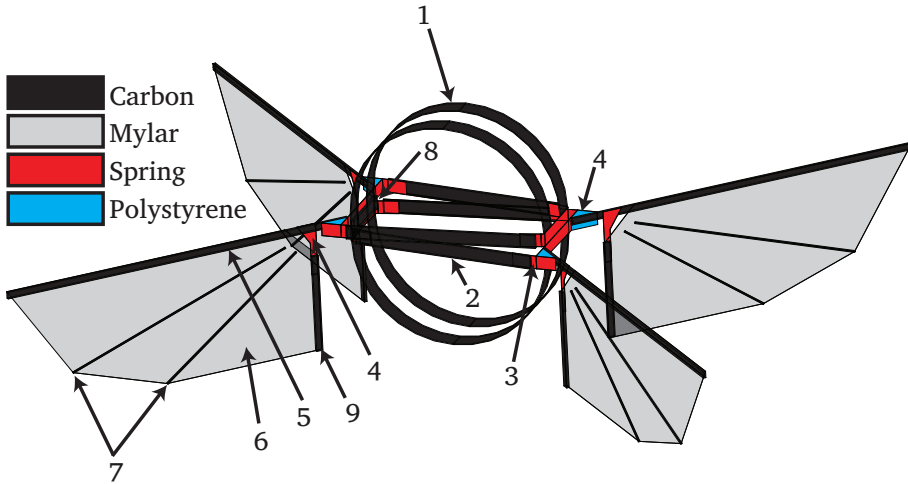
**Figure 7.1:** *The detailed design. The different materials have been indicated by the colors shown in the legend. The parts are, in numerical order: 1) The ring, one of two used for elastic energy storage. 2) Strut, part of the amplification mechanism. 3) Elastic hinge, part of the amplification mechanism. 4) Wing hinge. 5) Wing main spar. 6) Wing membrane. 7) Wing stiffening spars. 8) Crossbar to couple the rings. 9) Secondary wing spar.*

measurement while retaining the required accuracy. Since multiple prototypes might be tested, adaptability of the test setup is favored.
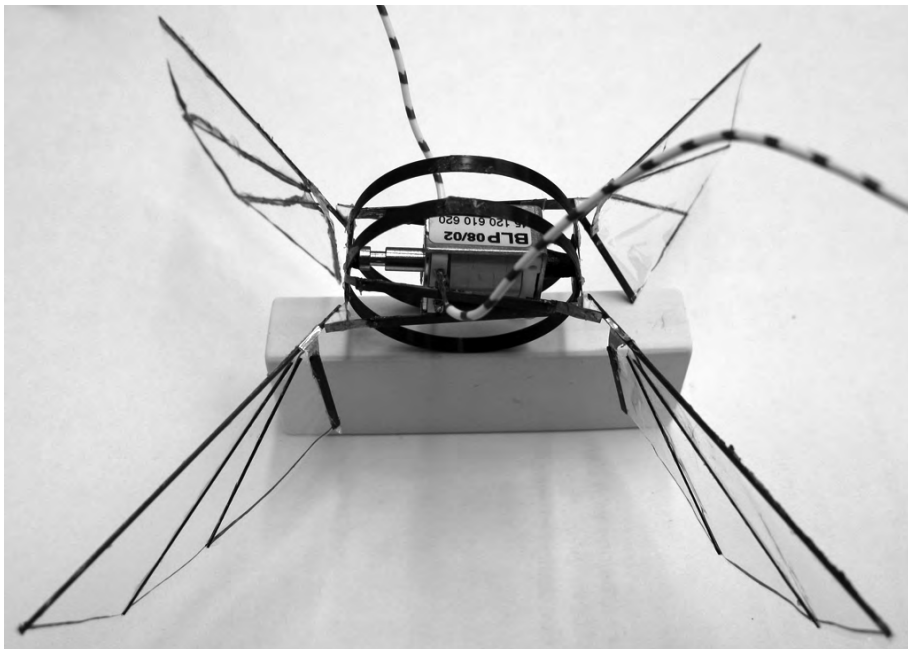
### 7.3.2   Test setup design

The first measurement setup is intended for the imaging of motion patterns: The movement of the structure is measured by suspending the model and using the strobe light to slow down the visible movement. This allows the visualization of the model in a range of motion from standstill, with the strobe light exactly at resonance frequency, or in a slow moving fashion when the strobe light is at a frequency near the resonance frequency. The choice for this method is made based on the aim for simplicity. Using this setup the movement of the prototype can be checked visually in real-time which is a huge benefit in this experimental stage. A consumer camera is used for obtaining video material, still images are used to review the motion. The suspension of the model is done in the test setup described below which is also used for lift measurements, the setup is shown in Figure 7.3 in which the camera, with top view on the model, can be seen.

The aspect of the test setup is designed to measure the lift produced is treated next. This aspect has been effectively integrated with the options for the review of motion. The requirements of simplicity and isolation of the vibration of the model have been fulfilled by selecting a fully mechanical measurement setup.

This is accomplished by suspending the model from a thin cantilever beam and using deflection changes to measure lift production, see Figure 7.3. Fenelon and Furukawa [56] used a similar setup to test their wing setup. The cantilever beam setup is suitable for the force range from 0 N to the weight of the structure including the actuator, which is the range for which the calibration has taken place. The beam is calibrated beforehand to a sensitivity of $1.25\pm0.1\times10^{-3}$N/mm in the intended range of measurement and behavior of the setup is linear in the expected lift force production range. Changes in beam deflection can be directly related to lift production. The setup has been tested and effectively isolated lift forces from vibration influences. This is due to two causes: First is the mechanical filtering introduced by suspending the model from curved power leads, and secondly the mechanical filtering introduced by the eigenfrequencies of the test setup combined with the model. Intended actuation frequencies are far higher than the eigenfrequencies of the test setup and consequently do not lead to significant vibration.

The integrated design of the test setup allows the imaging of motion patterns and the measurement of lift forces to be done using one setup. The benefits of this are that a model can be tested for both aspects in a relatively short period. The tuning of the resonant frequency has to be done once.



**Figure 7.2:** *The realized design including the actuator. Passive wing pitching provisions can be seen at the root of the wing.*
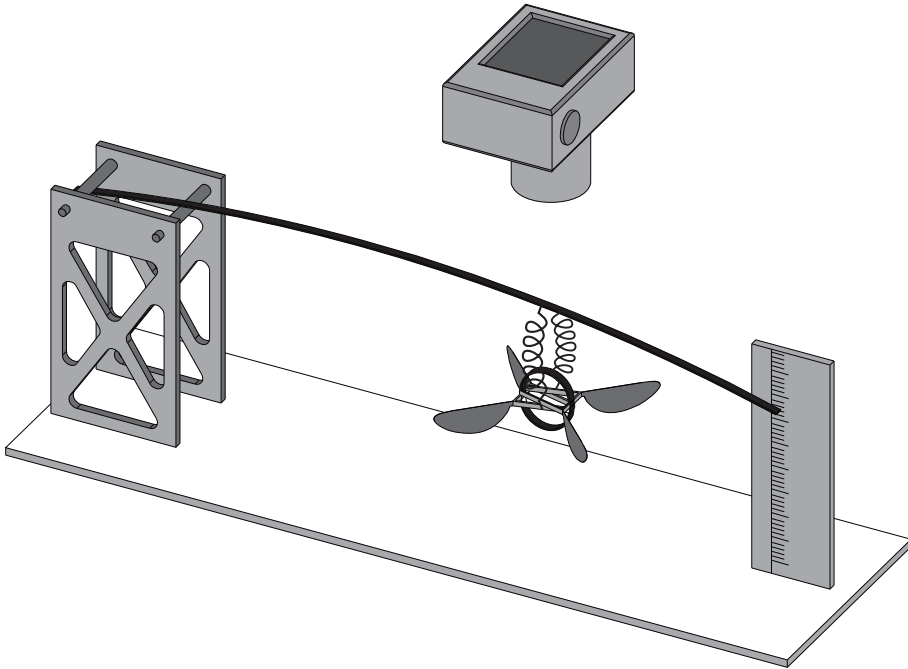
**Figure 7.3:** *Test setup for lift production based on a simple cantilever beam. The power leads are used to suspend the model, these leads effectively decouple the beam from vibrational influences of the prototype. Lift measurement setup is integrated with camera for reviewing wing motion. Integrated setup allows for efficient time usage.*

## 7.4   Experiments

### 7.4.1   Review of motion

The review of the kinematics is based on analysis of a sequence of pictures. The movement can be seen in Figure 7.4 in a sequence that shows one flapping cycle. It can be clearly seen that large amplitude wing sweeping is accomplished, comparable to the experiments with the resonant thorax with non-functional wings (see Section 5.6.5). Wing sweeping deflections are in the order of 65–70°. The resonant frequency was found to be $27\pm0.5$ Hz which is identical to the earlier resonant experiments mentioned above. An analysis of the pitching angle with respect to the sweeping angle shows that the wing pitching movement follows the kinematic pattern found when testing a single wing in the wing testing setup (see Section 6.6). This pattern closely corresponds to the simple kinematic pattern commonly used to describe insect-wing kinematics, *i.e.*, harmonic wing sweeping and harmonic wing pitching with phase shift with respect to the sweeping.

It can be clearly seen that the wing pitching deflection is not purely the result

of wing hinge action, but also partially due to deformations of the wing membrane. It can be seen that the lower right wing exhibits different behavior when compared to the other wings. This wing has been produced in a different batch using slightly different methods. Although this influences lift production negatively it does not significantly influence the resonant behavior of the total structure.

### 7.4.2    Test of lift production

The lift production for one wing will be, based on numerical calculations in Chapter 6, in the order of $2.32 \times 10^{-3}$N to $5.70 \times 10^{-3}$N for one wing. Beforehand it is known that with this value lift-off is not expected as the weight of the actuator prohibits this.

The prototype structure is actuated and driven in its resonant state, which is very close to the previously described 27 Hz for this prototype. The input to the solenoid is a sinusoidal signal with 12 V amplitude. Care has to be taken that the solenoid contracts for both the positive and negative part of the sinusoidal signal. Vibration of the cantilever induced by the resonant prototype is negligible compared to deflection changes induced by lift production. The prototype induces a $7\pm0.5$ mm deflection of the beam, corresponding to a lift production of $8.75\pm0.5\times10^{-3}$N or approximately $0.9\pm0.05$ g.

### 7.4.3    Wing performance

In order to give an indication of the wing performance, a rough estimate of the mean lift coefficient has to be calculated. Since the intended flight mode researched here is hovering flight, the analysis is straightforward. The mean lift coefficient is reviewed at the radius of gyration of the wing. In insects this corresponds to approximately half the wing radius, see [43, 81, 134], and is defined by

$$R_g = \sqrt{\frac{1}{S} \int_0^R r^2 c(r)\, dr}, \tag{7.1}$$

in which $S$ is the surface area of a single wing, $R$ is the radius of the wing and $c(r)$ is the chord at distance $r$ from the wing root. For the current wings a slightly different approach has to be used. This is due to the fact that the wing root has an offset which originates in the topology of the amplification mechanism, see Figure 5.19 on Page 87. The area radius of gyration is determined by

$$R_g = \sqrt{\frac{I}{S}}, \tag{7.2}$$

in which $I$ is the second moment of area with respect to the axis of rotation of the wing. Using the current wing, as described in Section 6.3, $R_g$ is approximately
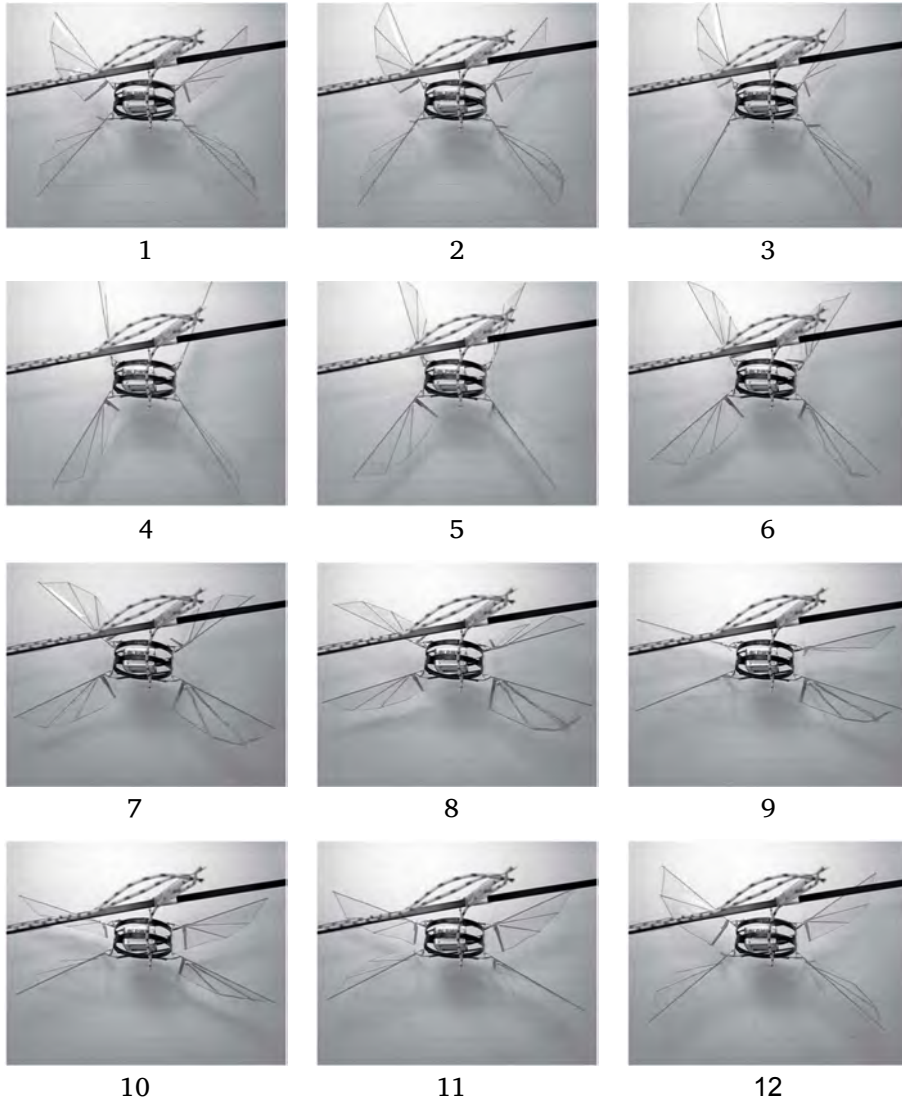
**Figure 7.4:** *Sequence of figures representing one flapping cycle, resonant frequency of 27 Hz, 65–70° wing sweeping angle. Passive wing pitching can be clearly seen, phase shift with respect to the wing sweeping motion can be clearly seen.*

30 mm. The velocity definition used for the mean lift coefficient estimate is the mean of the velocity squared at $R_g$. This is obtained by integrating the simple harmonic wing motion and given by

$$\bar{u} = \tfrac{1}{2}\sqrt{2}R_g A\omega. \tag{7.3}$$

$A$ and $\omega$ are the flapping amplitude and angular frequency, respectively. The mean lift coefficient is then defined as

$$\bar{C}_L = \frac{2L}{\rho\bar{u}^2 A}, \tag{7.4}$$

where $L$ and $\rho$ are the lift force for one wing and the density of air. Using the measured frequency, lift generation for one wing, $L$, and flapping amplitude: 27 Hz, $2.19\times10^{-3}$N and 0.57 rad, yields a mean lift coefficient of 0.95. Note that this value is very sensitive to the measured values of the flapping amplitude and flapping frequency. For comparative reasons the lift coefficient of the hawkmoth *Manduca sexta* is given here. Using the measured values of the wing kinematics during hovering flight, obtained from Willmott and Ellington [135], yields and mean lift coefficient of 1.38.

### 7.4.4   Review of performance

The wing motion patterns produced by the prototype when actuated in resonance look very similar to the patterns produced by an individual wing in a test setup. Uncertainty in the produced motion patterns has different sources listed below:

- The manufacturing techniques used to build the models. Especially local errors in mass and membrane tension might influence motion patterns significantly. Sensitivities with respect to errors in mass distribution are, however, not analyzed.

- Mechanical assumptions introduce differences between predicted and observed kinematics. In the modeling and testing the wing base is assumed to be rigid. The wing base in the prototype is, due to the compliant nature of the structure, not rigid and will therefore allow movements not present in the modeling.

- Aerodynamic modeling assumptions introduce differences between measured and predicted lift values. In the modeling the wing is assumed rigid. Observed membrane deformations are significant.

The lift production of the prototype is significantly smaller when compared to results of the quasi-steady aerodynamic model. This can be partially explained by the previously mentioned manufacturing inaccuracies. A factor is the limitation of the chosen aerodynamic modeling strategy. Quasi-steady models are known to

possess limited accuracy. The choice of modeling the wing as a rigid plate does not have a large influence mechanically but due to the finesses of lift producing mechanisms in insect flight small deviations in wing kinematics may have a large effect on lift production. A large factor in the creation of lift is the wing pitching angle. The mid stroke pitching angle of the wing base, shown in Figure 6.12 on Page 124 for the individually tested wings, is low for efficient lift production. A rough estimate of the pitching angle during resonant excitation of the completed structure, based on review of Figure 7.4, indicates that the maximum pitching angle at the base is between 30–35°. For efficient lift production a mid-stroke pitching angle should be higher, in the order of 45–50° as it is in the hawkmoth.

## 7.5   Concluding remarks

The current structure is capable of reproducing insect-like wing motion in a resonant setting. The current thorax structure implementation, based on a ring-type resonant structure, is able to produce the large amplitude wing sweeping motion. The wings, which include a tuned hinge for passive wing pitching motion, add the pitching motion to the wing sweeping. The combination can be seen as a successful step towards more optimized design.

Improvements of the structure may be expected in the following areas: Wing kinematics, wing planform and actuator technology. The lift production is larger than the mass of the structure, however, the current actuator is far too heavy to achieve lift-off. When using a different actuator technology, which has a higher specific power density, lift-off may be within reach. The wing sweeping amplitude can be enlarged to values just above 90°. Higher values are restricted by the structure. The current simplified pitching motion shows the feasibility of creating complex motions using passive system and is a starting point for more intricate patterns to improve lift production values. Maximum wing pitching angles can be increased using the current design, while this may not lead to lift-off the mean lift coefficient can be increased.

The current wing technology uses spars which are over dimensioned. This means that, while keeping the current wing inertia, effective area can be increased. In this way larger, more optimal wings, may be added to the existing thorax structure. The reference wing motion can be tuned further. Especially the pitching motion has been chosen for simplicity. More intricate movement patterns may be obtained by adding nonlinear springs and optimizing for lift production not a reference kinematics. The fastest manner to do this is to use the elegant combination of numerical models and experimental testing. It is the current view of the author that lift force generation could be improved by a factor of two using only newly designed and optimized wings.

# Chapter 8

# Conclusions and Recommendations

## 8.1 Conclusions

The structure of the conclusions in this thesis has been based on the major developments which form the basis of the current wing actuation mechanism. The conclusions in this chapter will be presented in the same ordering as the chapters. The topics are: The exploitation of resonance in flapping-wing MAVs, the use of compliant structures to facilitate wing actuation in flapping-wing MAVs, the use of ring-based elastic structures to facilitate resonance and the exploitation of passive wing pitching. These topics are pillars supporting the development of the wing actuation mechanism which was the central aim of this project. The overall project dictates a high degree of integration of the individual aspects. This, while separately reviewed here, was a guiding principle for all developments within the current design setting.

### 8.1.1 Resonance in flapping-wing MAVs

Perhaps the most essential aspect in the development of flapping-wing MAVs is the focus on simplicity. Since the setting of the current work is that of mechanics, the aspects of simplicity must be seen within this mechanically oriented setting. The inspiration for micro scale flapping wing flight originates in the fascination with and study of insects. While insects are mechanically seen very intricate and complex structures, see Chapter 2, the analysis of current flapping-wing MAV projects in Chapter 3 has brought forward that the designs that excel in mechanical simplicity are those that have most success of achieving flight.

The mechanical complexity of the insect flight mechanism can be overlooked when reviewing the design principles on a higher level. A number of lessons can be learned from insects and, consequently, be used in the design and analysis of flapping-wing MAV designs. Looking solely at the structural and dynamic aspects of the insect thorax-wing system, it can be concluded that the resonant principles employed by insects to obtain large wing sweeping angles can be given an interpretation within the flapping-wing MAV setting.

The benefits of implementing resonance to achieve the wing sweeping motion can be summarized in the following aspects which, in essence, constitute the design guidelines for the flapping-wing MAV wing actuation mechanism currently under design:

- The exploitation of resonance allows for a reduced energy signature for the wing sweeping motion. This reduction is realized by the fact that the mechanism is designed such that the sweeping motion is coupled to an energy storage structure. Thus, the wings are decelerated by storing energy in the structure which is retrieved to accelerate the wings leading to a harmonic wing sweeping motion. A minimum in energy expenditure can be found when the driving frequency is close- or equal to the resonant frequency of the structure.

- The subject of amplitude amplification is highly coupled to the first aspect. It should be noted, however, that the current view on amplitude amplification is seated on the assumption the wing actuation mechanism is compliant in origin and is not kinematically restricted to a certain wing sweeping motion. Amplitude amplification can be exploited to increase the stroke angle of the wing sweeping motion, this increase allows for generation of larger aerodynamic forces and thereby increases useful lift production.

- A less powerful actuator is required to achieve a certain wing sweeping amplitude when resonance is exploited, as compared to a system which does not exhibit resonant properties. This implies reduced actuator requirements which can be directly translated into an actuator of smaller mass. When looking at the overall requirements for the wing actuation mechanism a smaller mass means higher chances of lift-off or increased payload capacity.

These three points constitute the intention to base the current wing actuation mechanism design around the exploitation of resonant principles. The choice of implementation has to conform to the requirements of simplicity that span all aspects of the design.

The implementation of resonance does limit the design in certain aspects. The first of which is the wing driving frequency. Depending on the quality factor of the resonant system a change in drive frequency will have detrimental effects on the wing sweeping amplitude. Therefore, this change limits control options. Other methods which rely on influencing the resonant state are available for control purposes.

## 8.1.2   Compliant wing actuation

The implementation of resonant principles can be accomplished in a plethora of different manners. Perhaps the most obvious candidate for implementing these principles are compliant structures. Compliant structures, either in the form of compliant mechanisms or fully compliant structures, lend themselves in a natural way for the incorporation of resonant principles. The use of compliant structures implies a move away from standard flapping-wing MAV manufacturing techniques and requires a search for other techniques which can be found in other research areas.

While the exploitation of resonance comes in a natural way when employing compliant structures, another equally important factor exists. While the current design has dimensions which are easily reachable using current manufacturing principles, future developments will point towards the direction of miniaturization. It is this factor that makes developing expertise on the use of compliant structures for wing actuation mechanisms a viable direction, since compliant structures are far better suited for realizing mechanisms at a very small scale.

Both compliant mechanism- and compliant structure based wing actuation mechanisms have been proposed in Chapter 4. The intention of both these designs is to make certain that the first eigenmode of the structure coincides with the wing sweeping motion. Within the current design setting, compliant mechanisms based structures are more promising. The fully compliant structures introduce large difficulties when imposing design requirements on the wing sweeping amplitude.

The choice to base the design on a compliant mechanism introduces, implicitly, the choice for a linear actuator technology, which is inherently more suited to drive a resonant compliant structure. While the focus in this work is not on actuator selection and development, general requirements are imposed by the framework of low mass and simplicity. Many linear actuator technologies exist today. However, those immediately suited to apply in the current setting will have to be developed.

## 8.1.3   Ring-based compliant structures

The developments of the resonant compliant wing actuation mechanism require the selection of two structural components as presented in Chapter 4. The first is the structure used for storage of potential energy. This structure can be seen as the heart of the structure. The second component is the compliant mechanism which is used to transform and amplify the deformation of the elastic storage unit into the large sweeping motion at the wing root. The integration of these two parts is in essence the equivalent of the flapping-wing MAV thorax. It should be noted here that the sought after insect wing kinematics are split into the sweeping motion and pitching motion, in the current developments this division lies between the thorax structure and the wing. The thorax therefore provides only the sweeping motion.

The selection of an elastic storage unit is based on the exclusion and selection of the deformation mode. Bending has been found to be most suited for this setting due to the lower loads involved. Besides elastic storage levels another requirement is present. Namely, the requirement to be self contained. This implies that the elastic storage unit should not rely on external means of stabilization and support but instead provide these intrinsically. A ring-type structure has been found to meet these requirements. The ring essentially functions as a self-stabilized equivalent of a coil spring. Ring sizing has been performed based on material selection, required amount of elastic storage and selected operating range.

The deflections associated with the chosen ring-type structure are small and translational. A compliant mechanism is presented which transforms and amplifies this motion into the wing sweeping motion. The restriction to only the wing sweeping motion allowed for the use of a planar four-bar mechanism. The required amplification factor is determined by kinematic analysis of the structure and requirements imposed on input and output. In the realization phase the mechanisms are built using materials that are selected based on performance in this low mass setting.

Chapter 5 presents the analysis of the combination and the specification of various two- and four-winged designs. These designs have been realized and tested, the measured performance closely matches predicted behavior. Two series of prototypes are presented: the first is to test predictive qualities of the chosen analysis techniques and evaluate possibilities of the compliant mechanism–ring combination. The second series is geared towards more detailed design and focus is on rigorous materials selection. The structures show that sufficient wing sweeping amplitude and flapping frequency can be obtained using the current combination of ring and compliant mechanism.

Four-winged structures are most promising since they allow for beneficial positioning of the center of mass. The current realization and actuator techniques restrict the possible mechanism design to Concept 2 which is the combination of a ring-type structure with two compliant mechanisms driving four wings. In the current realization the mechanism has one degree of freedom.

## 8.1.4  Passive wing pitching

Chapter 6 demonstrates the design and analysis of the wings. The decoupling of the wing sweeping and pitching motion requires provisions to obtain the latter in the wing. Based on the analysis of insect-wing motion presented in literature, the choice has been made to strive for passive wing pitching motion. The wing pitching motion of insects is passive in origin and therefore allows for further mass reduction of the wing actuation mechanism by removing the need for pitching actuators.

The wings are based on the modification of an existing design. The modification encompasses the addition of an elastic element in the wing root which

constitutes a compliant hinge for the wing pitching motion. The tuning of this elastic element requires the selection of a suitable aerodynamical and mechanical modeling strategy. The mechanical model is straightforward while the selection of the aerodynamical model is more involved. Based on the qualitative comparison of various models the selection has been made to use a quasi-steady model with empirical corrections.

A tuning procedure has been proposed to fit the dynamic response of the model to a prescribed reference motion obtained from the design and analysis of the wing actuation mechanism. The results show that a simple linear spring can be used to accurately represent the intended pitching motion. The realization and testing of the wings is done separate from the wing actuation mechanism. It has been shown that the current passively pitching wing design can be made to accurately reproduce a reference pitching motion.

The modeling assumptions have been based on a rigid wing. Experiments have shown that, although small compared to total pitching motion, membrane deformations are present and have currently not been modeled. The influence of these deformations is beneficial since they increase effective pitching towards the wing tip.

### 8.1.5   Overall conclusion

The research presented in this thesis illustrates the possibilities of introducing lessons learned from studying insects to design and realization of wing actuation mechanisms for flapping-wing MAVs. The chapters present design and analysis of various parts required for the realization of the total structure. Modeling techniques chosen to analyze the design choices have been kept simple intentionally to allow for fast analysis and reanalysis after design changes. This aim for simplicity resounds throughout this thesis.

The culmination of the design is found in Chapter 7 in which all the constituents are combined to from the prototype structure, the ring-based structure as proposed in Chapter 4 and analyzed in Chapter 5 and the wings analyzed in Chapter 6. The resulting prototype structure produces significant lift when driven in the resonant state, while showing significant wing sweeping and kinematically correct pitching motion. While the lift produced is significantly larger than the mass of the structure, the heavy actuator prevents lift-off.

The exploitation of resonance in no way restricts the envelope of possible wing motions. In fact the chosen design allows for large possible range of flapping frequencies and wing sweeping motions. It is expected that future developments wining the Atalanta program can make valuable use of the developments within this thesis.

## 8.2    Recommendations

Although this thesis is aimed at the mechanical development of an insect-inspired wing actuation mechanism, there are still numerous topics that could be explored. The developments in the subjects required to fulfill the main objective have brought forward many options for improvements. These options for improvement are presented here. Besides the topics directly related to the developments in this thesis, the Atalanta project is aimed at the development of the total autonomous flying platform. Looking from the mechanical developments presented here a number of suggestions can be done for fields which are not directly included but closely related. These suggestions are also included in this section.

### 8.2.1    Wings

The currently developed wings have proven to be very promising. The current wings, while easy to manufacture, still have a large potential for improving performance. When looking for even higher performance a more complex wing design has to be used. Various options have been reviewed in Section 3.2.13 and these are guiding in exploring the expanded design space. Perhaps and even more important step in the design and optimization of new wings is the selection of an accurate but fast and elegant method for analysis and tuning. The selection of the analysis method will have to be based on the possibility to include a tunable mechanical model as well as an accurate aerodynamical model. New selection process has to be done because new wing designs require more detailed knowledge on localized aerodynamical loading conditions and the corresponding mechanical response. The aim should be to find a wing structure that is able to facilitate the passive wing pitching motion as well as an increasing twist in spanwise direction.

### 8.2.2    Actuators

The currently used actuator is of the COTS type, while very powerful and therefore feasible for the current setting, future developments require another actuator technology. The search for a weight optimized actuator should include a thorough review of actuator technologies. This review should not share the current limitation to electric actuation technologies but should be extended to include all types. Especially actuators based on the combination of chemical energy including a thermal cycle seem particularly promising in this setting of resonant motion.

When restricted to the electrical actuators a huge step can be made. The flapping-wing MAV setting is inherently of low accuracy when compared to settings for which actuators are commonly developed. This focus on accuracy has led to actuators which usually have a very low power density. When focusing on electromagnetic actuators large improvements can be expected when the design

of the actuator is optimized for power density. This implicitly assumes developments for a flapping-wing MAV of similar dimensions. When looking at decreasing scales piezo actuators seem more promising despite the high voltage drawback.

### 8.2.3  Integration

The current state of integration could be improved. The exploratory nature of this thesis has favored manufacturing solutions based on off-the-shelf materials. In order to perform a weight optimization of the structure, various individual components could be integrated into fewer components. Besides a possible reduction in vehicle weight the assembly process is simplified by a reduction of part numbers. When continuing the current exploratory setting, rapid prototyping techniques could be used to simplify the design and realization cycle.

In the current flapping wing prototype, the actuator is not highly integrated with the structure. In future developments the co-design of the resonant structure and actuator may lead to concepts in which the actuator is heavily integrated in both the structural as well as the control aspects of the wing actuation mechanism. An example of total integration would be to make the rings of an active material.

### 8.2.4  Control

Various options for control have been mentioned throughout this thesis. The current resonant setting can be exploited to explore methods for control. Many of these options have been mentioned in Section 3.4 and the proposed options can be explored. For this setting an extension of the concepts to four-winged applications will have to be made. The actuator requirements necessary to facilitate the exploitation of resonant modes for control have to be included in the design and development of the actuator.

Other control options have been proposed for integration in the wings. These options suggest including valves in the wing to influence the local aerodynamic loading condition. Making the wing permeable inherently reduces aerodynamic efficiency. Another option would be to include mechanisms to locally influence the stiffness of the wing membrane. Due to the fluid–structure coupling this could be an elegant method for obtaining control moments.

### 8.2.5  High level control

While control systems in insects are very complex valuable lessons can be learned from their functioning. Stabilization control in, for example, *Diptera* is based on a local control loop coupling the halteres and the wings. In flapping-wing MAVs, flapping and non flapping, however, this simplicity is usually not present. MAVs usually carry large amounts of CPU power which imply a large burden on the available energy. Large improvements can be made, from an energy perspective, when stabilization methods are inspired by the methods used by insects.

# Bibliography

[1] Aeromechanical Systems Group, 2009. Cranfield University, Shrivenham, Swindon, United Kingdom.
URL `http://www.cranfield.ac.uk/cds/aeromechanical/index.html`

[2] Airbus A380-800, 2010. Airbus (part of EADS Company), Toulouse, France.
URL `http://www.airbus.com`

[3] Alexander, R. M., 1995. Springs for wings. Science 268 (5207), 50–51.

[4] Andersen, A., Pesavento, U., Wang, Z., 2005. Analysis of transitions between fluttering, tumbling and steady descent of falling cards. The Journal of Fluid Mechanics 541, 91–104.

[5] Andersen, A., Pesavento, U., Wang, Z. J., 2005. Unsteady aerodynamics of fluttering and tumbling plates. The Journal of Fluid Mechanics 541, 65–90.

[6] Ansari, S. A., Żbikowski, R., Knowles, K., 2006. Aerodynamic modelling of insect-like flapping flight for micro air vehicles. Progress in Aerospace Sciences 42, 129–172.

[7] Ashby, M. F., 1999. Materials Selection in Mechanical Design. Butterworth-Heinemann.

[8] Balint, C. N., Dickinson, M. H., 2001. The correlation between wing kinematics and steering muscle activity in the blowfly *Calliphora vicina*. The Journal of Experimental Biology 204 (24), 4213–4226.

[9] Banala, S. K., Agrawal, S. K., 2005. Design and optimization of a mechanism for out-of-plane insect winglike motion with twist. Journal of Mechanical Design 127 (4), 841–844.

[10] Bar-Cohen, Y., March 2004. Electroactive Polymer (EAP) Actuators as Artificial Muscles: Reality, Potential, and Challenges, 2nd Edition. SPIE–The International Society for Optical Engineering.

[11] Bergou, A. J., Xu, S., Wang, Z. J., 2007. Passive wing pitch reversal in insect flight. The Journal of Fluid Mechanics 591, 321–337.

[12] Berman, G. J., Wang, Z. J., 2007. Energy-minimizing kinematics in hovering insect flight. The Journal of Fluid Mechanics 582, 153–168.

[13] Biomimetics & Intelligent Microsystem Laboratory, 2010. Konkuk University, Seoul, South-Korea.
URL http://bimil.konkuk.ac.kr/index.html

[14] Birch, J. M., Dickinson, M. H., 2003. The influence of wing-wake interactions on the production of aerodynamic forces in flapping flight. The Journal of Experimental Biology 206, 2257–2272.

[15] Blum, S. M., 1985. Fundamentals of Insect Physiology. Wiley-Interscience.

[16] Bolsman, C. T., Goosen, J. F. L., van Keulen, F., 2008. Insect-inspired wing actuation structures based on ring-type resonators. In: Ahmadian, M. (Ed.), Active and Passive Smart Structures and Integrated Systems, SPIE, San Diego, United States of America. Vol. 6928. SPIE.

[17] Bolsman, C. T., Goosen, J. F. L., van Keulen, F., June 2009. Compliant structure design for reproducing insect wing kinematics in mavs. In: Snyder, R. (Ed.), Proceedings of IFASD conference,Seattle,Washington,USA,June 21–25.

[18] Bolsman, C. T., Goosen, J. F. L., van Keulen, F., Porto, Portugal, Juli 2009. Design and realization of resonant mechanisms for wing actuation in flapping wing micro air vehicles. In: Silva Gomes, J., Mequid, S. (Eds.), Integrity, Reliability and Failure (IRF), Porto, Portugal, July 20–24,2009.

[19] Bolsman, C. T., Goosen, J. F. L., van Keulen, F., December 2009. Design overview of a resonant wing actuation mechanism for application in flapping wing mavs. International Journal of Micro Air Vehicles 1 (4), 263–272.

[20] Bolsman, C. T., Pålsson, B., Goosen, J. F. L., Munnig-Schmidt, R. H., van Keulen, F., Toulouse, France, Sept 17–21 2007. The use of resonant structures for miniaturizing FMAVs. In: 3rd US-European Competition and Workshop on Micro Air Vehicle Systems (MAV07) and European Micro Air Vehicle Conference and Flight Competition.

[21] Bos, F. M., 2009. Numerical simulations of flapping foil and wing aerodynamics - mesh deformation using radial basis functions. Ph.D. thesis, Delft University of Technology.

[22] Brodsky, A. K., 1994. The evolution of insect flight. Oxford University Press, Unites states of America.

[23] Brown, D., 2001. Deception Point. Corgi Books Limited.

[24] Bunget, G., Seelecke, S., 2009. Actuator placement for a bio-inspired bone-joint system based on sma. Vol. 7288. SPIE, p. 72880L.

[25] Büttgenbach, S., Bütefisch, S., Leester-Schädel, M., Wogersien, A., 2001. Shape memory microactuators. Microsystem Technologies 7 (4), 165–170.

[26] Chapman, R. F., 1969. The Insects Structure and Function. The English Universities Press LTD.

[27] Combes, S. A., Daniel, T. L., 2003. Flexural stiffness in insect wings I. scaling and the influence of wing venation. The Journal of Experimental Biology 206, 2979–2987.

[28] Combes, S. A., Daniel, T. L., 2003. Into thin air: contributions of aerodynamic and inertial-elatic forces to wing bending in the hawkmoth *Manduca Sexta*. The Journal of Experimental Biology 206, 2999–3006.

[29] Cox, A., Monopoli, D., Cveticanin, D., Goldfarb, M., Garcia, E., 2002. The development of elastodynamic components for piezoelectrically actuated flapping micro-air vehicles. Journal of Intelligent Material Systems and Structures 13, 611–615.

[30] Daniel, T. L., Combes, S. A., 2002. Flexible wings and fins: Bending by inertial or fluid-dynamic forces? Integrative and Comparative Biology 42 (5), 1044–1049.

[31] de Croon, G., De Clercq, K. M. E., Ruijsink, R., Remes, B., de Wagter, C., 2009. Design, aerodynamics, and vision-based control of the delfly. International Journal of Micro Air Vehicles 1 (2), 71–97.

[32] Delfly, May 2010. Aerospace Software and Technologies Institute, Delft University of Technology, Delft, The Netherlands.
URL http://www.delfly.nl

[33] Deng, X., Schenato, L., Sastry, S. S., 2006. Flapping flight for biomimetic robotic insects: part II-flight control design. Robotics, IEEE Transactions on 22 (4), 789–803.

[34] Deng, X., Schenato, L., Wu, W. C., Sastry, S. S., 2006. Flapping flight for biomimetic robotic insects: part i-system modeling. Robotics, IEEE Transactions on 22 (4), 776–788.

[35] Dickinson, M. H., Lehmann, F. O., Sane, S. P., 1999. Wing rotation and the aerodynamic basis of insect flight. Science 284, 1954–1960.

[36] Dickinson, M. H., Lighton, J. R., 1995. Muscle efficiency and elastic storage in the flight motor of drosophila. Science 268 (5207), 87–90.

[37] Dickinson, M. H., Tu, M. S., 1997. The function of dipteran flight muscle. Comparative Biochemistry and Physiology–Part A: Physiology 116 (3), 223–238.

[38] Du, H., Hu, M., Xie, J., Ling, S. F., 2005. Control of an electrostrictive actuator using newton's method. Precision Engineering 29, 375–380.

[39] Dudley, R., 2000. The biomechanics of insect flight: form, function, evolution. Princeton University Press.

[40] Dudley, R., Ellington, C. P., 1990. Mechanics of forward flight in bumblebees: I. kinematics and morphology. The Journal of Experimental Biology 148 (1), 19–52.

[41] Eich-Soellner, E., Führer, C., 1998. Numerical methods in multibody dynamics. Teubner Stuttgart.

[42] Ellington, C. P., 1984. The aerodynamics of hovering insect flight. i. the quasi-steady analysis. Royal Society of London Philosophical Transactions Series B 305, 1–15.

[43] Ellington, C. P., 1984. The aerodynamics of hovering insect flight. ii. morphological parameters. Royal Society of London Philosophical Transactions Series B 305, 17–40.

[44] Ellington, C. P., 1984. The aerodynamics of hovering insect flight. iv. aerodynamic mechanisms. Royal Society of London Philosophical Transactions Series B 305, 79–113.

[45] Ellington, C. P., 1984. The aerodynamics of hovering insect flight. v. a vortex theory. Royal Society of London Philosophical Transactions Series B 305, 115–144.

[46] Ellington, C. P., 1984. The aerodynamics of hovering insect flight. v. lift and power requirements. Royal Society of London Philosophical Transactions Series B 305, 145–181.

[47] Ellington, C. P., 1985. Power and efficiency of insect flight muscle. The Journal of Experimental Biology 115, 293–304.

[48] Ellington, C. P., 1991. Limitations on Animal Flight Performance. The Journal of Experimental Biology 160 (1), 71–91.

[49] Ellington, C. P., 1999. The novel aerodynamics of insect flight: applications to micro-air vehicles. The Journal of Experimental Biology 202 (23), 3439–3448.

[50] Ellington, C. P., Machin, K. E., Casey, T. M., 1990. Oxygen consumption of bumblebees in forward flight. Nature 347 (6292), 472–473.

[51] Ellington, C. P., van den Berg, C., Willmott, A. P., Thomas, A. L. R., 1996. Leading-edge vortices in insect flight. Nature 384, 626–630.

[52] Ennos, A. R., 1987. A comparative study of the flight mechanism of diptera. The Journal of Experimental Biology 127, 355–372.

[53] Ennos, A. R., 1988. The importance of torsion in the design of insect wings. The Journal of Experimental Biology 140, 137–160.

[54] Ennos, A. R., 1988. The inertial cause of wing rotation in diptera. The Journal of Experimental Biology 140, 161–169.

[55] Ennos, A. R., 1989. Inertial and aerodynamic torques on the wings of diptera in flight. The Journal of Experimental Biology 142, 87–95.

[56] Fenelon, M. A. A., Furukawa, T., 2010. Design of an active flapping wing mechanism and a micro aerial vehicle using a rotary actuator. Mechanism and Machine Theory 45 (2), 137–146.

[57] Friend, C. M., Kaley, A., Hameed, A., 2003. Shape-memory alloy actuation of insect-like flapping wings. Journal de physique. IV 112, 1193–1196.

[58] Fry, S. N., Sayaman, R., Dickinson, M. H., 2003. The aerodynamics of free-flight maneuvers in *Drosophila*. Science 300, 495–498.

[59] Galinski, C., Żbikowski, R., June 2005. Insect-like flapping wing mechanism based on a double spherical scotch yoke. Journal of the Royal Society: Interface 2 (3), 223–235.

[60] Galinski, C., Żbikowski, R., 2007. Materials challenges in the design of an insect-like flapping wing mechanism based on a four-bar linkage. Materials & Design 28 (3), 783 – 796.

[61] Giraudo, O., Osmont, D., 2006. A simple mechanical system for a flapping wing MAV: modeling and experiments. In: Society of Photo-Optical Instrumentation Engineers (SPIE) Conference Series. Vol. 6173. pp. 91–103.

[62] Greenewalt, C. H., 1960. The wings of insects and birds as mechanical oscillators. Proceedings of the American Philosophical Society 104 (6), 605–611.

[63] Haas, F., Gorb, S., Blickhan, R., 2000. The function of resilin in beetle wings. Proceedings of the Royal Society B: Biological Sciences 267 (1451), 1375–1381.

[64] Hall, A., Allahverdi, M., Akdogan, E. K., Safari, A., 2005. Piezoelectric/electrostrictive multimaterial PMN-PT monomorph actuators. Journal of the European Ceramic Society 25, 2991–2997.

[65] Harvard Microrobotics Laboratory, 2009. Harvard University, Cambridge, United States of America.
URL http://micro.seas.harvard.edu/

[66] Hengstenberg, R., 1988. Mechanosensory control of compensatory head roll during flight in the blowfly&lt;i&gt;calliphora erythrocephala&lt;/i&gt; meig. Journal of Comparative Physiology A: Neuroethology, Sensory, Neural, and Behavioral Physiology 163, 151–165.

[67] Ho, S., Nassef, H., Pornsinsirirak, T. N., Tai, Y. C., Ho, C. M., 2003. Unsteady aerodynamics and flow control for flapping wing flyers. Progress in Aerospace Sciences 39 (8), 635–681.

[68] Howell, L. L., 2001. Compliant Mechanisms. Wiley.

[69] Hu, M., Du, H., Ling, S. F., Zhou, Z., Li, Y., 2004. Motion control of an electrostrictive actuator. Mechatronics 14, 153–161.

[70] Josepson, R. K., Malamud, J. G., Stokes, D. R., 2000. Asynchronous muscle: A primer. The Journal of Experimental Biology 203, 2713–2722.

[71] Karpelson, M., Wei, G. Y., Wood, R., 2008. A review of actuation and power electronics options for flapping-wing robotic insects. In: Robotics and Automation, 2008. ICRA 2008. IEEE International Conference on. pp. 779–786.

[72] Kawamura, Y., Souda, S., Nishimoto, S., Ellington, C. P., 2008. Clapping-wing Micro Air Vehicle of Insect Size. Springer, Ch. Bio-mechanisms of Swimming and Flying, pp. 319–330.

[73] Kawamura Laboratory, 2009. Fukuoka Institute of Technology, Fukuoka city, Japan.
URL http://www.fit.ac.jp/~y-kawa/e-index.html

[74] Keennon, M. T., Grasmeyer, J. M., 2003. Development of the black widow and microbat mavs and a vision of the future of mav design. AIAA/ICAS International Air and Space Symposium and Exposition: The Next 100 Years.

[75] Khan, Z. A., Agrawal, S. K., 2005. Force and moment characterization of flapping wings for micro air vehicle application. In: Proceedings of the American Control Conference. Vol. 3. pp. 1515–1520.

[76] Khan, Z. A., Agrawal, S. K., 2007. Design and optimization of a biologically inspired flapping mechanism for flapping wing micro air vehicles. In: 2007 IEEE International Conference on Robotics and Automation. pp. 373–378.

[77] Kornbluh, R. D., Pelrine, R., Pei, Q., Oh, S., Joseph, J., 2000. Ultrahigh strain response of field-actuated elastomeric polymers. In: Bar-Cohen, Y. (Ed.), Society of Photo-Optical Instrumentation Engineers (SPIE) Conference Series. Vol. 3987. pp. 51–64.

[78] Langelaar, M., December 2006. Design optimization of shape memory alloy structures. Ph.D. thesis, Delft University of Technology.

[79] Lee, S. K., Kim, Y. S., Park, H. C., Yoon, K. J., Goo, N. S., Yu, Y., Cho, C., 2005. Performance analysis of a lightweight piezo-composite actuator considering the material non-linearity of an embedded pzt wafer. Smart Materials and Structures 14 (6), 1101–1106.

[80] Lehmann, F. O., 2004. Aerial locomotion in flies and robots: Kinematic control and aerodynamics of oscillating wings. Arthropod Structure & Development 33, 331–345.

[81] Lentink, D., Dickinson, M., 2009. Biofluiddynamic scaling of flapping, spinning and translating fins and wings. The Journal of Experimental Biology 212 (16), 2691–2704.

[82] Lentink, D., Jongerius, S. R., Bradshaw, N. L., 2009. The Scalable Design of Flapping Micro-Air Vehicles Inspired by Insect Flight. Springer, Ch. 14, pp. 185–205.

[83] Lilienthal, O., Reprint from 2003, original in 1889, Berlin. Der Vogelflug als Grundlage der Fliegekunst. Friedland i. Meckl.

[84] Malolan, V., Dineshkumar, M., Baskar, V., January 2004. Design and development of flapping wing micro air vehicle. 42nd AIAA Aerospace Sciences Meeting and Exhibit.

[85] Martin's Shark, 2008. Martin Newell's Flying Machines.
URL http://mnewell.rchomepage.com

[86] Matbase, 2009. Mechanical and Physical Properties of Materials.
URL http://www.matbase.com/

[87] McIntosh, S. H., Agrawal, S. K., Khan, Z., 2006. Design of a mechanism for biaxial rotation of a wing for a hovering vehicle. IEEE/ASME Transactions on Mechatronics 11 (2), 145–153.

[88] McMasters, J. H., 1989. The Flight of the Bumblebee and Related Myths of Entomological Engineering. American Scientist 77, 164–169.

[89] Mechanical Systems Laboratory, 2009. Department of Mechanical Engineering, University of Delaware, Delaware, Unites States of America.
URL `http://mechsys4.me.udel.edu/index.php`

[90] Mesicopter Project, 1999. Aircraft Aerodynamics and Design Group, Stanford University, United States of America.
URL `http://adg.stanford.edu/mesicopter/`

[91] MFI project website, Biomimetic Millisystems Laboratory, May 2010. University of California, Berkeley, United States of America.
URL `http://robotics.eecs.berkeley.edu/~ronf/MFI/index.html`

[92] Michelson, R. C., Naqvi, M. A., November 2003. Beyond biologically-inspired insect flight. von Karman Institute for Fluid Dynamics RTO/AVT Lecture Series on Low Reynolds Number Aerodynamics on Aircraft Including Applications in Emerging UAV Technology.

[93] Michelson, R. C., Reece, S., Arpil–March 1998. Update on flapping wing micro air vehicle research-ongoing work to develop a flapping wing, crawling entomopter. In: 13th Bristol Intl. RPV/UAV Systems Conference Proceedings.

[94] Miyake, H., 2008. Bio-mechanisms of Swimming and Flying. Springer Japan, Ch. Micro-structural Approach to Developing the Resonance Model of the Indirect Flight Mechanism, pp. 129–139.

[95] Muijres, F. T., Johansson, L. C., Barfield, R., Wolf, M., Spedding, G. R., Hedenstrom, A., 2008. Leading-edge vortex improves lift in slow-flying bats. Science 319 (5867), 1250–1253.

[96] Nguyen, V. Q., Syaifuddin, M., Park, H. C., Byun, D. Y., Goo, N. S., Yoon, K. J., 2008. Characteristics of an insect-mimicking flapping system actuated by a unimorph piezoceramic actuator. Journal of Intelligent Material Systems and Structures 19 (10), 1185–1193.

[97] Norberg, R. Å., 1972. The pterostigma of insect wings an inertial regulator of wing pitch. Journal of Comparative Physiology A: Neuroethology, Sensory, Neural, and Behavioral Physiology 81 (1), 9–22.

[98] Park, H. C., Kim, K. J., Lee, S., Lee, S. Y., Cha, Y. J., Yoon, K. J., Goo, N. S., 2004. Biomimetic flapping devices powered by artificial muscle actuators. In: Proceedings of US-Korea Conference on Science, Technology and Entrepreneurship, Durham, NC, USA.

[99] Pawlowski, K. J., Belvin, H. L., Raney, D. L., Su, J., Harrison, J. S., Siochi, E. J., 2003. Electrospinning of a micro-air vehicle wing skin. Polymer 44 (4), 1309–1314.

[100] Pelrine, R., Kornbluh, R. D., Pei, Q., Stanford, S., Oh, S., Eckerle, J., Full, R. J., Rosenthal, M. A., Meijer, K., juli 2002. Dielectric elastomer artificial muscle actuators: toward biomimetic motion. In: Bar-Cohen, Y. (Ed.), Society of Photo-Optical Instrumentation Engineers (SPIE) Conference Series. Vol. 4695 of Society of Photo-Optical Instrumentation Engineers (SPIE) Conference Series. pp. 126–137.

[101] Pesavento, U., Wang, Z. J., 2004. Falling paper: Navier-stokes solutions, model of fluid forces, and center of mass elevation. Physical Review Letters 93 (14), 144501.

[102] Pornsin-Sirirak, T. N., Lee, S. W., Nassef, H., Grasmeyer, J., Tai, Y. C., Ho, C. M., Keennon, M., 2000. Mems wing technology for a battery-powered ornithopter. In: Proc. of IEEE 13th Annual Intl Conf on MEMS. Citeseer, pp. 799–804.

[103] Pornsin-Sirirak, T. N., Tai, Y. C., Nassef, H., Ho, C. M., 2001. Flexible parylene actuator for micro adaptive flow control. In: Micro Electro Mechanical Systems, 2001. MEMS 2001. The 14th IEEE International Conference on. pp. 511–514.

[104] Pornsin-Sirirak, T. N., Tai, Y. C., Nassef, H., Ho, C. M., 2001. Titanium-alloy MEMS wing technology for a micro aerial vehicle application. Sensors and Actuators A: Physical 89 (1-2), 95–103.

[105] Ramamurti, R., Sandberg, W. C., 2002. A three-dimensional computational study of the aerodynamic mechanisms of insect flight. The Journal of Experimental Biology 205, 1507–1518.

[106] Raney, D. L., Slominski, E. C., 2004. Mechanization and control concepts for biologically inspired micro air vehicles. Journal of Aircraft 41, 1257–1265.

[107] Rees, C. J. C., 1975. Form and function in corrugated insect wings. Nature 256, 200–203.

[108] Sane, S. P., 2003. The aerodynamics of insect flight. The Journal of Experimental Biology 206, 4191–4208.

[109] Sane, S. P., Dickinson, M. H., 2002. The aerodynamic effects of wing rotation and a revised quasi-steadi model of flapping flight. The Journal of Experimental Biology 205, 1087–1096.

[110] Schwab, A. L., Meijaard, J. P., 2006. How to draw euler angles and utilize euler parameters. In: Proceedings of IDETC/CIE 2006, ASME 2006 International Design Engineering Technical Conferences & Computers and Information in Engineering Conference, September 10-13, 2006, Philadelphia, USA.

[111] Sedov, L. I., 1965. Two-Dimensional Problems in Hydrodynamic and Aerodynamics. Interscience Publishers.

[112] Shaninpoor, M., 2003. Ionic polymer-conductor composites as biomimetic sensors, robotic actuators and artificial muscles - a review. Electrochimica Acta 48, 2343–2353.

[113] Shewry, P. R., Tatham, A. S., Bailey, A. J., 2002. Elastomeric proteins: structures, biomechanical properties, and biological roles. Cambridge University Press.

[114] Sitti, M., Campolo, D., Yan, J., Fearing, R. S., Su, T., Taylor, D., Sands, T. D., 2001. Development of pzt and pzn-pt based unimorph actuators for micromechanical flapping mechanisms. In: IEEE International Confonference on Robotics and Automation. Vol. 4. pp. 3839–3846.

[115] Smith, M., Wilkin, P., Williams, M., 1996. The advantages of an unsteady panel method in modelling the aerodynamic forces on rigid flapping wings. The Journal of Experimental Biology 199 (5), 1073.

[116] Snodgrass, R. E., 1993. Principles of insect morphology. Cornell University Press.

[117] Stevens, J. M., Buckner, G. D., 2005. Actuation and control strategies for miniature robotic surgical systems. Journal of Dynamic Systems, Measurement, and Control 127, 537–549.

[118] Sun, M., Du, G., 2003. Lift and power requirements of hovering insect flight. Acta Mechanica Sinica 19 (5), 458–469.

[119] Sun, M., Tang, J., 2002. Lift and power requirements of hovering flight in *Drosophila virilis*. The Journal of Experimental Biology 205, 2413–2427.

[120] Sun, M., Tang, J., 2002. Unsteady aerodynamic force generation by a model fruit fly wing in flapping motion. The Journal of Experimental Biology 205, 55–70.

[121] Syaifuddin, M., Park, H. C., Goo, N. S., 2006. Design and evaluation of a lipca-actuated flapping device. Smart Materials and Structures 15 (5), 1225.

[122] Tantanawat, T., Kota, S., September 2006. Design of compliant mechanisms for minimizing input power in dynamic applications. Proceedings of DETC 2006, International Design Engineering Technical Conference.

[123] Trease, B. P., Moon, Y. M., Kota, S., 2005. Design of large-displacement compliant joints. Journal of Mechanical Design 127, 788–798.

[124] Usherwood, J. R., Ellington, C. P., 2002. The aerodynamics of revolving wings I. model hawkmoth wings. The Journal of Experimental Biology 205, 1547–1564.

[125] Usherwood, J. R., Ellington, C. P., 2002. The aerodynamics of revolving wings II. propeller force coefficients from mayfly to quail. The Journal of Experimental Biology 205, 1565–1576.

[126] van der Linde, R. Q., Schwab, A. L., 2010. Multibody dynamics b. Lecture notes, Delft University of Technology.

[127] van Dijk Pultrusion Products, 2007. Characteristics of the high performance dpp micro pultrusions. Tech. rep.

[128] Wakeling, J. M., Ellington, C. P., 1997. Dragonfly flight. I. gliding flight and steady-state aerodynamic forces. The Journal of Experimental Biology 200, 543–556.

[129] Wakeling, J. M., Ellington, C. P., 1997. Dragonfly flight. II. velocities, accelerations and kinematics of flapping flight. The Journal of Experimental Biology 200, 557–582.

[130] Wakeling, J. M., Ellington, C. P., 1997. Dragonfly flight. III. lift and power requirements. The Journal of Experimental Biology 200, 583–600.

[131] Warrick, D. R., Tobalske, B. W., Powers, D. R., 2005. Aerodynamics of the hovering hummingbird. Nature 435 (7045), 1094–1097.

[132] Weis-Fogh, T., 1960. A rubber-like protein in insect cuticle. The Journal of Experimental Biology 37 (4), 889–907.

[133] Weis-Fogh, T., 1972. Energetics of hovering flight in hummingbirds and in drosophila. The Journal of Experimental Biology 56 (1), 79–104.

[134] Weis-Fogh, T., 1973. Quick estimates of flight fitness in hovering animals, including novel mechanisms for lift production. The Journal of Experimental Biology 59 (1), 169–230.

[135] Willmott, A. P., Ellington, C. P., 1997. The mechanics of flight in the hawkmoth *Manduca Sexta*. I. kinematics of hovering and forward flight. The Journal of Experimental Biology 200, 2705–2722.

[136] Willmott, A. P., Ellington, C. P., 1997. The mechanics of flight in the hawkmoth *Manduca Sexta*. II. aerodynamic consequences of kinematic and morphological variation. The Journal of Experimental Biology 200, 2723–2745.

[137] Wood, R. J., 2007. Design, fabrication, and analysis of a 3DOF, 3cm flapping-wing MAV. In: IEEE/RSJ International Conference on Intelligent Robots and Systems, 2007. IROS 2007. pp. 1576–1581.

[138] Wood, R. J., October 2007. Liftoff of a 60mg flapping-wing MAV. In: IEEE/RSJ IROS International Conference on Intelligent Robots and Systems. pp. 1889–1894.

[139] Wood, R. J., Avadhanula, S., Fearing, R. S., 2003. Microrobotics using composite materials: the micromechanical flying insect thorax. IEEE Int. Conf. on Robotics and Automation, Taipei, Taiwan.

[140] Wood, R. J., Avadhanula, S., Menon, M., Fearing, R. S., 2003. Microrobotics using composite materials: The micromechanical flying insect thorax. In: IEEE International Conference on Robotics and Automation. Vol. 2. Citeseer, pp. 1842–1849.

[141] Wood, R. J., Steltz, E., Fearing, R. S., 2005. Optimal energy density piezoelectric bending actuators. Sensors and Actuators A: Physical 119, 476–488.

[142] Wootton, R. J., 1992. Functional morphology of insect wings. Annual review of Entomology 37 (1), 113–140.

[143] Wootton, R. J., Herbert, R. C., Young, P. G., Evans, K. E., 2003. Approaches to the structural modelling of insect wings. Philosophical Transactions of the Royal Society B: Biological Sciences 358 (1437), 1577–1587.

[144] Yan, J., Wood, R., Avadhanula, S., Sitti, M., Fearing, R. S., May 2001. Towards flapping wing control for a micromechanical flying insect. IEEE International Conference on Robotics and Automation, pp. 3901-3908, Seoul, Korea.

[145] Yang, L. J., Hsu, C. K., Ho, J. Y., Feng, C. K., 2007. Flapping wings with pvdf sensors to modify the aerodynamic forces of a micro aerial vehicle. Sensors and Actuators A: Physical 139 (1-2), 95–103, selected Papers From the Asia-Pacific Conference of Transducers and Micro-Nano Technology (AP-COT 2006), Asia-Pacific Conference of Transducers and Micro-Nano technology.

[146] Yoon, K. J., Shin, S., Park, H. C., Goo, N. S., 2002. Design and manufacture of a lightweight piezo-composite curved actuator. Smart Materials and Structures 11 (1), 163–168.

[147] Żbikowski, R., 2002. An aerodynamic modelling of an insect-like flapping wing in hover for micro air vehicles. Philosophical Transactions of the Royal Society of London Series A 360, 273–290.

# Samenvatting

**Vleugelactuatie gebaseerd op resonerende compliante mechanismen**
**Een op insecten geïnspireerd ontwerp**

Dit proefschrift beschrijft het ontwerp en de analyse van het vleugelactuatiemechanisme voor een op insecten geïnspireerd micro vliegtuig met flappende vleugels. In de natuur behoren insecten tot de meest capabele vliegers en daardoor vormen zij een grote bron van inspiratie. De menselijke inspanning om flappende vliegtuigen op insectenschaal te realiseren heeft de laatste jaren een grote ontwikkeling doorgemaakt. De focus van dit proefschrift ligt op het toepassen van resonante principes voor het verkrijgen van insect-achtige vleugelbewegingspatronen. Het vleugel–thorax systeem van insecten is in feite een resonant systeem. Insecten gebruiken de resonante aspecten van dit systeem voor het verminderen van de energie die nodig is voor het in stand houden van de vleugelbeweging evenals voor het vergroten van de vleugelslag door resonante amplificatie. De toepassing van resonante principes in micro flappendevleugelvliegtuigen is bedoeld om de zelfde aspecten uit te buiten. De vleugelbeweging van insecten kan in twee delen worden opgedeeld, het eerste deel is de flap beweging, het tweede deel is de vleugelrotatie. Het onderzoek in dit proefschrift ingedeeld volgens dezelfde lijn. Het vleugelactuatiemechanisme, dat de flap beweging in stand houdt, wordt parallel ontwikkeld aan de vleugels, die zorgen voor de vleugelrotatiebeweging.

Voor het uitbuiten van resonantie is het invoegen van een elastisch element in het vleugelactuatiemechanisme ontwerp noodzakelijk. Verschillende mogelijkheden worden bekeken en een optie gebaseerd op het toepassen van buiging is gekozen. De gekozen elastische structuur is de ring. Het toepassen van een ring geeft veel mogelijkheden voor het plaatsen van de actuator en de vleugels. De vleugels worden aan de ring gekoppeld doormiddel van een compliant am-

157

plificatie mechanisme welke de inherent lineaire beweging van de ring omzet en versterkt tot de grote rotatie die de vleugel flap vormt. De ontwikkeling van de structuren volgt een tweeledige aanpak. De eerste stap is de selectie van vier prototypes waarmee de functionaliteit van op ringen gebaseerde structuren en de analyse daarvan beoordeeld wordt. Deze analyse wordt gedaan doormiddel van meerdere-lichaam dynamica en eindige elementen. De tweede set prototypes is gericht op het verkrijgen van een ontwerp met een hoger detailleringniveau dat gericht is op de uiteindelijke toepassing. Hierbij wordt veel aandacht gegeven aan het verkrijgen van een ontwerp met een laag gewicht. Na het bepalen van de initiële afmetingen worden deze prototypes geanalyseerd doormiddel van eindige elementen (Eigenwaarde en transiënt analyse). Gebaseerd op deze analyses worden de structuren gemaakt en getest. De structuren zijn in staat om een vleugelslag met grote amplitude te bereiken in een resonante toestand.

Het gekozen analyse pad maakt het mogelijk om de vleugels onafhankelijk te ontwerpen en te analyseren. In insecten is de vleugelrotatie en de timing daarvan van groot belang voor het verkrijgen van efficiënte liftproductie. De vleugelrotatie in insecten is overwegend van passief. Een technisch alternatief vereist de implementatie van een elastische structuur in de basis van de vleugel. Dit elastische element is in het huidige vleugelontwerp toegepast als modificatie van een bestaand ontwerp. De stijfheid van het elastische element is bepaald door een gekoppeld meerdere lichamen dynamisch en aerodynamische model. De referentie die is gebruikt voor de vleugelbeweging is de versimpelde versie van de vleugelbeweging van de pijlstaartvlinder. De vleugels zijn gerealiseerd en experimenteel getest om hun prestaties te vergelijken met de analyse.

De op een ring gebaseerde structuur wordt gecombineerd met de vleugels om experimenteel de prestaties van de samengestelde structuur te testen. Een experimentele opstelling is gebouwd om de liftproductie te kwantificeren. In de opstelling is het prototype opgehangen aan een flexibele balk, waarna veranderingen in uitwijking direct gerelateerd kunnen worden aan lift productie. Er is significante liftproductie, in de orde van grootte van het gewicht van de structuur zonder de actuator. De kinematische patronen zoals gemaakt tijdens resonante excitatie, laten correcte vleugelrotatie timing zien.

De huidige ontwikkelingen hebben geleid tot groter inzicht in de mogelijkheden van het uitbuiten van resonantie voor vleugelactuatie evenals inzicht in het toepassen van op ringen gebaseerde structuren. Verdere ontwikkelingen liggen in de selectie en toepassing van nieuwe actuator technologieën en het inbouwen van mogelijkheden voor besturing.

*Caspar Bolsman*

# Acknowledgements

structional aspects of the realization of the prototypes. I am especially thankful to Bjorn Pålsson for performing an excellent literature review which saved me huge amounts of time.

The technical support staff of the PME department, Rob Luttjeboer, Patrick van Holst and Harry Jansen have provided me with insight and technical support when building and testing the prototypes, which was very welcome. I would like to thank Marianne Stolker for her help and assistance with many aspects of my work including streamlining the process of maintaining two workplaces.


*Amsterdam,*                                                                                 *Caspar Bolsman*
*August 2010*

# About the author

Caspar Bolsman was born on June 23, 1978, in Zaanstad, The Netherlands. He graduated secondary school at the Montessori Lyceum Amsterdam. In 1996 he started his study biology at the Faculty of Biology of the University of Amsterdam. He finished his Propedeuse in 1997. Following he studied mechanical engineering at the Mechanical Engineering Faculty at the Delft University of Technology.

Caspar obtained his master's degree within the Structural Optimization and Computational Mechanics group. As a part of obtaining his Master of Science degree he visited Airbus GmbH, Hamburg, Germany two times. During the first visit, which was in the form of an internship, he investigated the validity of equivalent beam models. The second visit was part of his Master's thesis. The topic of the thesis was a numerical investigation into the usage of measured Frequency Response Functions for updating finite element models, Title of the MSc thesis: *FE-model updating using measured FRFs*. Supervised by Dr. J. Brink-Spalink of Airbus GmbH and Prof. dr. ir. A. van Keulen. He graduated in 2005.

In November 2005 he started his Ph.D. project within the DevLab and the Structural Optimization and Computational Mechanics group, part of the Precision and Microsystems Engineering department, supervised by Prof. dr. ir. A. van Keulen and cosupervised by Dr. ir. J. F. L. Goosen. The topic is the development of an insect-inspired wing actuation mechanism for a flapping-wing MAV. The results are presented in this thesis.